CVR JOURNAL OF SCIENCE & TECHNOLOGY

Vol. No.: 4, June 2013 ISSN 2277-3916

CVR COLLEGE OF ENGINEERING

In Pursuit of Excellence

PATRONS

Dr. Raghava V. Cherabuddi, President & Chairman

Dr. K. Rama Sastri, Director

Dr. L.V.A.R. Sarma, Principal

Editor : Dr. K. V. Chalapati Rao, Professor & Dean, Research

Associate Editor : Wg Cdr Varghese Thattil, Professor, Dept. of ECE

Editorial Board :

Dr. K. Lal Kishore, Vice Chancellor, JNTU, Anantapur.

Dr. S. Ramachandram, Vice Principal, College of Engineering & Professor Dept. of CSE, Osmania University.

Prof. L. C. Siva Reddy, Vice Principal and Professor & Head, Dept. of CSE, CVRCE

Dr. A. D. Raj Kumar, Dean, Academics, CVRCE

Prof. S. Sengupta, Dean, Projects and Consultancy, CVRCE

Dr. K. Nayanathara, Professor, Head, Dept. of ECE, CVRCE

Dr. K. Dhanvanthri, Professor & Head, Dept. of EEE, CVRCE

Dr. M. S. Bhat, Professor & Head, Dept. of EIE, CVRCE

Dr. E. Narasimhacharyulu, Professor & Head, Dept. of H&S, CVRCE

Dr. N. V. Rao, Professor, Dept. of CSE, CVRCE

Dr. T. A. Janardhan Reddy, Professor & Head, Dept. of Mech. Engg., CVRCE

Dr. Bipin Bihari Jaysingh, Professor, Dept. of IT, CVRCE

CVR JOURNAL OF SCIENCE & TECHNOLOGY

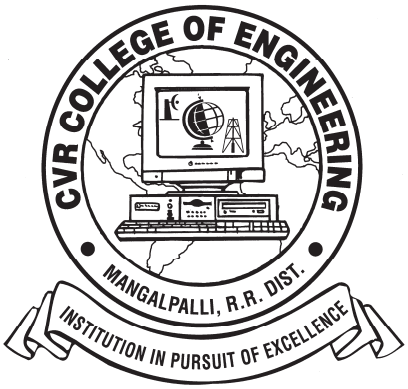

CVR COLLEGE OF ENGINEERING

(An Autonomous College affiliated to JNTU Hyderabad)
Mangalpalli (V), Ibrahimpatan (M),
A.P. – 501510
http://cvr.ac.in

EDITORIAL

We are happy to bring out Volume 4 of CVR Journal of Science and Technology. The breakup of papers in the present Volume from the various departments is:

CSE-2, Civil-1, ECE-6, EIE-2, H&S-4, IT-2, Medical-1

Apart from the technical papers of specialized nature, the current issue contains two papers which are of general interest. One of them is a review article on Environmental Problems in India, coauthored by a Professor from University of Phoenix, USA. The article is highly educative and gives a timely warning on the dangers of environmental pollution caused by lack of proper planning and indiscriminate disturbances to the ecosystem. The second article by the Medical Officer of our College contains valuable information to computer users on the professional hazards likely to be faced by them and on how best to avoid or minimize their impact.

It is gratifying to note the continuing research culture in the college and the interest shown by the staff members in contributing technical papers on the work done by them. It is an established fact that research plays a significant role in academic institutions, with research and teaching complementing each other. Research calls for focus and study in depth while teaching requires breadth of knowledge and general awareness. A balanced admixture of the two is conducive to giving quality education to the students and equipping them for their future career in industry where R&D is gaining increasing importance. Research of an interdisciplinary nature is likely to become more and more prominent, and it will be our endeavor to encourage inclusion of such contributions in our future issues.

I wish to place on record the assistance rendered in various ways by Dr. Bipin Bihari Jaysingh (Professor, IT), Sri Venkateswara Rao (Associate Professor, CSE) and Deepak (Programmer, CSE) in the preparation of the present issue of the journal. I wish to specially thank the members of the Editorial Board for their support.

I look forward to continuing support from the Management and the staff members in bringing out the future issues in tune with changing times.

K.V. Chalapati Rao
Editor

CONTENTS

CVR Journal of Science and Technology, Volume 4, June 2013 ISSN 2277 – 3916

Segmentation Based Image Mining Algorithms for Productivity of E-Cultivation

Dr. Hari Ramakrishna[1] , Ms. A. Kalyani [2] and Ms. M. Kavitha [3]
[1] Professor, Department of CSE, CBIT,Hyderabad, INDIA
Email: dr.hariramakrishna@rediffmail.com
[2,3] Students of Department of CSE, CBIT, Hyderabad, INDIA

***Abstract*— Image Mining techniques are suggested for agriculture for crop quality-evaluation and defect identification. A review of some of the important segmentation based algorithms and recent trends in image processing techniques which are applicable to crop quality evaluation and defect identification is presented. Image segmentation techniques are used for the detection of diseases. This demonstrates the use of the Agriculture information system, E-Cultivation process for increasing the productivity. Sample Results of some of the image segmentation algorithms used for crop disease identification and productivity measurement in E-Cultivation which are obtained using math lab are presented.**

***Index Terms*—e-cultivation, Image mining, Image segmentation, Agricultural framework, Image Segmentation, Math Lab**

I. INTRODUCTION

Countries like India and Srilanka depends more on agriculture. The communication and information technology is focusing more on supports techniques to channelize the modern technology for improving the agricultural domain. Several domains like Agricultural Information systems and Web based Agriculture can be seen in this context.

Intelligent Process Controlling Models are available to monitor any process in a distributed environment. Using Web based technologies, Web mining, Image Mining web based cultivation is possible. The process of cultivation for optimum yield and quality can be achieved with the support of such techniques. Agricultural field need computer based techniques for crop quality evaluation and defect identification. Image mining is one of such techniques suitable for agricultural applications.

For Agricultural field image processing techniques are useful for identifying the quality and defects by using image segmentation techniques. In case of plant the disease is defined as any impairment of normal physiological function of plants, producing characteristic symptoms. The quality can be achieved by segmenting the image of plant. For example, by counting the number of flowers in an image day by day we can identify the production of a flower plant. The main feature of the Agricultural information system is the availability of agricultural information to various users through the Internet.

Image processing, Image segmentation and image mining can be used in agricultural applications for following purposes:

i) To Identify diseased leaf, stem, fruit.
ii) To measure and monitor productivity of crop.
iii) To measure affected area of disease and to advise.
iv) To identify the intensity of diseases on the productivity.
v) To count the number of fruits and flowers etc on plants and trees.

For example we can identify disease of a plant on its leafs and other parts based on the affected area and symptoms. Consider a mango tree we can identify the fruits productivity like number of fruits, size of and quality. A symptom is considered as a phenomenon and evidence of its existence. Automatic detection of plant disease is an evolving research topic useful for e-cultivation. It benefits in monitoring large fields of crops, automatically detecting the symptoms of disease helps in documentation of Agricultural knowledge based in the form of software code and environment.

Generally diseases of a plant will be observed on leaves or stems of the plant. Monitoring such parts of plants plays a major role in successful cultivation. Diseases cause heavy crop losses amounting to several millions and billion dollars annually. Collecting such information from forms along with other attributes of the cultivation environment raise scope to new research problems in the domain of agriculture.78

The objective is to use Information Technology in agriculture, specifically in cultivation for improving the quality of cultivation and productivity useful for countries like Indian. Sample work is presented to find the flowers productivity in plant image and to identify the crop quality and diseases in plants. This is useful for agricultural information system to automate the process of finding the diseases in uploaded images.

II. IMAGE SEGMENTATION

Partitioning the image into different regions depending on domain requirements and given attributes is considered as Image segmentation in Image Processing.

The segmentation considers measurements of other attributes like grey level, color, texture, depth and motion. The final objective is to cluster pixels of image into salient image regions or segments, such as regions of individual surfaces, objects, or natural parts of objects

etc. Such methods can be used in object recognition, occlusion boundary estimation within motion or stereo systems, image compression, image editing, or image database look-up.

The outcome of this process is a set of regions, clusters or segments that cover the total given image, or a set of contours extracted from the image. In a clustered region each pixel is similar with respect to some characteristic like color, intensity, texture. Other regions and adjacent segments are significantly different. For example in Medical images , the resulting contours after image segmentation can be used to create 3D reconstructions based on interpolation algorithms such as Marching cubes.

The Image segmentation is defined as a partitioning of the set F into a set of connected subsets or regions (S1, S2, • • • , Sn) such that [ni=1Si = F with Si \ Sj = _ when i 6= j. The uniformity predicate P(Si) is true for all regions Si and P(Si [Sj) is false when Si is adjacent to Sj.

Where F will be be the set of all pixels and P( ) be a uniformity (homogeneity) predicate defined on groups of connected pixels.

The same definition is used for different types of domains like Medical images, Agricultural images etc. The objective of image segmentation is to locate certain objects of interest which may be depicted in the image. Some tile segmentation can be compares similar to a problem of computer vision.

It can be seen as a process of thresholding a grayscale image with a fixed threshold t where each pixel p will be assigned to one of two classes, P0 or P1, depending on whether I(p) < t or I(p) >= t.

Typical segmentation approaches for intensity images (represented by point-wise intensity levels) are :

i). *Threshold techniques*: Threshold techniques depends on the local pixel information and are effective when the intensity levels of the objects fall squarely outside the range of levels in the background as the spatial information is ignored, but blurred region boundaries can create havoc.

ii). *Edge based methods*: This will work on contour detection and its weakness in connecting together broken contour lines make them, too, prone to failure in the presence of blurring.

iii). *Region-based techniques*: In this method input image is partitioned into connected regions by grouping neighboring pixels of similar intensity levels and adjacent regions are then merged under some criterion involving homogeneity and sharpness of region boundaries.

iv). *Connectivity-preserving relaxation technique:* This is also known as the active contour model.

It will start at initial boundary shape represented in the form of spine curves; it iteratively modifies applying various operations like shrink, expansion as per the some energy function. Coupling it with the maintenance of an "elastic" contour model gives it an interesting new twist; this is a difficult task comparing with other models. Unless handled properly, risk involved in it is more comparing with other models.

Segmentation is classified base on grayscale, texture and motion.

i). Segmentation based on grayscale

ii). Segmentation based on texture

iii). Segmentation based on motion

III. IMAGE SEGMENTATION FOR E-CULTIVATION

Agricultural field need computer based techniques for crop quality evaluation and defect identification. Image mining is one of such techniques suitable for agricultural applications.

Monitoring of the crops for managing the e-cultivation is an important process. Agricultural images are uploaded for monitoring, for e-advisory, for identifying the faulty portions and for measuring the productivity. This will have high impact on the overall productivity of the e-cultivation systems.

The image processing and image mining can be used in agricultural applications for following purposes:

i). Identification of diseased leaf, stem, fruit

ii). Identification and quantification of affected area by disease.

iii). Identification of intensity of diseases and its effect on productivity.

In case of plant the disease is defined as any impairment of normal physiological function of plants, producing characteristic symptoms.

Observing the images of plants, leaves, and stems and finding out the diseases, percentage of the disease plays a key role in successful cultivation of crops. It is helpful in preventing heavy crop losses due to diseases.

E-Cultivation Models

E-Cultivation models are web based agricultural system; Information communications and technology (ICT) are used for agriculture. These models are used for developing new technologies in agriculture field. By using E-Cultivation models agriculture experts can identify the diseases and quality over internet online without visiting the forms physically. This method works on a web based architectural model that creates a agricultural nodal system. Automation of measuring the status of cultivation and collecting requirements are possible through such models. The models used in this work are more suitable for such applications.

IV. DISEASE IDENTIFICATION IN PLANTS USING K-MEANS ALGORITHM

The natural spectral groupings present in a dataset are identified using K-Means clustering. It identifies a fixed number of disjoint, flat or non-hierarchical clusters. It is useful for the globular clusters. The K-Means method is well known for numerical, unsupervised, non-deterministic and iterative.

Properties of K-Means Algorithm

i) K- Clusters which are all non empty that means at least one item in each cluster are required

ii) The behavior of these clusters will be non-overlapping and non-hierarchical.

iii) All members are closer to its respective cluster.

Image Segmentation by clustering

Technique based on clustering like K-Mean can be applied for Image Segmentation. Such techniques are used for clustering the medical and Agricultural images for the identification of defective parts in medical images or required parts in agricultural images. In agricultural images there is a need to identify and measure defective part as well as required regions like fruits and flowers etc.

Color-Based Segmentation

In this model the process is automated to segment colors using the L*a*b* color space. We apply the K-means clustering method for this clustering. The following steps describe this process of clustering:

Step 1: Read and formalize Image
Step 2: Colour Recognition and formatting
Step 3: Image K Means classification
Step 4: Labelling identified section
Step 5: Rebuilding image
Step 6: Finding specified Sections

V. IDENTIFYING THE FLOWERS IN A PLANT

The objective of the work is to detect the flower region and regions of interest (ROIs) from the agricultural image. The process involved in the extraction of flowers region from image is described in the following steps:

i) Original image
ii) Bit plane slicing
iii) Erosion
iv) Median Filter
v) Dilation
vi) Outlining
vii) Flowers Border Extraction
viii) Flood Fill Algorithm
ix) Flowers Extracted Image

The image processing methodologies used in these models are Bit-Plane Slicing, Erosion, Median Filter, Dilation, Outlining, flower Border Extraction and Flood-Fill algorithms.

The first step is applying bit plane slicing algorithm to the scan image. The different binary slices are resulted from this algorithm. The best suitable slice applied for better accuracy, sharpness and the further enhancement of flower region.

As a next step the Erosion algorithm is applied to enhances on the sliced image for reducing the noise. The dilation and median filters are also used for further improvement for filtering other type of distortion. Outlining algorithm used to find the outline of the regions after obtained noise reduced images. The flower border extraction technique is applied to find the flower border region. Flood fill algorithm is used to fill flower border with the flower region. Finally the flower region will be extracted. This flower region can be used for segmentation for the identification of flowers. Unlike Medical images lot of customization is required on these methods if applied on different types of plants as attributes and requirements change from case to case.

The result obtained is presented as sequences of figures:

Original flowers image

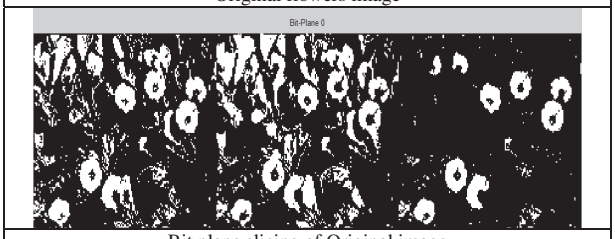

Bit plane slicing of Original image

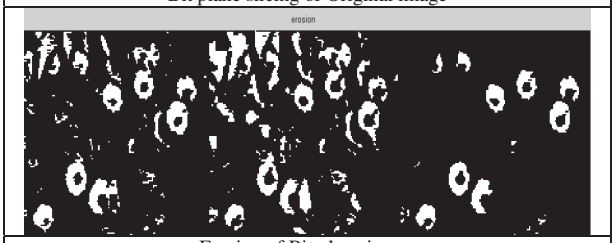

Erosion of Bit plane image

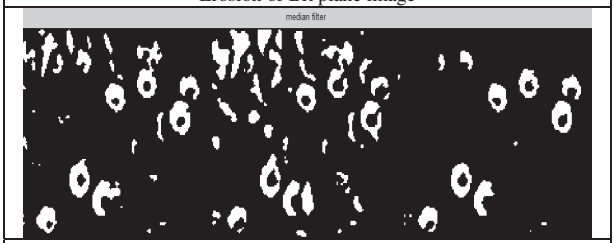

Median filtered image

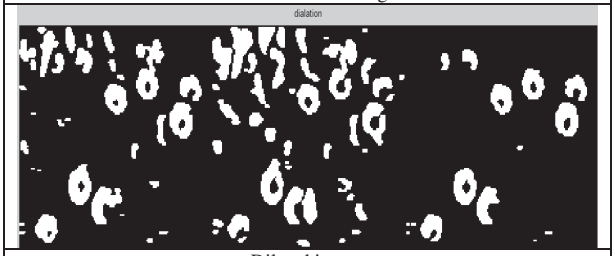

Dilated image

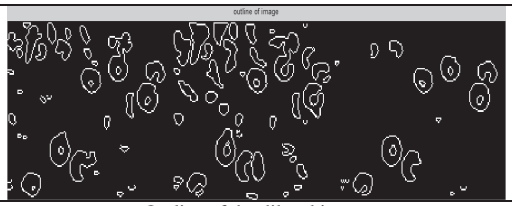

Outline of the dilated image

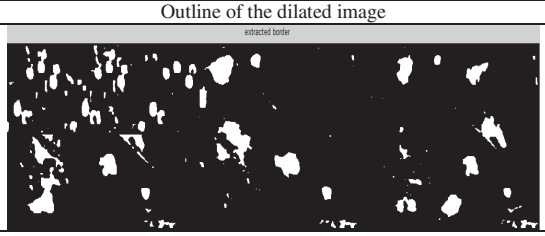

Extraction of border

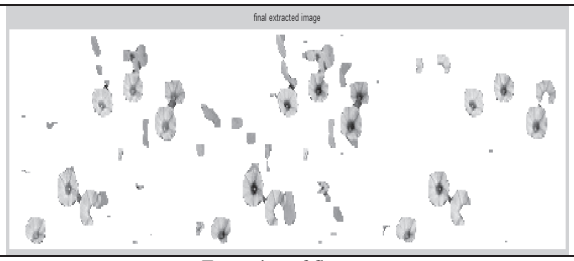

Extraction of flowers

VI. IDENTIFYING DEFECTIVE SEGMENTS

Identifying the defective segments for measuring the quality and productivity of plant can be obtained in a similar methodology. Result of Mat lab code for the processes is presented in the following figures. Similar things can be applied on quality of vegetables.

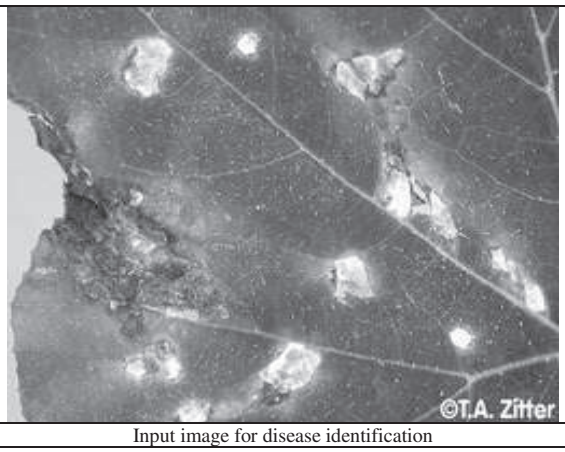

Input image for disease identification

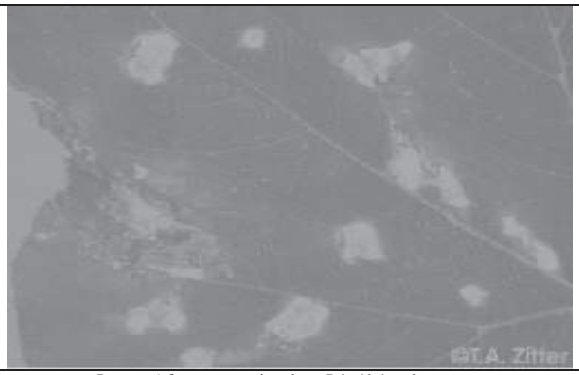

Image After converting into L*a*b* color space

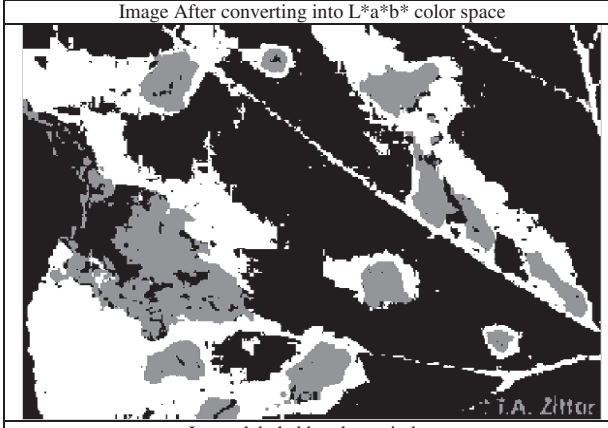

Image labeled by cluster index

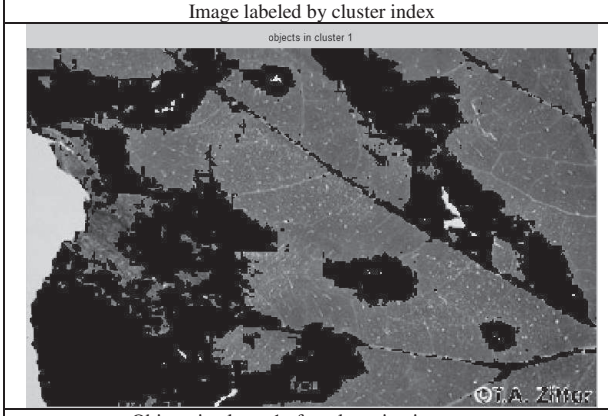

Objects in cluster1 after clustering image

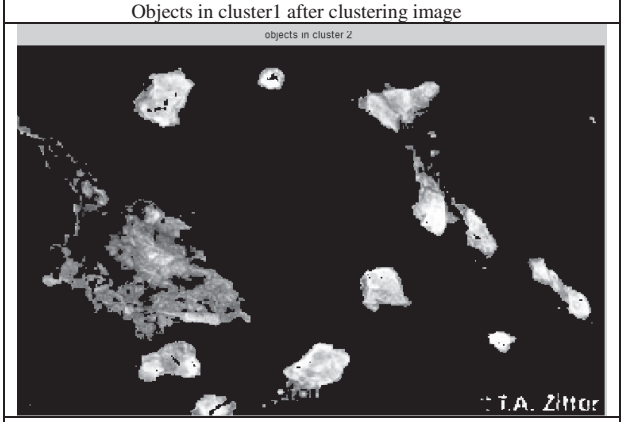

Objects in cluster2 after clustering image

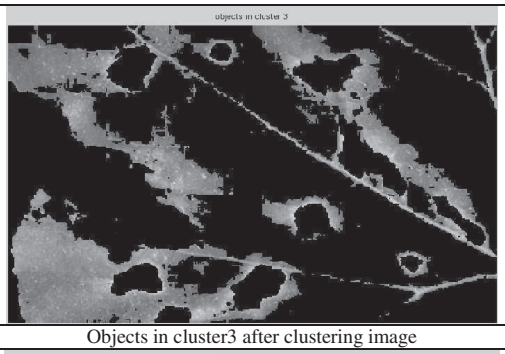

Objects in cluster3 after clustering image

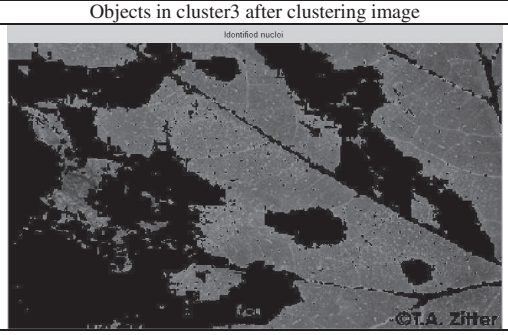

Identified specified nuclei in image

CONCLUSIONS

The main objective of the paper is to use different image mining techniques like K-means Clustering algorithm in image segmentation techniques for e-cultivation requirements. Unlike medical images e-Cultivation raises several different types of challenges as the type of requirements and attributes change from case to case. A lot of customization of image segmentation and other algorithms are required for each case. This will raise scope for lot of research in this domain.

The model presented as sample in this paper can be extended to problems like count the number of flowers in images. Such techniques can be applied on satellite images also to monitor the cultivation process in spatial domain. The model presented is objected to small image samples of e-cultivation nodal system for evaluation of crop quality and productivity useful for e-cultivation advisory models.

ACKNOWLEDGMENT

The authors Dr.Hari Ramakrishna and his students Ms. A.KALYANI and Ms. M.KAVITHA wish to thank the faculty of Department of CSE-CBIT for their support and motivation for the work.

REFERENCES

[1] H. Al-Hiary, S. Bani-Ahmad, M. Reyalat, M. Braik and Z. ALRahamneh "Fast and Accurate Detection and Classification of Plant Diseases", International Journal of Computer Applications (0975 – 8887) Volume 17– No.1, March 2011

[2] Yu-Hsiang Wang "Tutorial:Image Segmentation" Graduate Institute of communication Engineering, National Tiwan University.

[3] Dr.Hari Ramakrishna,T.S.Praveena, Prof. N.Rama Devi "SEGMENTATION BASED IMAGE MINING FOR AGRICULTURE" International Journal of Engineering Research and Technology Vol. 1 (02), 2012, ISSN 2278 – 0181.

[4] http://www.wikipedia.com/image segmentation applications

[5] O.N.N. Fernando and G.N. Wikramanayake"Web Based Agriculture Information System"submitted in University of Colombo.

[6] Schmid, P.: Image segmentation by color clustering, http://www.schmid-saugeon.ch/publications.html, 2001

[7] http://www.cs.ioc.ee/~khoros2/one-oper/bit-slice/front-page.html

[8] http://www.pages.drexel.edu/~weg22/edge.html

[9] http://www.eng.auburn.edu/users/jzd0009/matlab/doc/help/toolbox/images/imclearborder.htm

[10] http://en.wikipedia.org/wiki/Flood_fill

A Model for Safety-Critical Real-Time Systems by making use of Architectural Design Patterns

U.V.R. Sarma[1], Sahith Rampelli[2] and Dr. P. Premchand[3]

[1]CVR College of Engineering, Department of CSE, Ibrahimpatan(M), R.R. District, A.P., India
Email: sarmauvr@yahoo.co.in
[2] CVR College of Engineering, Department of CSE, Ibrahimpatan(M), R.R. District, A.P., India
Email: sahith.indian@gmail.com
[3]Osmania University, Department of CSE, Hyderabad, A.P., India
Email: p.premchand@uceou.edu

***Abstract*—Design Patterns, which give abstract solutions to commonly recurring design problems, have been widely used in the Software and Hardware domain. This paper presents the principles of Architectural & Design patterns for Real-Time Software Systems. For the successful application of design patterns for Safety-Critical Real-Time systems, an integration of a number of architectural design patterns is desirable. For this reason, a pattern catalog is constructed that classifies commonly used Hardware and Software design methods. Moreover, it is intended to construct the catalog such that an automatic recommendation of suitable design patterns for a given software application can be made. The paper focuses on reliability patterns and studies the impact of the patterns on the QoS. To support the designers, a tool is developed to suggest the patterns that are appropriate for the software based on the characteristics of the problem. This tool will be able to help generate the code template for the selected design pattern.**

***Index Terms*— Design Pattern, Real-Time Systems, Non-Functional Requirements, Safety-Critical Systems.**

I. INTRODUCTION

Over the last few years, Real-Time systems have been increasingly used in safety-critical applications where failure can have serious problems. Designing of Real-Time systems is a complex process, which requires the assimilation of common design methods both in hardware and software to implement functional and non-functional requirements for these safety-critical applications.

Design patterns provide abstract solutions to commonly recurring design problems in the software and hardware domain. In this paper, the concept of design patterns is adopted in the design of safety-critical real-time system. A catalog of design patterns is constructed to support the design of real-time systems. The proposed catalog contains a set of software and hardware design patterns to cover frequent design problems such as handling of random and systematic faults and safety monitoring, Furthermore, the catalog provides a decision support component that supports the decision process of choosing a suitable pattern for a particular problem based on the available resources and the requirements of the applicable patterns. The Proposed Tool Provides the Code Template for the selected pattern.

Bruce Douglass proposed several design patterns for the Safety-Critical Real-Time applications based on the well-known design methods. The UML (*Unified Modeling Language*) provides a notation for design patterns but this notation is targeted primarily towards mechanistic design patterns. In this proposed paper, we are not discussing the Design patterns in a detailed way in order to limit its size.

II. DESIGN PATTERN TEMPLATE

In this section, we proposed a Design Pattern Template to represent the well-known design patterns for Safety-Critical Real-Time Software applications. As shown in Figure 1, the upper part of the template includes the traditional representation of a design pattern and also listing of the pattern implications on the non-functional requirements. Moreover, further support is given by stating implementation issues, summarizing the consequences, side effects, related patterns and Code Template as well.

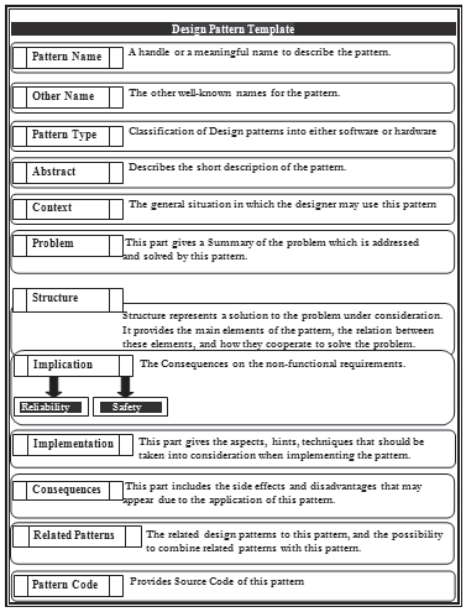

Figure 1: Design Pattern Template

The proposed design template includes a part for pattern implication on the non-functional requirements such as reliability and safety. In order to add these side effects into the pattern concept, we propose an extended template for an effective design pattern representation for Safety-Critical Real-Time applications.

Section III describes the Architecture of the proposed Model. Section IV provides the implementation details. Section V deals with the Code generation part.

Types of Architectural Design Patterns

Hardware Patterns*:* It includes the patterns that contain explicit hardware redundancy to improve either reliability or safety. This group contains the following 8 patterns:

- Triple Modular Redundancy Pattern.
- Homogeneous Redundancy Pattern.
- Heterogeneous Redundancy Pattern.
- M-Out-Of-N Pattern.
- Monitor-Actuator Pattern.
- Sanity Check Pattern.
- Watchdog Pattern.
- Safety Executive Pattern.

Software Patterns

- N-Version Programming Pattern.
- Recovery Block Pattern.
- Acceptance Voting Pattern.
- N-Self Checking Programming Pattern.
- Recovery Block with Backup Voting Pattern

Triple Modular Redundancy Pattern (TMR)

Let us consider the "Triple Modular Redundancy Pattern" and then generate the code template using our proposed tool.

Type: Hardware

1)*Pattern Name*:Triple Modular Redundancy Pattern (TMR)

2) *Other Name*:2-oo-3 Redundancy Pattern, Homogeneous Triplex Pattern.

3) *Abstract*: The TMR pattern operates three channels in parallel rather than operating a single channel and switching over to an alternative when a fault is detected. By operating the channels in parallel, the TMR pattern detects random faults.

The TMR pattern runs the channels in parallel and at the end compares the results of the computational channels together. As long as two channels agree on the output, then any deviating computation of the third channel is discarded. This allows the system to operate in the presence of a fault and continue to provide functionality.

*4) Context:*The TMR pattern offers an odd number channels that are operating in parallel, and this pattern is used to enhance reliability and safety in real-time applications where there is no fail-safe state.

5) *Problem*: TMR pattern provides protection against random faults.

6) *Implication:* To enhance reliability and safety.

7) *Implementation:* The development of the TMR pattern is common to replicate the hardware and software to avoid common mode faults so that each channel uses its own memory, CPU and so on.

8) *Consequences:* The TMR Pattern can only detect random faults. High recurring cost because the hardware and software in the channels must be replicated. The TMR pattern is a common one in applications where reliability needs are very high and worth the additional cost to replicate the channels.

9)*Related Patterns:* Heterogeneous redundancy, Homogeneous Redundancy Pattern.

Following Figure 2 details about TMR pattern implementation in UML and sample code in Java.

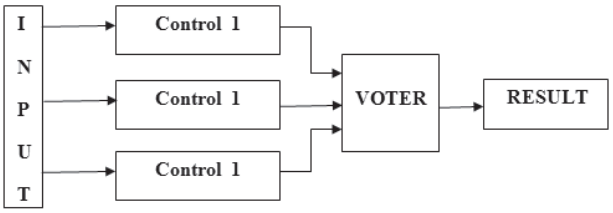

Figure 2: TMR Pattern

The class diagram is given as Figure 3 below.

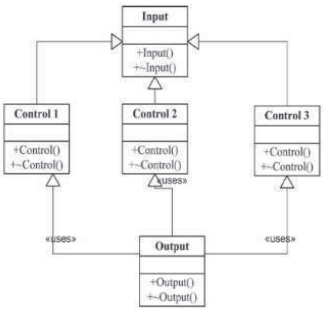

Figure 3: UML - Class Diagram Representation for TMR Pattern

III. ARCHITECTURE

This section describes the architecture that will be used to develop the catalog program. To implement the required features for the current catalog, the software is divided into a set of modules where each module is implemented in a package.

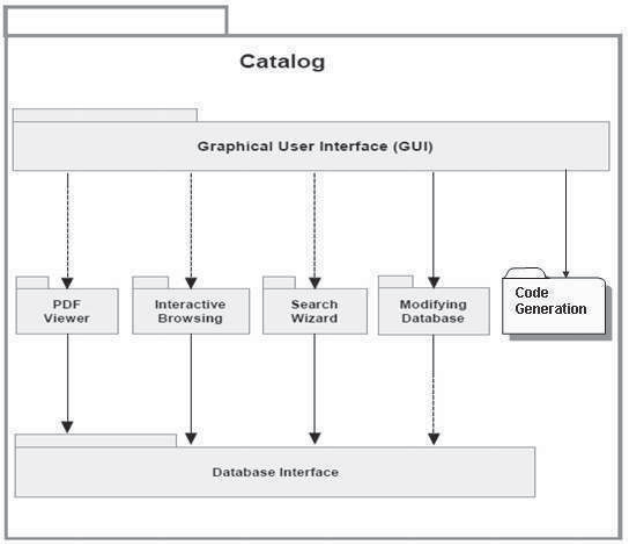

Figure 4: The architecture of the Catalog software

The Graphical User Interface (GUI) represents an intermediate connection between the user and the other modules. It handles the interaction with the user and the application. For example, the interactive browsing interface provides a graphical display for the pattern structure and the ability to navigate the different components, while the PDF Viewer includes a plug-in to display the PDF files.

The PDF Viewer provides a list of PDF files for the available patterns, divided into three groups. Furthermore, it has been implemented using a PDF plug-in, which gives users the ability to browse, save, and print the patterns similar to the original Adobe Acrobat Reader software.

The interactive browsing module provides the second method for pattern presentation. It includes a selective navigation of the contents of the pattern. This feature gives users the ability to select, retrieve, and copy complete information about any part of the selected pattern.

The search wizard module includes the decision support feature provided by this tool. It gives users the ability to find a suitable pattern or a combination of patterns for the desired application by answering questions in an oriented step by step wizard.

This module serves two purposes. First, it allows users to modify the catalog contents, such as the fields of the patterns, solutions, decision points (requirements), problems and decision trees. Second, it provides the functionality to add new elements to the database such as creating a new pattern, a new solution, or a new decision tree. These two features offer an easy way to modify and extend the current catalog.

IV. Implementation

A. Presentation Layer

The presentation layer allows querying the Database for editing the design patterns and updating the catalog, connecting with the Database locally through JDBC. Sophisticated interface is provided for the administrators and end user. The proposed application provides assistance to developers and other functionalities dealing with object-oriented framework such as UML representation and code generation for the design patterns. The user interface is a stand-alone application. The following Fig 4 shows an interface for the management of the Design Patterns Catalog. Users can browse the list of patterns. Advanced users may add new patterns.

Figure 5: Interface for Design Pattern Catalog

Here, we believe that modeling of Architectural Design Patterns should be standardized to meet the needs of developers. Our proposed application can generate class diagrams for the specified design pattern and thereby generate the source code for Architectural Design Pattern.

B. The Design Pattern Search Wizard and other screens

We collect a set of criteria from the description of Design Patterns and classify by their applicability. In order to extract Patterns from the Database, we opted for a categorization of design patterns. This is mainly restricted to the applicability part of Design Patterns and can easily be extended to cover other literal description parts. The set of criteria and the corresponding keywords database must be thinking out for the related patterns. Our proposed tool provides the end-user with a comprehensive list of keywords, that we have collected, to be used automatically and the tool will help end-users to choose the appropriate Design Patterns.

The Java based search wizard enables the effective search and the selection of suitable Design Patterns with respect to the situations in which to use the desired Design Pattern.

*Filtering:*The first constraint involves the selection of keywords that match the scope of the user query. The search operation intends filtering and refining of the user's ideas in order to reduce the search scope and have closer results to the desired Patterns.

Second constraint, the program will suggest a list of all the situations matching the selected keyword. The user is required to read the criteria and select those that best describe the situations he queries for. By checking appropriate statements the user is ready to generate the suitable Design Patterns.

The following figure 6 is the Design Pattern search wizard interface.

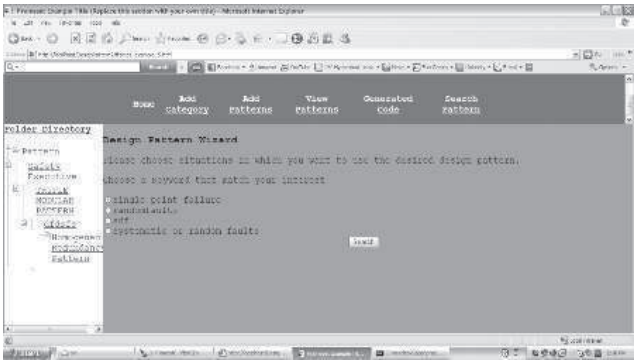

Figure 6: Design Pattern Search Wizard interface

This is how the login page will look like, as shown in figure 7.

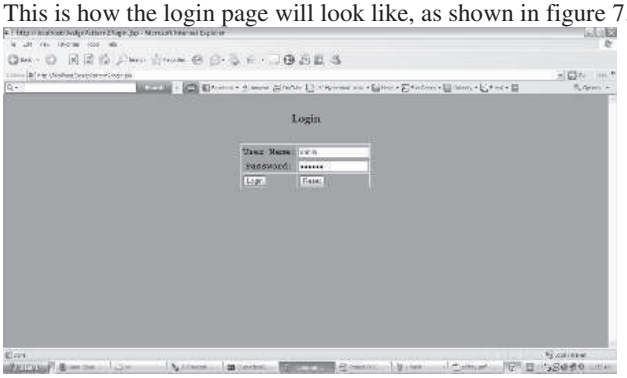

Figure 7: Login Page.

The users can also register; the "PDF conversion" page as given in figure 8.

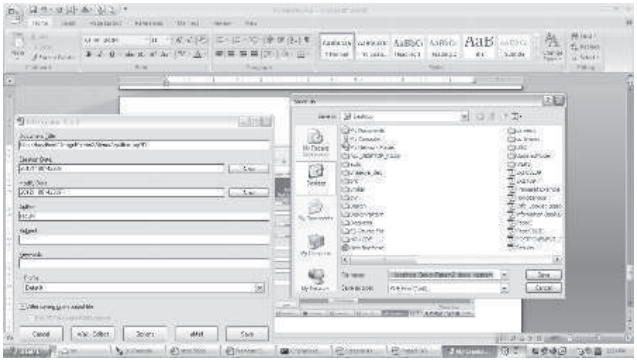

Figure 8: PDF Conversion

The home screen of the Admin is given in figure 9.

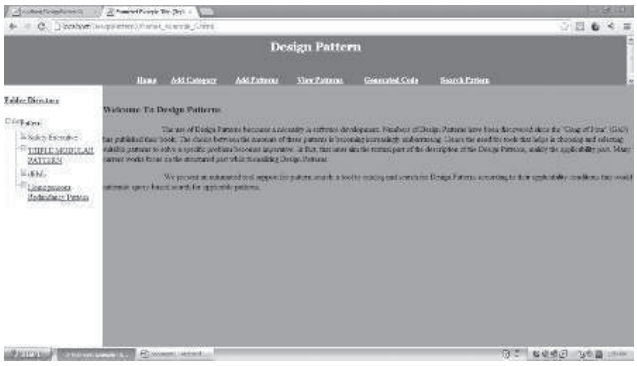

Figure 9: Home Admin

Code generation output screens are given in the following figures 10. The code is generated using the tool.

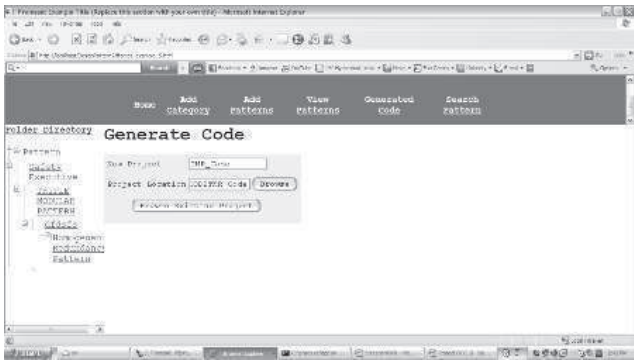

Figure 10: Code Generation

As specified in figure 10, we can give the class details; attribute details and operation details in the tool.

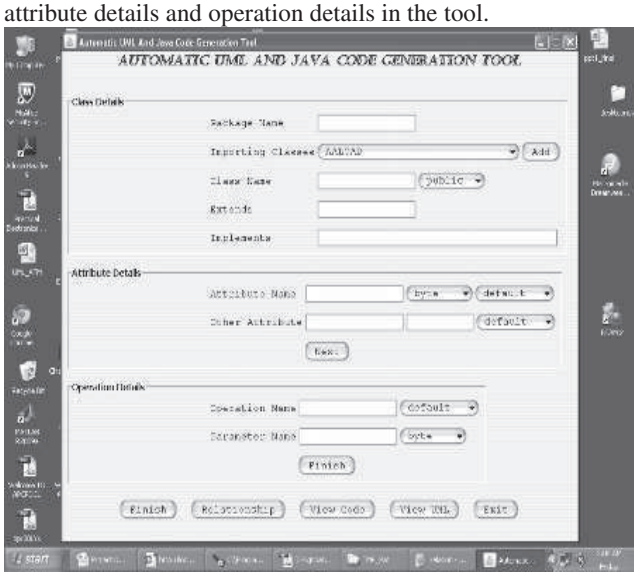

Figure 11: Automatic UML and JAVA Code generation tool.

C. Relationship

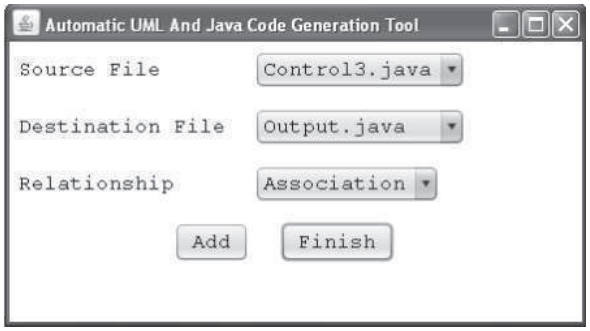

Figure 12: Relationships within Classes

The above Figure 12 allows the user to maintain the relationships with the given classes.

Source Class and Destination class are selected along with the Relationship (i.e., Association, Aggregation and Generalization etc).

V. CODE GENERATION FOR TRIPLE MODULAR REDUNDANCY(TMR) PATTERN

Fig. 13 is the UML diagram for the TMR pattern. In Fig 14 View Code, the Java file is selected to view the Java Code, which consists of Classes, Attributes and Methods. Skeleton Code will be provided to the user and can be customized/enhanced in future as per the requirements.

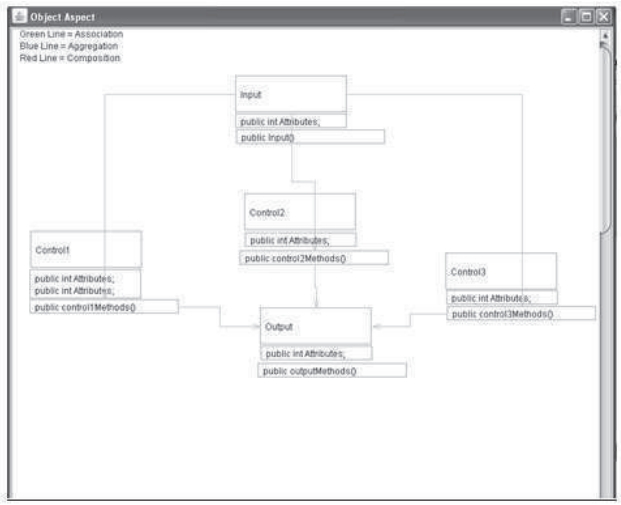

Figure 13: UML diagram for TMR Pattern using Proposed Tool.

Figure 14: View Pattern Code

The following figures Figure 15, 16, 17 and 18 provide the Skeleton Code (Code Template) for the TMR Pattern.

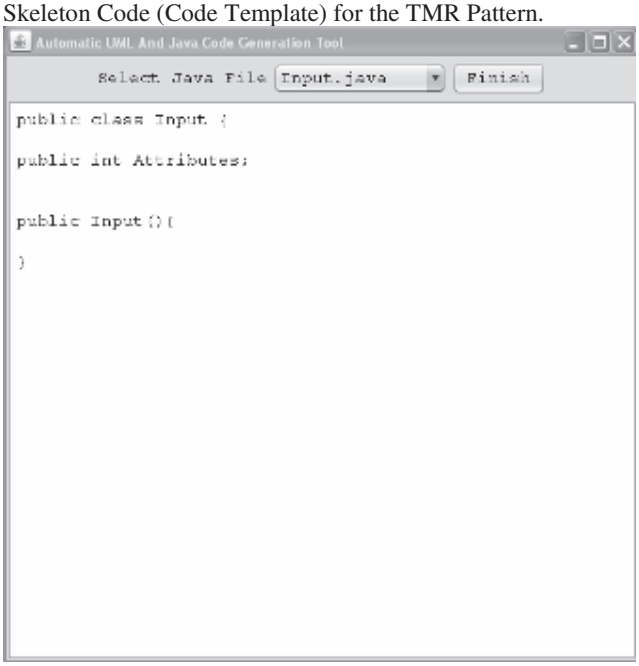

Figure 15: Code Template for TMR Pattern

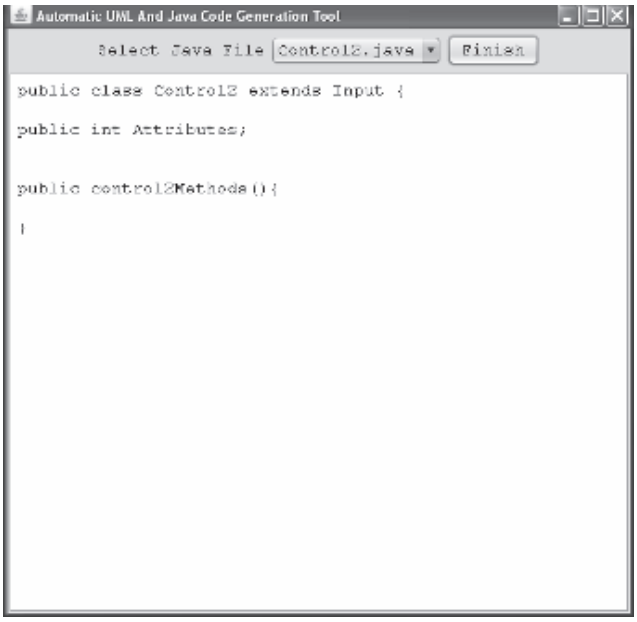

Figure 16: Code Template for TMR Pattern

Figure 17: Code Template for TMR Pattern

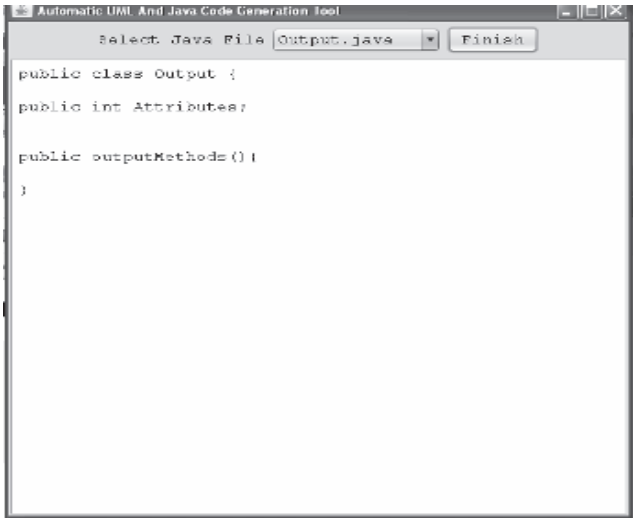

Figure 18: Code Template for TMR Pattern

View UML link will provide the UML Diagram.

VI. CONCLUSION

Integration of design patterns is desirable for the successful development of the real-time applications. In order to achieve a successful application, we presently constructed a Design Pattern catalog, where we maintain a collection of design patterns that are commonly used in hardware and software domain. Moreover, the constructed catalog provides an automatic recommendation of suitable design method for a given application.

In order to support the designers, we proposed a tool that suggests a suitable design pattern based on the software characteristics. This tool will be helpful in generating the source code for the suitable design pattern.

VII. FUTURE ENHANCEMENTS

The work presented in this paper introduces some possible directions for future work. This catalog can be extended to include other design techniques that address the design problems for Safety-Critical Real-Time systems.

The Simulation module can be developed. Therefore, the construction of a comprehensive simulator that provides reliability and safety simulation for all design patterns would be desirable and useful for comparison and assessment.

ACKNOWLEDGMENT

The authors would like to thank the student Mr. Datta Virivinti of B. Tech. (IT), CVR College of Engineering, for his contribution in developing the interface. The authors would also like to thank the college for providing its amenities.

REFERENCES

[1] Design Pattern Representation for Safety-Critical Embedded Systems, Ashraf Armoush, Falk Salewski, Stefan Kowalewski,2009.

[2] Design Patterns for Safety-Critical Embedded System, Ashraf Armoush, 2010.

[3] Design patterns to implement safety and Fault Tolerance, Hemangi Gawand, R.S,Mundada, P.Swaminathn, International Journal of Computer Applications(0975 – 8887), Volume 18-No. 2, March 2011.

[4] Application-Level Fault Tolerance in Real-time Embedded Systems, Francisco Afonso, 2008.

[5] Design Patterns: Element of Reusable Object-Oriented Software by Erich Gamma, Richard Helm, Ralph Johnson and John Vlissides, 2012.

[6] http://www.patternrepository.com

[7] Real-Time Software Design Patterns, Janusz ZALEWSKI.

[8] Pattern-Based Architectures Analysis and Design of Embedded Software Product Lines, Public version,EMPRESS,2003.

[9] Modeling Real-Time applications with Reusable Design Patterns, Saoussen Rekhis, Nadia Bouassida,Rafik Bouaziz MIRACL-ISIMS, Vol. 22, September, 2010.

[10] A. Armoush, E. Beckschulze, and S. Kowalewski. Safety assessment of design patterns for safety-critical embedded systems. In 35th Euromicro Conference on Software Engineering and Advanced Applications (SEAA 2009). IEEE CS, Aug. 2009

Traffic Noise Study on Muzaffarnagar Byepass

S. Praveen[1] and Dr. S.S. Jain[2]
[1] CVR College of Engineering, Civil Engineering Department, Ibrahimpatan, R.R.District, A.P, India
Email: samarthipraveen@gmail.com
[2] Professor, Indian Institute of Technology Roorkee, Civil Engineering Department, Roorkee, Uttarakhand, India
Email: ssjanfce@iitr.er.net

Abstract— **Noise Pollution has become a major concern to planners, regulatory agencies affecting individuals and communities. Most of the countries, keeping in view the alarming increase in environmental noise pollution has set permissible noise standards. Road surface, speed of the traffic, gradient of the road, traffic flow etc. are the different factors affecting noise level on a highway. The Bureau of Indian Standards (BIS) has recommended an acceptable noise level of 25-35 dB (A) for non-Urban areas. A number of noise predicting models have been developed over the past 30 years that attempted to model the highway conditions under study. Useful correlations has been found to exist between traffic parameters like traffic volume, average speed of traffic stream and noise parameters like Equivalent sound energy level (Leq) in the locations. With the help of these correlations, it is possible to predict the impact of traffic developments in terms of noise pollution in future.**

Index Terms— **Noise pollution, Traffic Speed, Traffic flow and Models**

I. INTRODUCTION

Noise is defined as unwanted sound. Sound is produced by the vibration of sound pressure waves in the air. Sound pressure levels are used to measure the intensity of sound and are described in terms of decibels. The decibel (dB) is a logarithmic unit which expresses the ratio of the sound pressure level being measured to a standard reference level. Sound is composed of various frequencies, but the human ear does not respond to all frequencies.

Frequencies to which the human ear does not respond must be filtered out when measuring highway noise levels. Sound-level meters are usually equipped with weighting circuits which filter out selected frequencies.

It has been found that the A-scale on a sound-level meter best approximates the frequency response of the human ear. Sound pressure levels measured on the A-scale of a sound meter are abbreviated dB (A). Noise is unacceptable and causes trouble to human beings. Noise pollution has become a major concern of communities living in the vicinity of major highway corridors. The exposure of noise from highways affects more people than noise from any other source. Several federal and State agencies have implemented regulations that specify procedures to conduct noise studies. These regulations have led to the advancement of computerized method for predicting highway noise. In general noise has three sources

i. Operational noise from transportation system
ii. Occupational or Industrial Noise
iii. Community Background Noise.

Among these operational noises from transportation system alone contribute about 70% of total noise whereas road traffic noise is responsible for 55% of total noise.

Sound intensity decreases in proportion with the square of the distance from the source. Generally, sound levels for a point source will decrease by 6 dB (A) for each doubling of distance. Sound levels for a highway line source vary differently with distance, because sound pressure waves are propagated all along the line and overlap at the point of measurement. A long closely spaced continuous line of vehicles along a roadway becomes a line source and produces a 3 dB (A) decrease in sound level for each doubling of distance. However, experimental evidence has shown that where sound from a highway propagates close to "soft" ground (e.g., plowed farmland, grass, crops, etc.), the most suitable drop off rate to use is not 3 dB (A) but rather 4.5 dB (A) per distance doubling. This 4.5 dB (A) drop off rate is usually used in traffic noise analyses.

For the purpose of highway traffic noise analyses, motor vehicles fall into one of three categories:

i. Automobiles -vehicles with two axles and four wheels,
ii. Medium trucks - vehicles with two axles and six wheels, and
iii. Heavy trucks - vehicles with three or more axles

The emission levels of all three vehicle types increase as a function of the logarithm of their speed.

The level of highway traffic noise depends on three things:

a. The volume of the traffic,
b. The speed of the traffic, and
c. The number of trucks in the flow of the traffic.

Generally, the loudness of traffic noise is increased by heavier traffic volumes, higher speeds, and greater numbers of trucks. Vehicle noise is a combination of the noises produced by the engine, exhaust, and tyres. The simulation techniques for unrestricted traffic in urban situations and Sabir (1988) conducted noise level survey for community noise & peak noise emission. The survey was conducted at six sites in the eastern province of Saudi Arabia and two sites in New Delhi, India.

II. METHODOLOGY

To determine noise studies some of the organization like CPCB (situated in New Delhi), CRRI, Delhi traffic

police, Delhi administration and Centre of transportation Engineering (COTE), Roorkee have conducted a number of traffic flow noise pollution studies at selected mid block and important highway intersection in Delhi. Most of the studies were confined to only evaluating the noise pollution.

Kumar, Mehndiratta and Sikdar in 1993 studied the variation in noise pollution for buses running in different gears. The noise pollution data were recorded inside the running bus and trucks near the driver seat (near engine), in the middle of the bus and on the back seat of bus. Various correlations between the engine gear vehicle speed and noise parameter have been developed.

Gupta, Khanna and Gangil (1979) attempted to develop relationship between the vehicular noise and strem flow parameters. The Uttarakhand state highway No.45 passing through Roorkee was selected as the study area between Polaris intersection to Roorkee Talkies inter-section. The developed prediction equation for the noise level L_{10} is given below.

$$L_{10} = 18.092433 + 19.90357 * \log_{10}(Q_w) \quad dB(A) \qquad (1)$$

Where Q_W = Traffic volume in EPCU/hr.

In the present study, 117th km on NH58, Muzaffarnagar Byepass Road was selected for field studies. The data collection was carried out in two locations L1 and L2 respectively.L1 indicates Delhi to Roorkee road and L2 indicates Roorkee to Delhi road at Muzaffarnagar Byepass.

At the site the following data have been collected:

1. Traffic Noise Levels
2. Classified Traffic Volume
3. Speed

Individual vehicle noise levels were taken and classified in to different categories.

1. Car, Jeep, Van
2. Scooter, Motor cycle (2-Wheeler)
3. Bus,
4. Truck
5. 3-Wheelers

III. STUDY AREA

The traffic study area considered was 117th km Road, NH58, Muzaffarnagar Byepass Road in Uttarkhand state. Data has been collected for traffic noise levels for different category of vehicles, spot speed and traffic volume simultaneously. The locations that were considered are Delhi-Roorkee Road (L1) and Roorkee-Delhi Road (L2). Traffic sample data was collected for one hour duration at three points which are away from the pavement edge (namely S1, S2, S3).Details of different measurements carried were given below.

A. Noise level

To record the traffic noise levels, noise level meter no. NL 2100B was used. It was placed at a specified distance from the pavement edge and at a height of 1.2m from the ground level. Its microphone was placed right angle to the direction of traffic flow.

A noise sample size of 15 minute in each hour at a particular selected distance from the edge pavement was taken. Noise samples were collected in dB(A) scale at every 15 second interval (i.e. 4 counts per minute) or total 40 reading in one sample size.

For every noise sample, cumulative frequency data has been calculated. Similarly for both locations computations are shown in figure 1 and figure 2.

B. Traffic Volume

In India most commonly used method for traffic volume is the manual method for a shorter duration (up to 24 hrs) volume counts. The details such as vehicle classification and number of occupants can easily be obtained in manual method. Sometimes, when traffic volume is very high and manually it is not possible to record it more accurately time-lapse photographic technique (TLP) or VRT is employed.

In the present studies, it has been done through manual counts.

At the two selected study locations (L1 & L2) one hour classified traffic volume data were recorded, in a predesigned , hourly traffic volume recording proforma which are subdivided in 5 minute time interval columns.

For this purpose , four semi skilled persons were employed i.e. two in each direction.

C. Spot speed measurements

A Doppler speedometer was used for measuring the spot speeds in KMPH. Speed for all the categories of the vehicles were recorded in a predesigned proforma for hourly duration, which is sub-divided in to 5 minute interval columns.

To facilitate the computations, the first step in the analysis of the observed speed data of whole traffic stream was grouped into speed-class intervals and a frequency distribution table was prepared for every hourly observed spot speed data, at all study locations.

For each Location frequency distribution table has been prepared similar to location 1(Roorkee to Delhi) and Location 2 (Delhi to Roorkee).

IV. OBSERVATIONS, RESULTS AND DISCUSSIONS

A. General

The observations, analysis and discussions upon computations of noise, volume and Speed Data are presented. The traffic parameters such as Passenger Car Noise Equivalence (PCNE) have been calculated from the computations.

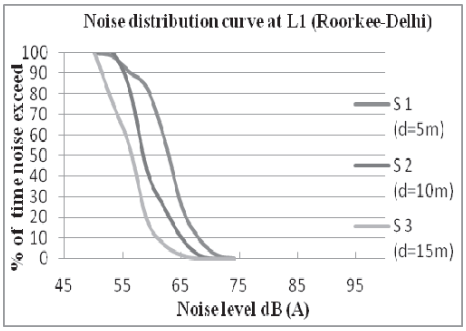

Figure 1 Noise Level Distribution Curve at L1

Location: 117th km Road, NH58, Muzaffarnagar Bye pass,

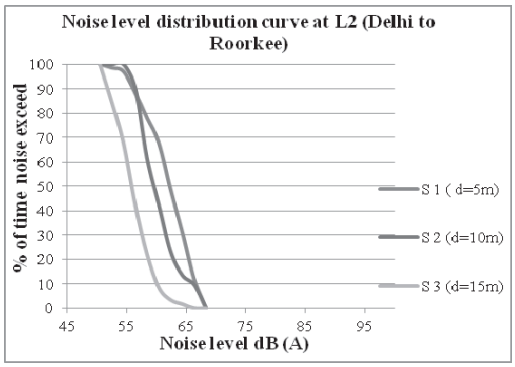

Figure 2 Noise Level Distribution Curve at L2

Location: 117th km Road, NH58, Muzaffarnagar Bye pass,

Note: S1,S2 and S3 are the samples , distance away from the pavement at 5m,10m and 15m respectively.L1 is location of Roorkee-Delhi route. L2 is location of Delhi-Roorkee route.

Interpretation of Results and Discussions:

The work consists of an exclusive study of traffic noise on a two way, two lane rural highway of Muzaffarnagar Byepass road. As observed from the analysis, the noise observed on 3 sample points that were taken on both locations show high noise levels than the permissible limit of rural highways. As according to BIS the acceptable noise level of 25-35 db(A) for non-Urban areas.

B. Determination of Speed Distribution Curve

Speed distribution curve has drawn for each sample and their fifty percentile speed has been calculated and presented.

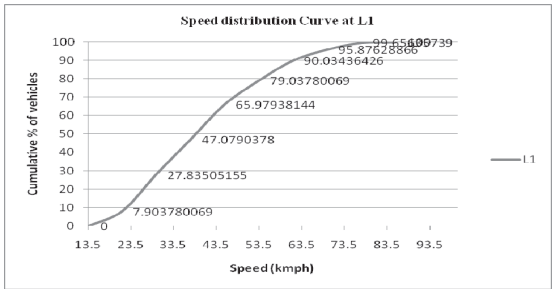

Figure 3 Cumulative Speed Distribution Curve at L1 (Delhi-Roorkee Road)

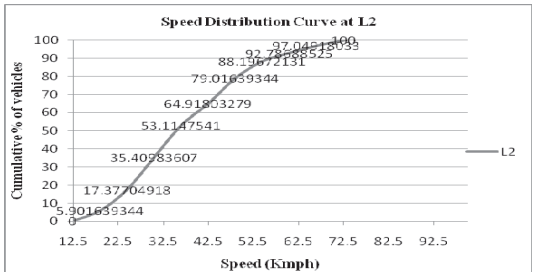

Figure 4 Cumulative Speed Distribution Curve at L2 (Roorkee-Delhi Road)

C. Determination of Passenger car noise equivalence (PCNE)

It is defined as that no. of free flowing passenger cars under standard traffic flowing passenger cars under standard traffic flow conditions which generate noise level equal to that of particular category of vehicle. The PCNE for any particular type of vehicle whose noise levels is L_T dB (A) is given by

$$n = 10^{(L_T - L_C)/10} \quad (2)$$

Where L_T is noise level of the vehicle, L_C is noise level of car.

The Cumulative Noise Distribution for Different category of Vehicles for PCNEs are calculated.

TABLE 2
Determination of 50 Percentile Noise levels

Category of Vehicles	Bus	Truck	Car	2-wheelers	3-wheelers
50 Percentile Noise level dB (A) (L_T)	87.5	82	79	80	68

PCNE of Bus

$$n = 10^{(L_T - L_C)/10}$$
$$= 10^{(87.5-79)/10} = 7.08$$

Similarly, PCNE of Traffic Stream are calculated as follows:

TABLE 3
Determination of PCNE for different category of vehicles.

Category of Vehicles	Bus	Truck	2-wheelers	3-wheelers
PCNE	7.08	2.00	1.26	0.08

TABLE 4
Determination of Noise levels

Location Code	Noise Parameters dB(A)	S1 (d = 5m)	S2 (d =10m)	S3 (d =15m)
L1 (Delhi-Roorkee)	Leq TNI LNP	57.14 54 65.14	61.11 64.5 70.61	64.66 70 75.66
L2 (Roorkee-Delhi)	Leq TNI LNP	59.44 59 68.44	61.61 65 71.11	66.86 74 78.36
Location Code	Percentile Levels	S1 (d = 5m)	S2 (d = 10m)	S3 (d = 15m)
L1 (Delhi-Roorkee)	L10 L50 L90	60 56 52	66 59.5 56.5	67 62.5 56
L2 (Roorkee-Delhi)	L10 L50 L90	62 58 53	66.5 60 57	69.5 64.5 58

TABLE 5
FHWA Noise Standards

Land Use	Design Noise Level L_{10}	Description of Land Use Category
A	60dB(A) (exterior limit)	For parks and open spaces where quietness is of primary importance
B	70 dB (A) (exterior limit)	Residential areas Hotels, Schools, Churches, Libraries, Hospitals etc.
C	75 dB(A)	Developed areas
D	55 dB(A) (interior limit)	Residential areas, Hotels, Libararies

F. Relation Between Noise and Volume

The correlation between volume and noise is found by plotting the values of Noise, Leq in dB(A) on Y-axis and Volume in EPCNE/hr in X-axis respectively.

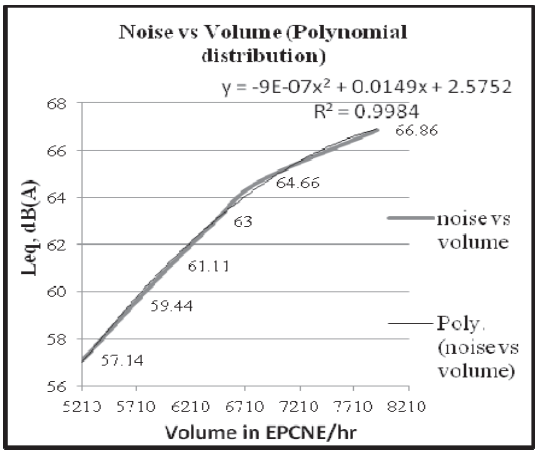

Figure 5 Noise vs Volume (Polynomial distribution)

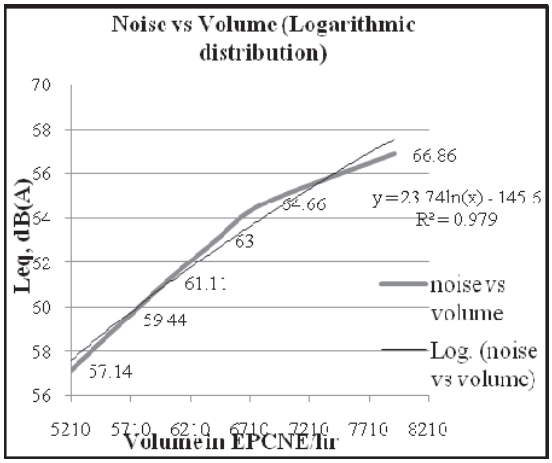

Figure 6 Noise vs Volume (Logarithmic distribution)

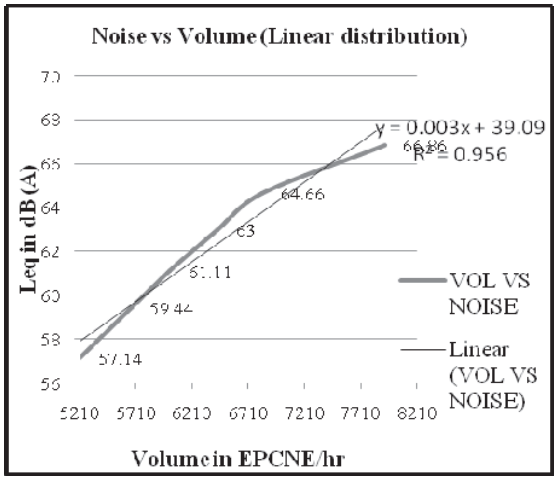

Figure 7 Noise vs Volume (Linear distribution)

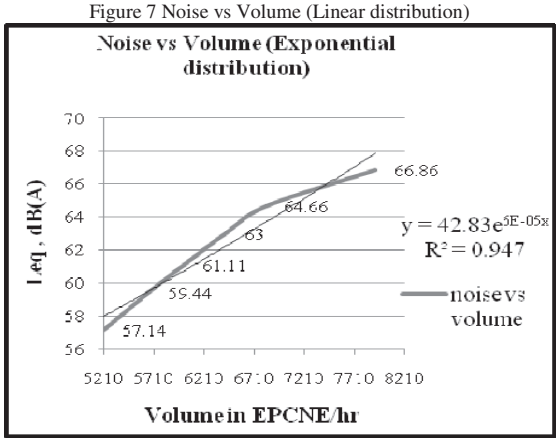

Figure 8 Correlation between Noise and Volume

Interpretation of Results and Discussions: A curve is plotted between noise and volume for a road having a capacity in terms of EPCNE/hr. Initially the curve shows the similar trend for the steady flow of traffic. But in case of congested flow it is expected that the noise level will show increasing trend up to certain value of volume and then it will again decrease at the very small value of volume. The reasons of expecting the above trend in case of congested flow were that the flow changes from steady to congested region the horning by the rear vehicles becomes more frequent either to get way to the vehicles or to overtake the frontal one. But none of the operations are possible in the congested flow and hence the chain of horning started as the vehicles arrive at the site. The decrease of noise level may be noticed, if the vehicle comes to the site at a big crowd, as the horning of vehicle stops. Therefore, in the total jam condition the noise level will be mainly because of the engines, and a chain of engine noise may lead to a higher noise level. As observed the Polynomial distribution gives the good correlation between Noise and Volume as its R^2= 0.998

G. Relation Between Noise and Speed

The correlation between Noise and Speed is found by plotting the values of Leq in dB(A) on Y-axis and Speed in km/hr in X-axis respectively in below Figures

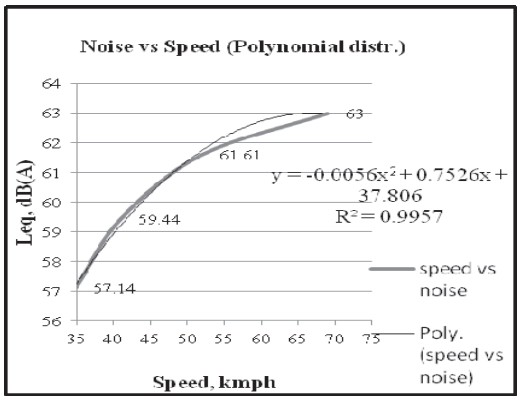

Figure 9 Noise vs Speed (Polynomial Distribution)

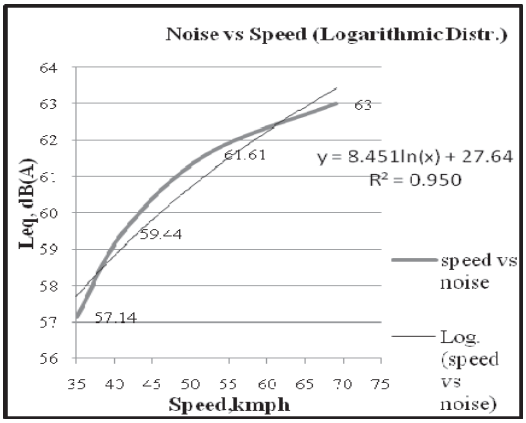

Figure 10 Noise vs Speed (Logarithmic Distribution)

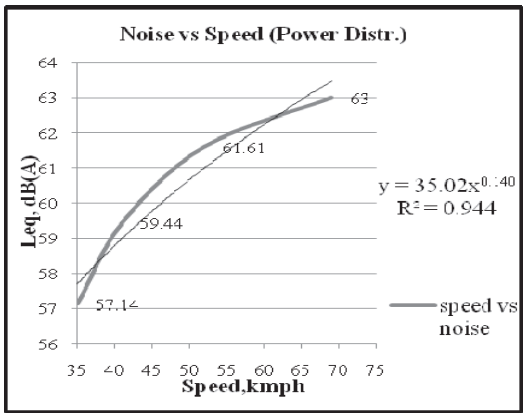

Figure 11 Noise vs Speed (Power Distribution)

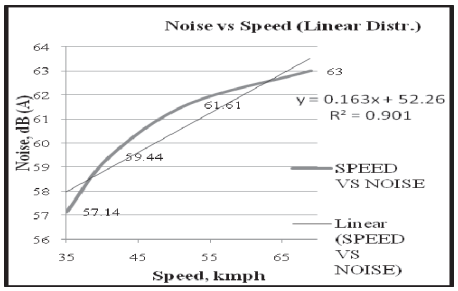

Figure 12 Noise vs. Speed (Linear distribution)

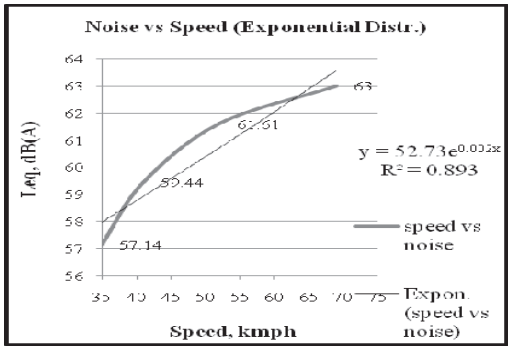

Figure 13 Noise vs Speed (Exponential Distribution)

Interpretation of results and discussions:Finally a curve is plotted between noise, Leq in dB(A) and Speed (kmph) on y-axis and x-axis respectively. As observed from the curve it shows that at a particular speed, the noise of the vehicles increases as the speed of vehicle is increasing. This is due to as the vehicle reduces its speed the noise emission of vehicle and its horning also reduced, this mainly occurs at a congested traffic. As observed from the above figures, the Polynomial Distribution between noise and speed shows a good correlation as its $R^2 = 0.9957$.

CONCLUSIONS

A. Conclusions

Following conclusions have been drawn based on the information presented in this report

1. The study has shown that the noise levels emitted by traffic noise in Location1 (Roorkee-Delhi) and Location2 (Delhi-Roorkee) were quite high.
2. The noise level decreases with the distance from the source of observation points.
3. Useful correlations have been found between traffic parameters like traffic volume, average speed and noise (Leq).
4. Traffic Volume affects the noise. As 200 vehicles passing in one hour sound half as loud as 2000 vehicles. So Volumes need to have a noticeable effect.
5. Reducing speed is the most immediate and equitable way of minimizing traffic noise.
6. A small increase in the percentage of heavy vehicles in the composition of flow may increase the noise level to a greater extent.
7. Major Traffic noise models throughout the world differ in some respects in detail but overall, the methodology is similar.
8. In order to overcome the problems the most effective one is to promote awareness on noise pollution and the risks of daily exposure to high noise levels.

B. Recommendations

1. Detailed studies are to be carried out in 4-lane highways in order to study the noise of different categories of vehicles.
2. Studies for Traffic noise pollution reduction through eco-friendly noise barriers like trees etc. Should be conducted under varying conditions of land uses

ACKNOWLEDGEMENT

It is my great pleasure to express my sincere gratitude and immense veneration to my supervisor Dr. S.S. Jain, Professor, Transportation Engineering Group, Department of Civil Engineering, Indian Institute of Technology Roorkee, for his intuitive and meticulous guidance, valuable assistance in scrutinizing the manuscript and his valuable suggestions during the period of project work. I am also thankful to all my friends who directly or indirectly helped me during the period of completion of project.

VI. REFERENCES

1. Alexander, A., Barde, J.Ph and Langdon.,(1975) "Road Traffic Noise", London Applied Science Publication, Vol.16, 34-38.
2. "FHWA MN Division Guidance for Evaluating Traffic Noise Impacts of local", federally funded projects that are exempt from State Noise Standards [31/1/2003].
3. IRC 104-1988,"Guidelines for Environmental Impact Assessment of Highway Projects", Jamnagar House , New Delhi.
4. "Highway Traffic Noise Analysis and Abatement Policy and Guidance" by U.S. Department of Transportation Federal Highway Administration Office of Environment and Planning Noise and Air Quality Branch, (1995). Washington, D.C.
5. Hothersall, David C., and Salter, Richard J.,(1979) "Transport and the Environment", Granada Publishing Limited, Crossby Lockwood staples, London.
6. Johnson, D.R., and Saunders, E.G., (1968) " The Evaluation of Noise from freely flowing Road Traffic", Journal of sound and vibration, Vol10, 287-309.
7. Kumar, V.,(1979) "Analysis of Urban Traffic Noise", M.E. Dissertation, Civil Engineering Department, University of Roorkee, Roorkee, India,.
8. Lloyd B. Arnold,.(2001) "Highway Noise Study Analysis", Environmental Engineer, Senior Environmental Division, Virginia Department of Transportation.
9. Pearson, D. Krik, and Sabir, S.M.,(1988) "Road Traffic in Developing Countries Assesssment and Prediction" Proceedings. ICORT, Centre of Transportation Engineering., Civil Engineering Department, University of Roorkee, Roorkee, India.
10. Rao, P.R., (1991) "Prediction of Road Traffic Noise", Indian Journal of Environmental Protection, Kalpana Corporation, Varanasi, Vol 11, 290-293.
11. Yap, X.W,, Bavani, N., Ramdzani (1999) "An Effect of Traffic Noise on Sleep: A Case Study in Serdang Raya, Selangor",Faculty of Environmental Studies, University Putra Malaysi.

Equalization Techniques for Time Varying Channels in MIMO based Wireless Communication

T Padmavathi[1] and Varghese Thattil[2]
[1]CVR College of Engineering, Department of ECE, Ibrahimpatan, R.R.District, A.P., India
Email:padmatp41@gmail.com
[2]CVR College of Engineering, Department of ECE, Ibrahimpatan, R.R.District, A.P., India
Email:mailthattil@gmail.com

Abstract - **In mobile integrated service digital network, high bit-rate data transmission is essential for many services such as video, multimedia etc. When data is transmitted at high bit-rate, wireless channels exhibit delay dispersion because of multipath components (MPC). Different propagation times from transmitter (Tx) to receiver (Rx) in MIMO systems produces different MPCs. This in turn leads to Inter Symbol Interference (ISI), which can greatly disturb the transmission of digital signals. If delay spread is smaller than the symbol duration, it can lead to considerable Bit Error Rate (BER) degradation. Equalization defines any signal processing technique used at receiver to make the signal less susceptible to delay spread. Equalizers require an estimate of channel impulse or frequency response to mitigate the ISI. In this paper the performance of equalization techniques are compared by considering 2 transmit and 2 receive antennas (resulting 2x2 MIMO Channel). Assume that channel is flat fading Rayleigh multipath- channel and modulation is BPSK.**

Index terms- **Delay spread, Inter Symbol Interference, Rayleigh multipath channel, Adaptive equalization**

I. INTRODUCTION

Wireless communication has been optimized due to growth of cellular Telephone and wireless internet access. This development opened a new direction for wireless communication to provide Universal personal and multimedia communication irrespective of the mobility or location. These services need to be provided with high data rates. To obtain this objective future wireless networks required to support a wide range of services including voice, data, facsimile, image and video.

Because of multipath fading, Inter Symbol Interference (ISI) is introduced in the received signal for mobile radio system through Radio channel. A strong equalizer is required to eliminate the ISI from signal. The design of equalizer requires knowledge of frequency selectivity, Channel Impulse Response (CIR) [1] to mitigate the ISI.

In multiuser, a multi carrier communication system, MIMO communication channels rapidly varies due to the mobility of user. Channel State Information (CSI) is available at transmitter or receiver with feedback in the communication system. This CSI introduces problems in the radio communication system. To overcome with this problems Channel equalization techniques are Introduced [2].

Equalizers need to learn the channel characteristics (training) with Impulse response. The knowledge of impulse response is useful to estimate the frequency response if channel changes continuously (tracking). The Adaptive equalization technique includes training and tracking.

In training process, the training sequence has been sent to the adaptive equalizer at the receiver. The training sequence is a binary signal which is either pseudorandom or fixed bit pattern. The adaptive equalizer at the receiver uses mathematical algorithm to estimate filter coefficients. This estimated filter coefficients, are modified to eliminate the noise which is created due to multipath fading effect of the channel. The training sequence along with user data is sent to the receiver. If the channel is transmitting with delay spread, deepest fades the training sequence is designed to allow the equalizer at the receiver to get exact filter coefficients. Once training sequence transmission finished, filter coefficients are optimized to receive user data [8].

Equalizer tracks the time varying characteristics of the channel continuously with recursive algorithm after receiving the user data. As a result adaptive equalizer rapidly changes its filter coefficients over time. The convergence of equalizer is obtained with proper training. Convergence time of equalizer is depends on equalizer recursive algorithm, structure of the equalizer and rate of change of multipath fading channel [4].

Equalizer design must balance the removal of ISI with noise enhancement because noise and signal passes through the equalizer, so that noise power is also increases. This noise enhancement is very less in the non Linear equalizers but design of non linear equalizer

is complex process. Linear equalizers are simple to implement. The Linear and Non Linear equalizers are implemented with lattice or traversal structure. The traversal structure of N-coefficient filter consists with N-1 taps, N-1 delay elements with complex weights. The structure of lattice filter is complex [3]. Adaptive equalizer requires recursive algorithm to update filter coefficients along with filter structure. In this paper equalization techniques for MIMO channels with linear equalizer are discussed. There are five adaptive linear equalizers. These are

1. Zero Forcing (ZF) equalization
2. Minimum Mean Square Error (MMSE) equalization
3. Zero Forcing equalization with Successive Interference Cancellation (ZF-SIC)
4. ZFSIC with optimal ordering.

II. MIMO SYSTEM MODEL

A MIMO Communication System is developed with *nT* ransmit and *nR* receive antennas shown in fig2.1 In this paper 2x2 MIMO systems are discussed with *nT* = *nR*.=2

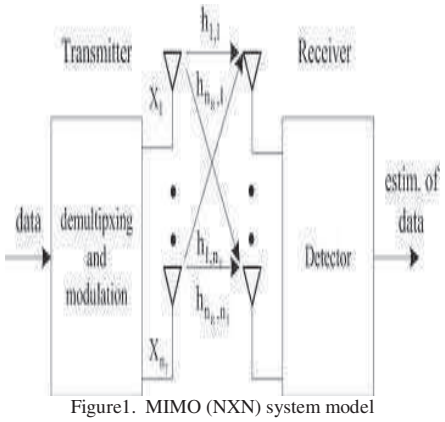

Figure1. MIMO (NXN) system model

A flat fading MIMO channel is assumed with *nT* transmit and *nR* receive antennas. These antennas are represented by a channel matrix (H) with nR × *nT* antennas. The elements of **H** are independent to each other and *Hj,i* ∈ *CN*(0, 1).The column vector X of is an input to the channel and channel output, AWGN Channel is represented by *nR* × 1 column vectors with **n** and y respectively. The elements of **n** are assumed to be independent and *nj* ∈ *CN* (0, σ2). For convenience, we define

m=min (*nT, nR*), *n*_=max (*nT, nR*), *d*_=*n* − *m*.

The channel input/output equation for channel can be written as

Y=Hx+n (1)

Where Y is the receive vector and x is the transmit vectors and H is the channel matrix and n is the noise vector respectively.

To represent 2x2 MIMO transmission channel a 2 x 2 matrix is taken with four complex-valued elements. Based on known pilot or training sequence the channel matrix elements are estimated. The signal at the receiver can be represented with

$$\begin{pmatrix} RxO \\ Rx1 \\ . \\ RxN \end{pmatrix} = \begin{pmatrix} h_{1,1} & h_{2,1} & . & h_{N,1} \\ h_{1,2} & h_{2,2} & . & h_{N,2} \\ . & . & . & . \\ h_{1,N} & h_{2,N} & . & h_{N,N} \end{pmatrix} \begin{pmatrix} TxO \\ Tx1 \\ . \\ TxN \end{pmatrix}$$

Where

$$H(t) = \begin{pmatrix} h_{1,1}(t) & \dots & h_{1,m}(t) \\ \dots & \dots & \dots \\ h_{n,1}(t) & \dots & h_{n,m}(t) \end{pmatrix}$$

Rx0 To RxN, are the received symbols

$h_{1,1}$ is the fading coefficient from 1st transmit antenna to1st receive antenna,

$h_{1,2}$ is the fading coefficient from 1st transmit antenna to 2nd receive antenna,

$h_{2,1}$is the fading coefficient from 2nd transmit antenna to 1st receive antenna,

$h_{2,2}$ is the fading coefficient from 2nd transmit antenna to 2nd receive antenna,

Tx0 to TxN are the transmitted symbols and noise is represented

$$y(k,n) = \sum_{u=1}^{U} H_u^{(c)}(k,n) S_u(k,n) + \eta(k,n) \quad (2)$$

η(k,n) noise on receive vectors.[4]

III. ADAPTIVE EQUALIZER

If the time varying properties of communication channel is adapted automatically then equalizer is called adaptive equalizer.

Adaptive equalizers are implemented in the receiver either at the base band or at IF since channel response, base band signal, and demodulated signal represented with base band envelope expression. This adaptive equalizers are simulated and implemented at the base band receiver.

The original transmitter information signal represented with x(t) and combined complex base band channel impulse of the transmitter is represented with f(t). Base band noise signal at the channel input is represented with nb(t) , and signal received by equalizer can be represented by equation.

$$Y(t) = x(t) \otimes f(t) + n_b(t) \quad (3)$$

Where f*(t) denotes complex conjugate of f (t), and * denotes the convolution operation. If the impulse response of the equalizer is heq (t), then the output of equalizer is

$$d(t) = x(t) \otimes f(t) \otimes h_{eq}(t) + n_b(t) \otimes h_{eq(t)}$$

$$= h(t) \otimes g(t) + n_b(t) \otimes h_{eq}(t) \quad (4)$$

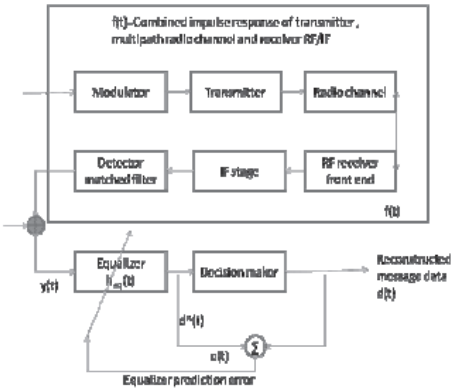

Figure2. Block diagram of a communication system with an adaptive equalizer in the receiver.

Where g(t) is the combined response of the transmitter, channel ,RF/IF sections of the receiver ,and the equalizer at the receiver. The complex base band impulse response of the traversal filter equalizer is given by

$$h_{eq}(t) = \sum_n c_n \delta(t - nT) \quad (5)$$

Where cn is the complex filter coefficient of the equalizer. The desired output of the equalizer is x (t), the original source data. Assume that nb (t). Then, in order to force d (t) =x (t), g(t) must be equal to

$$g(t) = f(t) \otimes h_{eq}(t) = \delta(t) \quad (6)$$

The Objective of equalization is to satisfy the given equation

$$H_{eq}(f)F(-f) = 1 \quad (7)$$

Where Heq (f) and F (f) are Fourier transforms of heq (t) and f (t) respectively, so that the combination of the transmitter, channel, and receiver appear to be an all pass channel [5].

A. Zero forcing (ZF) Equalizer

Zero Forcing Equalizer uses a linear equalizer algorithm for communication system. The linear equalizers are implemented based on inverse frequency response of the channel.

The name Zero Forcing corresponds to bringing down the ISI to zero in a noise free case. This will be useful when ISI is significant compared to noise. The zero frequency equalizer frequency response *C*(*f*) and Channel frequency response *F*(*f*) is constructed such that *C*(*f*) = 1 / *F*(*f*). Thus the combination of channel and equalizer gives a flat frequency response and linear phase *F*(*f*)*C*(*f*) = 1.If the channel response for a particular channel is H(s) then the input signal is multiplied by the reciprocal of this. This is intended to remove the effect of channel from the received signal, in particular the Inter symbol Interference (ISI).

For 2x2 MIMO Channel the received signal at the first receive antenna is represented as

$$y_1 = h_{1,1}x_1 + h_{1,2}x_2 + n_1 = \begin{bmatrix} h_{1,1} h_{1,2} \end{bmatrix} \begin{bmatrix} x_1 \\ x_2 \end{bmatrix} + n_1$$

The received signal on the second receive antenna is,

$$y_2 = h_{2,1}x_1 + h_{2,2}x_2 + n_2 = \begin{bmatrix} h_{2,1} h_{2,2} \end{bmatrix} \begin{bmatrix} x_1 \\ x_2 \end{bmatrix} + n_2$$

The equation can be represented in matrix notation as follows:

$$\begin{pmatrix} y_1 \\ y_2 \end{pmatrix} = \begin{pmatrix} h_{1,1} & h_{1,2} \\ h_{2,1} & h_{2,2} \end{pmatrix} \begin{pmatrix} x_1 \\ x_2 \end{pmatrix} + \begin{pmatrix} n_1 \\ n_2 \end{pmatrix}$$

Equivalently,

$$y = Hx + n \quad (8)$$

To solve for *x*, we need to find a matrix which satisfies *WH* = *I*. The Zero Forcing (ZF) detector for meeting this constraint is given by,

$$W = (H^H H)^{-1} H^H \quad (9)$$

Where W - Equalization Matrix and

H - Channel Matrix

This matrix is known as the Pseudo inverse for a general m x n matrix where

$$H^H H = \begin{pmatrix} h_{1,1}^* & h_{1,2}^* \\ h_{2,1}^* & h_{2,2}^* \end{pmatrix} \begin{pmatrix} h_{1,1} & h_{1,2} \\ h_{2,1} & h_{2,2} \end{pmatrix} = \begin{pmatrix} |h_{1,1}|^2 + |h_{2,1}|^2 & h_{1,1}^* h_{1,2} + h_{2,1}^* h_{2,2} \\ h_{1,2}^* h_{1,1} + h_{2,2}^* h_{2,1} & |h_{1,2}|^2 + |h_{2,2}|^2 \end{pmatrix}$$

The off diagonal elements in the matrix $H^H H$ are not zero, because the off diagonal elements are non zero in values. Zero forcing equalizer tries to null out the interfering terms when performing the equalization, i.e. when solving for *x*2 the interference from *x*1 is tried to be nulled and vice versa. During this process noise is also amplified. Hence the Zero forcing equalizer is not the best possible equalizer. However, it is simple and reasonably easy to implement. For BPSK Modulation in Rayleigh fading channel, the BER is defined as

$$P_b = \frac{1}{2}\left(1 - \sqrt{\frac{(E_b / N_o)}{(E_b / N_o) + 1}}\right)$$

Where

Pb - Bit Error Rate

Eb / No - Signal to noise Ratio

B. Minimum Mean Square Error (MMSE) Equalizer

A minimum mean square error (MMSE) estimator minimizes the mean square error (MSE), which is a common measure of estimator quality. MMSE equalizer does not eliminate ISI completely but, minimizes the total power of the noise and ISI components in the output. Let *x* be an unknown random variable, and let *y* be a known random variable. An estimator *x*^ (y) is any function of the measurement *y*, and its mean square error is given by

$$MSE = E\{(X^ - X2)\} \quad (10)$$

where the expectation is taken over both *x* and *y*.The Minimum Mean Square Error (MMSE) approach tries to find a coefficient *W* which minimizes the

$$E\{[W_{y-x}][W_{y-x}]^H\}$$

where W - Equalization Matrix
H - Channel Matrix and
n - Channel noise y- Received signal. To solve for *x*, we need to find a matrix *W* which satisfies *WH =I*. The Minimum Mean Square Error (MMSE) detector for meeting this constraint is given by,

$$W = [H^H H + N_o I)^{-1} H^H \quad (11)$$

This matrix is known as the pseudo inverse for a general m x n matrix.

When comparing the equation (9) with the equation (11) in Zero Forcing equalizer, apart from $N_o I$ the term both the equations are comparable. If the noise term is zero, the MMSE equalizer reduces to Zero Forcing equalizer.

C. Zero Forcing with Successive Interference Cancellation (ZF-SIC)

From the Zero Forcing (ZF) equalization approach, the receiver can obtain an estimate of the two transmitted symbols x_1, x_2

$$\begin{bmatrix}\hat{x}_1\\ \hat{x}_2\end{bmatrix} = (H^H H)^{-1} H^H \begin{bmatrix}y_1\\ y_2\end{bmatrix}$$

Take one of the estimated symbols (for example x2) and subtract its effect from the received vector y_1 and y_2

$$\begin{bmatrix}r_1\\ r_2\end{bmatrix} = \begin{bmatrix}y_1 - h_{1,2}\,\hat{x}_2\\ y_2 - h_{2,2}\,\hat{x}_2\end{bmatrix} = \begin{bmatrix}h_{1,1}\,x_1 + n_1\\ h_{2,1}\,x_1 + n_2\end{bmatrix}$$

$$r = hx_1 + n$$

The above equation is same as equation obtained for receive diversity case. In Maximum Ratio Combining (MRC) the received symbols are combined by taking the information from multiple copies.

$$\hat{x}_1 = \frac{h^H r}{h^H h}$$

This forms Zero Forcing Equalizer with Successive Interference Cancellation (ZF-SIC) approach.

D. Successive Interference Cancellation with 0ptimal Ordering

In successive Interference cancellation either x_1 or x_2 selected first and subtracted from y_1 or y_2. But to make that decision, let us find out the transmit symbol (after multiplication with the channel) which came at higher power at the receiver. The received power at the both the antennas corresponding to the transmitted symbol is x_1 is,

$$Px_1 = |h_{1,1}|^2 + |h_{2,1}|^2$$

The received power at the both the antennas corresponding to the transmitted symbol x2 is

$$Px_2 = |h_{1,2}|^2 + |h_{2,2}|^2$$

If $Px_1 > Px_2$ then the receiver decides to remove the effect of x_1 from the received vector y_1 and y_2 then re-estimate x_2.

$$\begin{bmatrix}r_1\\ r_2\end{bmatrix} = \begin{bmatrix}y_1 - h_{1,1}\,\hat{x}_1\\ y_2 - h_{1,2}\,\hat{x}_1\end{bmatrix} = \begin{bmatrix}h_{1,2}\,x_2 + n_1\\ h_{2,2}\,x_2 + n_2\end{bmatrix}$$

expressing in matrix notation,

$$\begin{bmatrix}r_1\\ r_2\end{bmatrix} = \begin{bmatrix}h_{1,2}\\ h_{2,2}\end{bmatrix} x_2 + \begin{bmatrix}n_1\\ n_2\end{bmatrix}$$

$$r = hx_2 + n$$

with Maximal Ratio Combining [6] (MRC) The equalized symbol for $\hat{x}_2$ is,

$$\hat{x}_2 = \frac{h^H r}{h^H h}$$

else if $Px_1 < Px_2$ the receiver decides to subtract effect of x_2 from the received vector y_1 and y_2, and then re-estimate expressing in x_1.

$$\begin{bmatrix}r_1\\ r_2\end{bmatrix} = \begin{bmatrix}y_1 - h_{1,2}\,\hat{x}_2\\ y_2 - h_{2,2}\,\hat{x}_2\end{bmatrix} = \begin{bmatrix}h_{1,1}\,x_1 + n_1\\ h_{2,1}\,x_1 + n_2\end{bmatrix}$$

Expressing in matrix notation,

$$\begin{bmatrix}r_1\\ r_2\end{bmatrix} = \begin{bmatrix}h_{1,1}\\ h_{2,1}\end{bmatrix} x_1 + \begin{bmatrix}n_1\\ n_2\end{bmatrix}$$

$$r = hx_1 + n$$

And the equalized symbol x1 with Maximal Ratio Combining [6] (MRC). is,

$$\hat{x}_1 = \frac{h^H r}{h^H h}$$

Doing successive interference cancellation with optimal ordering ensures that the reliability of the symbol which is decoded first is guaranteed to have a lower error probability than the other symbol. This results in lowering the chances of incorrect decisions resulting in erroneous interference cancellation. Hence gives lower error rate than simple successive interference cancellation. [7]

IV. RESULTS

A. Zero forcing (ZF) Equalizer

The zero-forcing equalizer removes all ISI, and is ideal when the channel is noiseless. However, when the channel is noisy, the zero-forcing equalizer will amplify the noise greatly at frequencies *f* where the channel response $H(j2\pi f)$ has a small magnitude (i.e. near zeroes of the channel) in the attempt to invert the channel completely.

From simulation results, Zero forcing equalizers improve the data rate, but not diversity gain.

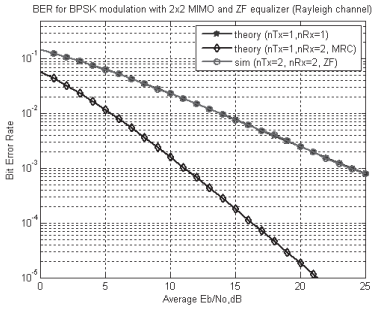

Figure 3. BER for BPSK modulation with 2x2 MIMO and ZF equalizer

B. Minimum Mean Square Error (MMSE) Equalizer

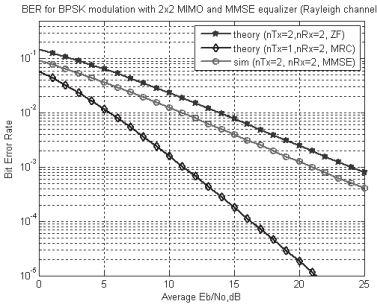

Figure 4. BER for BPSK modulation with 2x2 MIMO and MMSE equalizer

Minimum Mean Square Error (MMSE) equalizer results in around 3dB of improvement of BER at 10^{-3}

C. *Zero Forcing with Successive Interference Cancellation (ZF-SIC)*

Compare to Zero forcing equalizer, with successive Interference Cancellation 3.2dB improvement in BER.

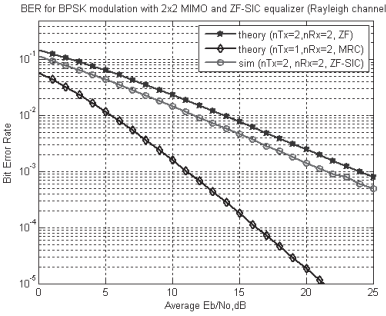

Figure4. BER for BPSK modulation with 2x2 MIMO and ZF SIC equalizer

D. Successive Interference Cancellation with optimal ordering (SIC).

Compared to Minimum Mean Square Equalization with simple successive interference cancellation case, addition of optimal ordering results in around 5.0dB BER improvement

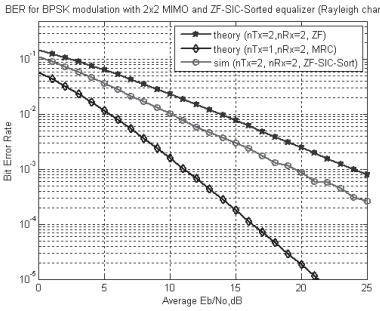

Figure 5. BER for BPSK modulation with 2x2 MIMO and ZF SIC Optimized equalizer

CONCLUSIONS

Due to mobility, multiuser, multicarrier and time varying property of Channels, MIMO requires equalization techniques for wireless communication. In this paper Equalization technique are compared for MIMO. From simulation results we can conclude that MMSE with SIC can cancel out interference with optimum level.

REFERENCES

[1] Ardavn malekhi- Tehrani,Babak Hasibi, John M. coeffi 'frequency selective channels Adaptive equalization techniques of Multi Input Multi Output' IEEE Transaction. Wireless Communication 1999.

[2] Sajid Ahmed¤, Sangarapillai Lambotharan, Andreas Jakobsson, Jonathon Chambers of' Parameter estimation 'and equalization techniques for MIMOfrequency selective channels with multiple frequency offsets.

[3] Zero-forcing equalization for timevaryingsystem with memory"byCassio B. Ribeiro, L. R. de Campos, and Paulo S.R.Diniz.

[4] zero-forcing frequency domain equalization for DMT systems within sufficient guard interval by Tanja Karp , Martin J. Wolf , Steffen Trautmann , and Norbert J. Fliege.

[5] Jun Shi Huiyu Luo Yu-Ching Tong, Adaptive Equalizer for MIMO WirelessCommunication Channels March 12, 2003.

[6] O. Simeone, Y. Bar-Ness, and U.Spagnolini, Linear and Nonlinear Preequalization/Equalization for MIMO SystemsWith Long-Term Channel State Information at the Transmitter, IEEE transactions on wireless communications, vol. 3, no. 2, march 2004.

[7] 'Wireless Communications' by F.Molish

[8] Wireless Communication, by "GoldSmith"

A Continuous-Time ADC and Digital Signal Processing System for Smart Dust and Wireless Sensor Applications

B. Janardhana Rao[1] and O.Venkata Krishna[2]
[1] CVR College of Engineering/ECE, Hyderabad, India
Email: janardhan.bitra@gmail.com
[2] CVR College of Engineering/EIE, Hyderabad, India
Email: venkatakrishna.odugu@gmail.com

Abstract— **In this paper an event-driven (ED) digital signal processing system (DSP), Analog-to-digital converter(ADC) and Digital-to-analog converter(DAC) operating in continuous-time (CT) with smart dust as the target application is presented. The benefits of the CT system compared to its conventional counterpart are lower in-band quantization noise and no requirement of a clock generator and anti-aliasing filter, which makes it suitable for processing burst-type data signals.**

A clock less EDADC system based on a CT delta modulation (DM) technique is used. The ADC output is digital data, continuous in time, known as "data token". The ADC used an un buffered, area efficient, segmented resistor string (R-string) feedback DAC. This DAC in component reduction with prior art shown nearly 87.5% reduction of resistors and switches in the DAC and the D flip-flops in the bidirectional shift registers for an 8-bit ADC, utilizing the proposed segmented DAC architecture. The obtained Signal to noise distortion ratio (SNDR) for the 8-bit ADC system is 55.73 dB, with the band of interest as 220 kHz and Effective number of bits(ENOB) of more than 9 bits.

Index Terms: **smart dust, continuous-time (CT), Delta modulation, Analog-to-digital converter (ADC), Digital-to – analog converter (DAC).**

I. INTRODUCTION

The target of this paper is to study and design a mixed-signal processing system consisting of an Analog-to-Digital Converter (ADC), Digital Signal Processor (DSP) and Digital-to-Analog Converter (DAC), for the smart dust application, in a top-down, test-driven design methodology. The complete system has to be operated in a CT mode without any sampling. The focus is to achieve low power consumption and area, without sacrificing the overall system performance.

There has been a new phenomenon emerging out in recent past called "smart dust" also known as "motes" or "wireless sensor networks" or "swarming". Smart dust is a tiny (size and density of a sand particle), ultra-low-power electronic sensory autonomous device packed with various sensors, intelligence and even wireless communication capability. A typical scenario could be smart dust motes deployed in large numbers to form an ad-hoc network, called as swarm, detects environment variables such as light, temperature, pressure, vibration, magnetic flux density or chemical levels. This network, formed by few tens or even millions of motes, can communicate with neighboring motes and pass on the data collected from one mote to another in a systematic way, which can be collected and processed further [1]. Smart dust can derive the energy necessary for its functioning either from batteries or from the environment itself, or from both. The power consumption of the smart dust decreases with the shrinkage in the size of the mote. It has to be in the order of few microwatts. This imposes a stringent constraint on the design, and has to be addressed by following various low power design techniques.

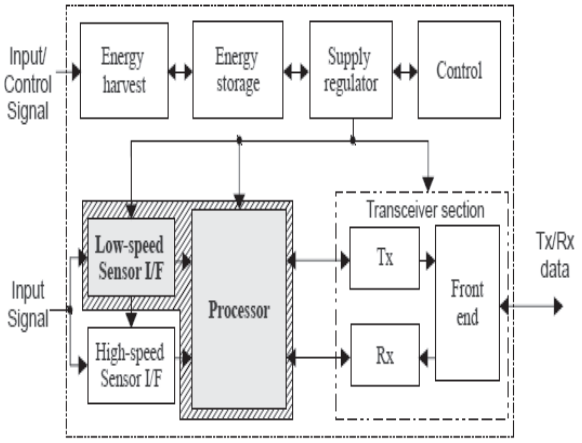

Figure 1. Block diagram of a typical smart dust mote.

Figure.1 shows the block level details of a single autonomous smart dust supply regulator, control, high-speed sensor interface, low-speed sensor interface, DSP and radio transceiver section. Energy harvester generates energy from the environment such as solar radiation, wind or even vibration. The generated energy is stored for future usage, using an energy storage element. The available energy is supplied efficiently, in the form of fixed voltages and currents, to the various circuits of the system with the help of the supply regulator. The control

circuitry is responsible for the various control mechanisms involved in a mote, which decides the operation of the mote. The sensors collect the environmental variations of interest and convert them to an equivalent electrical signal, analog in nature. The sensory interfaces are required to perform initial signal conditioning and analog to digital conversion of the sensed data. The data is processed digitally using a DSP. DSPs can essentially perform various kinds of operations on the digital signals, such as filtering, domain transformations, compression, encryption, etc. The processed data is reconstructed back to analog equivalent necessary for transmission, using a DAC (not shown in figure). The transceiver section up-converts the baseband signal to Radio Frequency (RF) signals and transmits them. It also receives the RF signals and down-converts them to the baseband signal. This paper targets the design of the low speed sensor interface and the DSP, as highlighted in figure 1.

The specifications of the CTDSP system, that is finally going to be deployed in the smart dust motes are shown in table 1. The major constraint imposed on the system is that all the blocks in the design should be clockless. Further, the system should be implemented in 90 nm advanced Complementary Metal Oxide Semiconductor (CMOS) process. The specifications of the ADC, DAC and the transversal direct-form Finite-Impulse-Response (FIR) Low Pass Filter (LPF) is as shown in table 1.

TABLE 1.
SPECIFICATIONS OF THE CT-DSP SYSTEM FOR SMART DUST.

Item	Parameter	Value
ADC	Resolution	8 bits
	Maximum input signal frequency	20 KHz
LPF	Sampling frequency	44 KHZ
	Passband edge frequency	5.2 KHZ
	Stopband edge frequency	10KHz
	Pass band ripple	1 dB
	Stopband attenuation	50dB
DAC	Resolution	8
Generic	Supply voltage	1 V
	Technology	90nm

A. Continuous time processing

A new emerging field of digital signal processing in CT has been presented by Prof. Yannis Tsividis of Columbia University [2, 3]. It is opposed to the conventional sampled systems where the processing is carried out in discrete time. This CTDSP system processes the data sensed by the analog Interface block of the sensor module and produce the output to the RF front-end. As the input data is of burst nature, occurring occasionally, it is highly desirable that the CTDSP system remains idle most of the time and operates only when there is a significant data to process. This is achieved by using level crossing technique, where the ADC operates only if there is a significant variation observed in the input signal. It doesn't produce a sample if there is a long silence or no data available to process.

A conventional DSP system operates with a global reference or clock signal. The input signal, $x(t)$, is sampled-and-quantized at the rising or falling edge of the clock signal for an edge triggered system. The quantized signal is encoded digitally and processed by the subsequent DSP section and the reconstruction of the digital signal to the analog equivalent by the output DAC.. The overall system is completely synchronized with respect to the global clock. The drawbacks of the conventional DSP systems are, A sampled system requires clock generator, which has a large fan-out, since it has to drive gates of many transistors. Hence, making it costly to implement, both in terms of the area and power consumption, the sampling frequency is decided based on the highest frequency component of the input signal. It is therefore necessary to implement a band-limiting filter known as an anti-aliasing filter, to avoid aliasing, whose implementation might also be a costly affair, the sampling results in the aliasing of higher frequency terms to the band of interest, even if the Nyquist theorem is followed and the deviation from the precise sample timing instances due to the clock jitter and the clock skew can cripple down the system performance to undesired levels, if not designed properly.

The signal to be processed by the smart dust module is of burst nature, which occurs occasionally. The clocked systems, although equipped with many advantages, are not an ideal choice for processing the burst-like signals. The drawbacks listed for the clocked system are more dominating compared to the advantages for the smart dust application. Hence in this paper the event-driven CT digital signal processing systems are discussed, which operates on the principle of level-crossing and are very suitable for burst-type data processing.

II. CONTINUOUS-TIME OR EVENT-DRIVEN DSP SYSTEMS

The CT or event-driven Digital Signal Processor (DSP) systems, as the name suggests, operates in continuous time mode [2,6]. The input signal, $x(t)$, is processed by the CTDSP system to produce output, $y(t)$. There is no clock involved anywhere in the system. A CT system can also be divided into three basic sub-systems: the CTADC, CTDSP and CTDAC. As pointed out above, there is no global clock involved anywhere in CTDSP system. Hence, all the three blocks operates in a CT mode and are represented with a prefix CT [5]. Figure 2 shows the block diagram of the CTDSP system with the three sub-systems. CTADC is the first block in the CTDSP system which quantizes and digitizes the input signal, $x(t)$, to a CT output, $bi(t)$. Unlike conventional system, the input signal is not sampled before quantization. The CT data is then processed by the

CTDSP sub-system to produce digital data, *dj*(*t*), which is reconstructed to analog signal, *y*(*t*), by the CTDAC block. Note that the time domain is represented in "t" as it is always continuous in nature.

Figure 2. CTDSP system with the basic building blocks CTADC-CTDSP-CTDAC.

The CTDSP system adopts non-uniform sampling approach, where samples are generated only when the event crosses predefined quantization reference level. The operation of the CTDSP system can be classified as quantization by the CTADC block and the processing of the digital (continuous) data by the CTDSP subsystem.

A. CTDSP quantization technique: A level-crossing approach.

A conventional DSP system adopts uniform quantization technique, where samples are taken and processed at every clock cycle. The maximum frequency of the input signal dictates the minimum possible clock frequency of sample generation. However, it turns out that, for signals with burst-like nature and long period of silence, exhaustive sampling is not required as done in conventional systems. The samples generated either contains no information or repetitive information. Further, additional dynamic power is required for the processing of these samples by the DSP section. A different class of the quantization technique, called a level-crossing sampling scheme, suggested by Sayiner et al., and further explained by Tsividis in [2, 3, 5]. It is a non-uniform sampling approach, where the samples are generated only when the event crosses the predefined quantization reference level. Since the quantization is based on the event and is continuous in time, it is called as an EDCT quantization [3].

The quantization steps can be uniform or non-uniform and can be customized further based on the application. To understand the CT quantization technique, let's consider figure.3. As shown, the input signal, *x*(*t*), when crosses the predefined quantization reference level, get quantized to signal, *xq*(*t*), and produces samples (*ti, x*(*ti*)). This is a non-uniform sampling operation, where the signals with faster slope generates samples more frequently ("faster") compared to signals with lesser slopes. Hence, signal-dependent sampling is achieved simply by utilizing the built-in feature of the quantizer. With this approach, the signal with less variation produces lesser number of samples to be processed by the subsequent DSP section; hence resulting in a signal dependant power consumption. This is a clear advantage of the CT systems, making it very suitable for processing burst type signals.

The continuous-time digital output, *bi*(*t*), of the CTADC block is processed by the CTDSP sub-system. Since the ADC output is digital in nature, the advantages of the digital signal processing can be utilized in the CT system as well. The design approach for the CTDSP system is described in [6]. Based on the transfer function, a conventional DSP system can be realized using multipliers, adders and delay taps as basic building blocks. A digital signal processor operating in the CT mode can be mapped from the discrete counterpart by replacing these blocks by the one operating in the CT domain. For Example, asynchronous multipliers and adders, which operates without clock, can be used in the CT system. One method of implementing the delay taps is by using chain of inverters. A better approach is presented in [9,10], where collection of delay cells connected in series are used to delay and hold the data. Handshaking is used between delay cells to ensure proper data transmission. The usage of these delay blocks are experimentally confirmed in [4, 11]. The CTDSP sub-system produces output, *dj*(*t*), as shown in figure 2, which is reconstructed back to the analog equivalent, *y*(*t*), by the CTDAC module. The CTDAC can be realized using architectures and circuit implementation techniques as mentioned in section V for the clocked counterpart. The only difference is that the DAC should operate without clock.

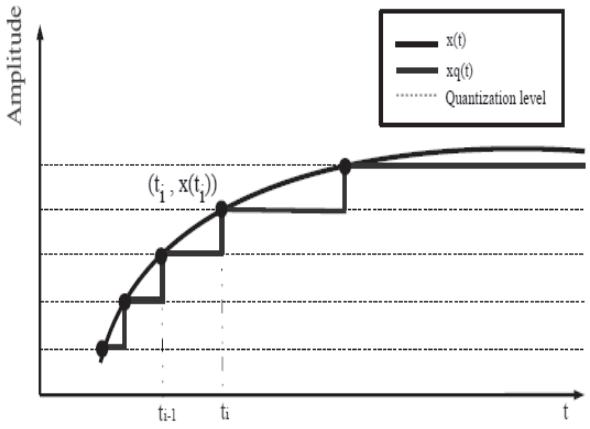

Figure 3. Level-crossing quantization technique in CTDSP system

III. EVENT-DRIVEN ADC

The first module in the ED DSP system is the CTADC or the ED ADC. It converts the analog input signal, *x*(*t*), provided by the Analog Interface (AI) to CT digital binary output signal, *bi*(*t*). A block diagram of the AI and the CTADC is shown in figure 4. The AI section

consists of a sensor network and an analog filter. The sensor network detects the variation in the input signal (temperature, pressure, humidity , etc. based on the application) and converts it to the electrical signal. The analog filter limits the frequency of the input signal to the operating range of the ADC.

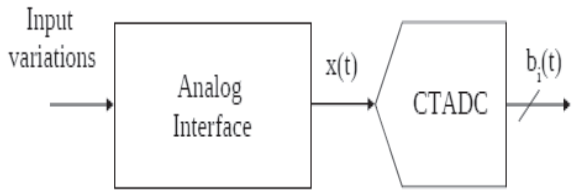

Figure 4. Block diagram of AI and CTADC.

The AI is designed based on the overall specification defined for the smart dust module, for e.g., the sensor interface is selected based on the application and the cutoff frequency of the analog filter is selected based on the frequency of operation of the system. As illustrated in figure 4, the AI provides a CT signal, $x(t)$, to the CTADC block. The CTADC consists of a CT quantizer and an encoder, which digitize the signal to, $bi(t)$. The digital output, $bi(t)$, is continuous in time and can be represented in many ways depending on the deployed ADC architecture [3].

A .Level-crossing sampling for the CTADC

The CTADC adopts a level-crossing sampling technique. In this section a detailed description of the level-crossing quantization technique is presented. Figure. shows the quantization procedure in the CTADC. When the input signal, $x(t)$, crosses a quantization reference level, it gets quantized to the nearest quantization level based on the direction of the input signal. The quantized signal, $xq(t)$, as shown in figure 5, is continuous in time and the samples are represented as $(ti, x(ti))$, where $ti-1$ and ti represent the time instances of the sample generation, respectively. The quantized signal, $xq(t)$, can be digitized in many ways [3], like the CT binary bits in a flash ADC or by using data token consisting of *change* and *direction* (increment/decrement) as in DM [15]. The former approach is illustrated in figure.5, where $b0$, $b1$ and $b2$ are the CT binary signals. The level-crossing sampling is a non-uniform sampling operation, where the faster signals with higher slopes generate samples more frequently ("faster") compared to signals with lower slopes. Hence, a signal-dependent sampling is achieved

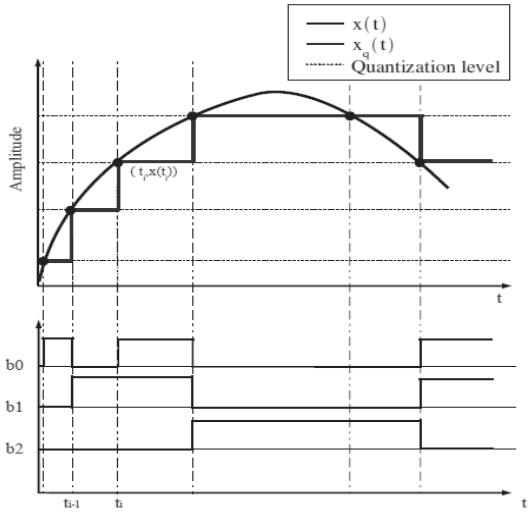

Figure 5. Level-crossing quantization in the CTADC with 3-bit CT digital output representation; $b0$, $b1$ and $b2$.

simply by utilizing the built-in feature of the quantizer. It means, that an input signal with lower variation generates lower number of samples to be processed by the subsequent DSP section, hence achieving lower dynamic power dissipation.

The frequency spectrum of an 8-bit CT quantizer as well as the sampled quantizer are shown in figure 6 and figure.7, respectively. The CT quantized signal spectrum has only the signal and its harmonic components. Whereas, the output spectra of the conventional sampled quantizer contains not only the signal and its harmonics, but also other undesirable tones, which are spread across the entire spectrum, and are not harmonically related to the signal frequency. This is an artifact due to aliasing of the higher frequency harmonic distortion components into the lower frequency band of interest and can be attributed to the sampling of the CT quantized output, which is just same as the conventional technique of quantization after sampling. Hence the difference between figure.6 and figure.7 is the noise floor added in the latter case due to aliasing, which is an inherent feature of sampling.

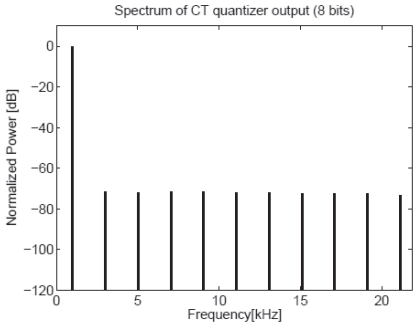

Figure 6: Frequency spectrum of an 8-bit CT quantizer with input amplitude $A = xmax$.

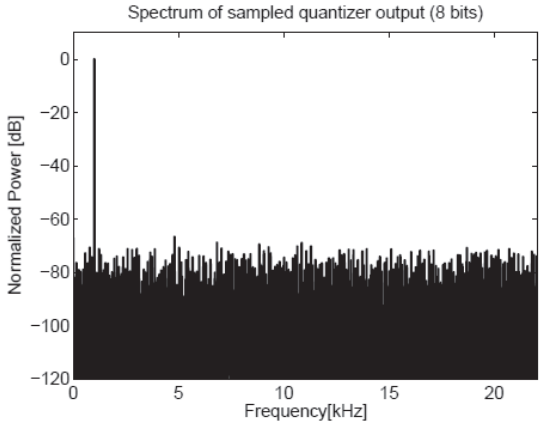

Figure 7: Frequency spectrum of an 8-bit sampled quantizer with frequency of sampling, fs = 44 kHz.

B. Proposed architecture of an event driven DM ADC

An ED DM ADC system consists of two comparators, a feedback DAC, a bidirectional Shift Register (SR) and an asynchronous digital control logic. The block diagram of the ED DMADC system is shown in figure.8. The DAC generates two reference signals: *VTop*(*t*) and *VBot*(*t*) for the upper and lower comparator, respectively. The upper (lower) comparator tracks the positive (negative) going signal and produces output *Inc* (*Dec*), which is high, when input signal is greater (lesser) than *VTop*(*t*) (*VBot*(*t*)) and zero when the signal is in between the two reference levels. Based on the value of *Inc/Dec*, the digital asynchronous control logic produces signals: *change* and *direction*, collectively called as "data token ". The data token is provided to the bi-directional SR which increments (decrements) the DAC outputs, *VTop*(*t*) and *VBot*(*t*), by _ (voltage resolution of the ADC), if *Inc* (*Dec*) is high. The data token is also provided to the subsequent DSP section, which processes the samples. The DSP section sends the acknowledge signal *Ack* back to the control logic.

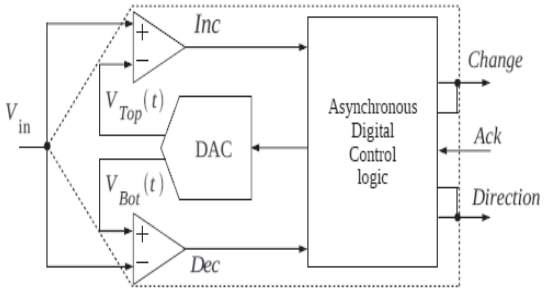

Figure 8: Event-driven ADC based on delta modulation technique.

IV. CONTINUOUS TIME DSP

After the CT quantization of the input signal picked up by the sensor, to infer the information content of the quantized and digitized tokens, one has to process it. The processing is done using a digital signal processor, before the data transmission. This can be performed either in CT or discrete-time. The CTDSP is preferred over the conventional sampled DSP, to avoid sampling clock and the drawbacks associated with it. CTFIR filter is considered for designing the CTDSP. The CT processing of the signals in digital domain can be achieved by using basic blocks such as adders, multipliers and delay elements, all operating in continuous mode. The subsequent discussion provides detail about the design of the DSPs system operating in CT.

A. Event-driven FIR filter with delta-modulation technique

An approach is to use an asynchronous DMADC. The two signals which collectively form the output data token from the DMADC are *change* and the *direction*. The *change* represents the time instance of the sample generation and the *direction* represents the sample value which can be "high" or "low". Note that, these two binary signal fully represents an *N*-bit signal and can be reconstructed back to the quantized signal, $q(t)$. Henceforth, *change* and *direction* are collectively called as a data token ([*change*, *direction*]). As shown in figure 9, the data token is passed to the up-down counter, which counts up or down by 1 LSB if the data token is [1,1] or [1,0], respectively. Counting up or down can simply be performed by adding or subtracting 1 LSB from the previous value stored in the counter. The output from the counter is $q(t - k.TD)$, which is multiplied with the tap coefficient, bk, to produce output, $mk(t)$, as given by

$$m_k(t) = b_k \cdot q(t - k \cdot T_D). \quad (1)$$

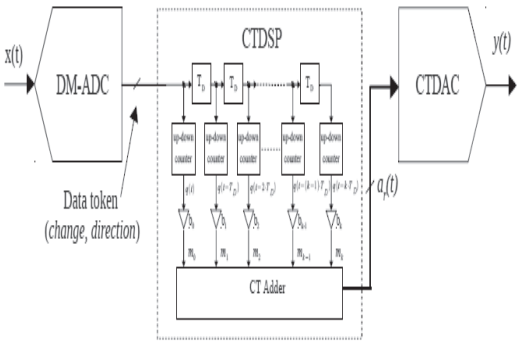

Figure 9: Event-driven FIR filter with DM encoding technique.

And the final output, $y(t)$, which is the weighted sum of $mk(t)$, is given by

$$y(t) = \sum_{k=0}^{K} m_k(t) = \sum_{k=0}^{K} b_k \cdot q(t - k \cdot T_D). \quad (2)$$

B. Design consideration of CTDSP system

In this section a few basic design parameters are discussed that are required for designing the CTDSP system. A transfer function of the CTDSP system is the filter transfer function, $B(s)$, can be determined by taking the Laplace transform of output, $y(t)$, as given by equation (2), where $y(t)$ is represented as the linear combination of the quantized input signal, $q(t)$. The output $Y(s)$ of a system with frequency response, $B(s)$, and a quantized input signal $Q(s)$ is given by

$$Y(s) = Q(s) \cdot B(s). \quad (3)$$

The expression for $Y(s)$ can be written as

$$Y(s) = [\sum_{k=0}^{K} b_k \cdot e^{-s \cdot T_D \cdot k}] \cdot Q(s). \quad (4)$$

The data token generated by the CTADC depends on the slope of the input signal. The total number of data tokens generated and the minimum possible distance between the two tokens are of primary importance, as it defines the functional requirement on the DSP section. Both, the number and the distance between the two data tokens has to be preserved, to achieve the correct filtering operation by the DSP block. Any missing data token or deviation in the distance between the two tokens, may result in undesirable variation in the frequency response of the filter.

The CTADC should be able to operate at the rate of $1/Tmin$, which for the above case of fb= 20 kHz is approximately equal to 16 MHz. This is equivalent to oversampling the ADC by a rate of 400. Hence, this system is suitable only for low frequency operation, because, for the high input frequency and considering the same oversampling ratio, the data token rate goes drastically high, which can be impractical for implementation with the mainstream CMOS process. Based on the above discussion and design parameters, fb and N of the ADC, it is possible to roughly define the power consumption of the CTDSP system.

V. CONTINUOUS TIME DAC

The CTDAC is the final block of the CTDSP system. It converts the digitally processed CTDSP sub-system output to an analog equivalent. In the previous sections, it is concluded that the DM-based ADC and DSP are preferred architectures for the smart dust application. Hence, the DAC architecture selection is based on the assumption that it is capable of accepting the 8-bit output word from the DM operated DSP sub-system. Also, as shown in figure 8, one feedback DAC is required inside the CTADC block. Hence, there are two DACs in the complete system. Target of the design is to reuse the same architecture in both the places. Any DAC which work asynchronously can be used for this purpose.

Few important points to take care, while selecting the DAC architecture, which is suitable for the feedback as well as the output DAC, are: The CTDAC shall generate two reference levels $V_{Top}(t)$ and $V_{Bot}(t)$ required as a reference for the top and bottom comparators shown in figure 8. The two reference levels are separated by Δ_{LSB} given by equation (2)

$$V_{Top}(t) - V_{Bot}(t) = \Delta_{LSB}. \quad (2)$$

Note that this constraint is not applicable for the output DAC, where only one output is required. The output shall increment or decrement by only one bit at a time to track the input signal continuously in the DMADC. It shall operate in an asynchronous mode without any clock, as no clock is used in the other sub-modules. It shall occupy very less area and it shall consume as less power as possible.

There are many possible architectures which can be used for realizing the required DAC structure with the constraints given above, e.g., resistor-string (R-string), current steering DAC, charge accumulation DAC and segmented DAC [7]. It has been shown in [11], that a resistor-string DAC architecture occupies lesser area, consumes less power, simple in design and can generate the two reference levels as described above. Due to these advantages a resistor-string DAC architecture is selected in this design.

A. Segmented resistor-string DAC

It is described that the resistor-string DAC architecture is preferred over the other DAC architectures. However, the simple resistor-string DAC may not be a cost effective solution for higher ADC is to use segmented resistor-string architecture, which produces same resolution as resistor-string architecture, with less hardware. Various possible segmented DAC architectures are available with the advantages and drawbacks. A final DAC architecture is presented, which is used in the design and block diagram is shown in figure 10.

The segmented $m \times n$ resistor-string DAC consists of two segments, where the first string with m resistors, resolves the Most Significant Bits (MSBs) and the second substring with n resistors, resolves the Least Significant Bits (LSBs) [7].

As shown in figure.10, two bi-directional SRs are required in this architecture, which based on the data token, produces m and n bit control signals for the MSB and LSB string, respectively. One possible selection of m and n is given by

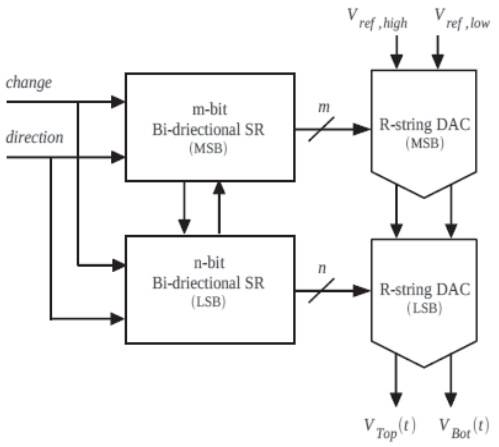

Figure 10: Block diagram of the $m \times n$ segmented resistor-string DAC with the $m \times n$ segmented bi-directional Shift registers.

$$m = \begin{cases} n = 2^{N/2}, & if\ N\ is\ even \\ n/2 = 2^{(N-1)/2}, & if\ N\ is\ odd. \end{cases} \quad (5)$$

Figure.11 presents the segmented resistor-string DAC architecture with the MSB and LSB strings. $V_{ref,high}$ and $V_{ref,low}$ are the highest and lowest output reference voltages, respectively, from the DAC and are applied across the MSB string. The control signals, m and n from the bi-directional SR, are applied to the switches used to tap the output of the MSB and LSB string, respectively. Only one output is high at a time for each m and n bits. The total number of resistors in the segmented DAC and the total number of flip-flops in the bi-directional SR are now given by $(m+n)$ and the total switches in the DAC are given by $(2) \cdot (m+n)$. The voltage step, Δ_{MSB}, resolved by each resistor in the MSB string is given by

$$\Delta_{MSB} = \frac{V_{ref,high} - V_{ref,low}}{m}, \quad (6)$$

which is further resolved by the LSB string to voltage step, Δ, given by

$$\Delta = \frac{V_{ref,high} - V_{ref,low}}{m \cdot n}, \quad (7)$$

where $m \cdot n = 2^N$. Hence, the segmented architecture produces the same resolution as obtained by an N-bit resistor-string DAC, with reduced hardware count.

This architecture, however, suffers from the loading effect of the LSB string to the tapped MSB resistor as explained next. Let R_{MSB} and R_{LSB} be the respective resistances of each resistor in the MSB and the LSB string. The total series resistance of LSB string, $R_{LSB,T\ otal}$, is given by

$$R_{LSB,T\ otal} = n.R_{LSB}. \quad (8)$$

The equivalent resistance, $R_{MSB,Equivalent}$, of the tapped MSB resistor in parallel to $R_{LSB,T\ otal}$ is given by

$$R_{MSB,Equivalent} = R_{MSB} \parallel (n.R_{LSB}), \quad (9)$$

which is different from R_{MSB}. Hence, the voltage drop across the tapped MSB resistor is not exactly equal to $\Delta_{MSB,}$ as given by equation (6). It results in the generation of incorrect reference voltages at the output of the DAC. The loading effect of the LSB string to the MSB string can be avoided simply by adding buffers between the MSB and the LSB string then

$$R_{MSB,Equivalent} = R_{MSB.} \quad (10)$$

It means, that effectively there are m resistors in series in the MSB string, with each resistor generating Δ_{MSB} as given by equation (6), which is exactly the same as required. Hence, with the proper choice of LSB string resistors, the loading effect can be avoided.

VI. Simulation results

Systematic top-down test-driven methodology is employed throughout the project. Initially, MATLAB models are used to compare the CT systems with the sampled systems. The complete CTDSP system is implemented in Cadence design environment. The architecture of the DM ADC system ,as shown in Fig.8. is used to realize a high level working model of an 8- bit ADC system employing the proposed segmented DAC architecture.

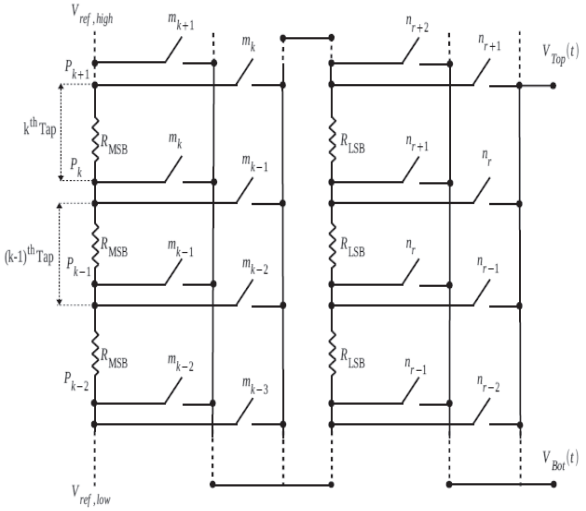

Figure 11: Resistor-string segmented DAC architecture.

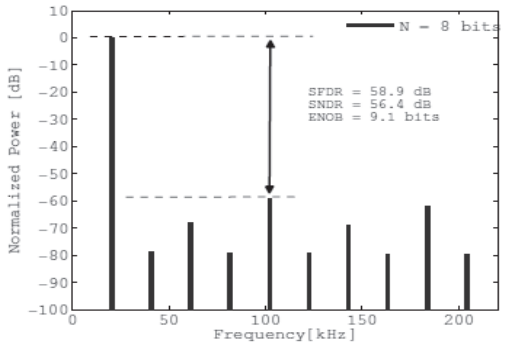

Figure 12. Output frequency spectrum of an 8-bit DM ADC with 16×16 shared MSB resistor DAC, 20.416 kHz input frequency and 220 kHz band of interest.

Table II. Comparision of components, SNDR and ENOB obtained for 8-bit system for different types of DACs.

Parameter	8-bit ADC with Resister string DAC	8-bit ADC with Segmented-Resister-string DAC
Frequency band	220	100
SNDR(dB)	56.5	67.5
ENOB	9.1	10.9
Resisters in DAC	512	64
Switches in DAC	256	33
D Flip-flop in DAC	256	32

The noise immunity to the system is provided by adding an offset of $\Delta/4$ to the lower comparator of the CTADC. The system is tested with an input sinusoid of frequency 20.416 kHz, the SNDR obtained for the 8-bit system is around 56.5 dB when considering the band of interest as 220 kHz. For the smart dust application, a resolution as high as 8-bit is not required. It is possible to reduce the number of bits to 3-bits and still be able to detect the signal at the input and process it.

The figure 12. presents the spectrum of an 8-bit ADC system plotted . It can be observed that the odd order harmonics are dominating in the spectrum and even order harmonics are suppressed by more than 80 dB. Hence no noise floor.

Table II presents a comparison of the SNDR and ENOB for an 8- bit ADC using resister string DAC and 8- bit ADC using segmented resister string DAC. The SNDR improvement can be observed when the band of interest is reduced from 220 kHz to 100 kHz and improvement of ENOB is also clearly observed.

It has been shown that the sensitive feedback DAC or resistor string DAC used in the ADC can be modified further to a segmented structure, which helps in reducing the overall components(resistors, switches, and D Flip-flops) observed is approximately 87.5%. in the design. The savings are doubled for systems utilizing similar DAC at the DSP output.

The hardware overhead for ADC system utilizing the proposed segmented architecture reduces drastically compared to the ADC using resistor string DAC. Hence, it is possible to design an N-bit ADC with a segmented DAC architecture which utilizes lesser hardware compared to its resistor string counterpart and provides better performance.

The transient response of the 8-bit system with 8-bit ADC, 8-bit DSP and 8-bit output DAC with 20.4 kHz input frequency. The overall output of the system is shown on the right side of the figure, *OutChange* and *outDirection* are the tokens generated by the digital delta modulator.

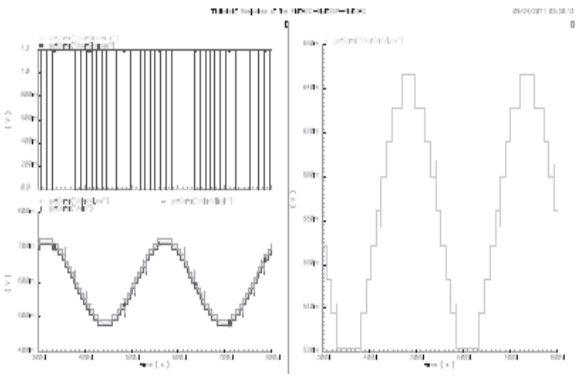

Figure 13. Transient response of the 8-bit system with a 8-bit ADC, 8-bit DSP and 8-bit output DAC and 20.4 kHz sinusoidal input frequency.

CONCLUSION

This paper presents Continuous time ADC and DSP system for smart dust and wireless applications it is concluded that the CT processing is very well suited for the smart dust application. The noise immunity to the system is provided by adding an offset of $\Delta/4$ to the lower comparator of the CTADC.

To validate the presented theory, an 8-bit ED ADC system is designed. It has been shown that the sensitive feedback DAC used in the ADC can be modified further to a segmented structure, which helps in reducing the overall components in the design. The Lower SNDR obtained for the 8-bit system as there is no noise present in the output spectrum.

The presented system CTADC or the ED ADC and CT DSP section can be potential area and energy saver and its suitability for smart dust and wireless applications is shown.

REFERENCES

[1] B.Warneke, M. Last, B. Liebowitz, and K. S. J. Pister, "Smart Dust: communicating with a cubic-millimeter computer," *Computer*, vol. 34, no. 1, pp. 44– 51, 2001.

[2] Y. Tsividis, "Continuous-time digital signal processing," *Electronics Letters*, vol. 39, no. 21, pp. 1551–1552, 2003.

[3] Y. Tsividis, "Event-Driven Data Acquisition and Digital Signal Processing_A Tutorial," *Circuits and Systems II: Express Briefs, IEEE Transactions on*, vol. 57, no. 8, pp. 577–581, 2010.

[4] B. Schell and Y. Tsividis, "A Continuous-Time ADC/DSP/DAC System With No Clock and With Activity-Dependent Power Dissipation," *Solid-State Circuits, IEEE Journal of*, vol. 43, no. 11, pp. 2472–2481, 2008.

[5] Y. Tsividis, "Digital signal processing in continuous time: a possibility for avoiding aliasing and reducing quantization error," *in Acoustics, Speech, and Signal Processing, 2004. Proceedings. (ICASSP '04). IEEE International Conference on*, vol. 2, pp. ii–589–92 vol.2, 2004.

[6] Y. Tsividis, "Event-driven data acquisition and continuous-time digital signal processing," *in Custom Integrated Circuits Conference (CICC)*, 2010 IEEE, pp. 1–8, 2010.

[7] D. Johns and K. W. Martin, Analog integrated circuit design. New York: Wiley, 1997.

[8] B. Schell and Y. Tsividis, "Analysis and simulation of continuous-time digital signal processors," *Signal Processing*, vol. 89, pp. 2013–2026, 10 2009.

[9] B. Schell and Y. Tsividis, "A Low Power Tunable Delay Element Suitable for Asynchronous Delays of Burst Information," Solid-State Circuits, IEEE Journal of, vol. 43, no. 5, pp. 1227–1234, 2008.

[10] M. Kurchuk and Y. Tsividis, "Energy-efficient asynchronous delay element with wide controllability," *in Circuits and Systems (ISCAS), Proceedings of 2010 IEEE International Symposium on*, pp. 3837–3840, 2010.

[11] B. Schell, Continuous-time digital signal processors : analysis and implementation. *PhD thesis, Columbia University*, 2008.

FPGA Implementation of OFDM Transceiver

R. Ganesh[1] and S. Sengupta[2]
[1]CVR College of Engineering/ECE Department, Hyderabad, India
Email: rachaganesh@gmail.com
[2] CVR College of Engineering/ECE Department, Hyderabad, India
Email: sengupta_santudas@yahoo.co.in

Abstract—**The OFDM is a multi-carrier modulation scheme in which the available carrier bandwidth can be divided into N number of orthogonal carrier frequencies and the data can be shared by these multiple carriers. This paper describes the design and implementation of OFDM transceiver using single FPGA board. The design methodology used is the 8-point IFFT/FFT with radix-2 with QPSK modulation scheme. The design unit consists of a back to back connected OFDM transmitter and receiver with QPSK framer, IFFT, PISO, SIPO, FFT and QPSK de framer etc. All these blocks are designed and simulated using Xilinx ISE 12.4 design suite. Finally the transceiver is implemented on Xilinx Virtex 5 LX110T FPGA with a data rate of 8, 16, 32 Mbit.**

Index Terms— **OFDM, FFT, IFFT, FPGA, QPSK**

I. INTRODUCTION

The growth of the wireless communication has produced a strong demand for advance wireless communication. Orthogonal Frequency Division Multiplexing (OFDM) is a state of the art modulation technique for high speed wireless communication with resistant to fading. The OFDM is a special form of Multi carrier Modulation which was originally used in high frequency radio. An efficient way to implement OFDM by means of Discrete Fourier Transform (DFT).The computational complexity would be reduced by a Fast Fourier Transform (FFT).Recent advances in VLSI Technology have enabled cheap and fast implementation of FFT's and IFFT's.

The data transmission over a wireless communication channel can be done by using a carrier signal with the help of modulation. The transmission can be done by using either a single carrier modulation or multi carrier modulation. In a single carrier modulation scheme each data symbol is transmitted sequentially on a single carrier i.e. signaling interval equal to data symbol duration [4]. The problem with single carrier modulation is the modulated carrier is occupies the entire available bandwidth. This problem can be solved by using multi carrier modulation. In a multi carrier modulation scheme N sequential data symbols are transmitted simultaneously on N multiple carriers i.e. signaling interval equal to N time's data symbol duration [4]. Here the available band width is divided into N number of sub carriers; hence it is bandwidth efficient compared to single carrier modulation.

The Orthogonal Frequency Division Multiplexing (OFDM) is one of the multi carrier modulation techniques for data transmission. In OFDM all the sub carriers are orthogonal to each other. The concept of conventional multi carrier and orthogonal multi carrier techniques are shown in Fig.1 (a) and Fig.1 (b) [5].

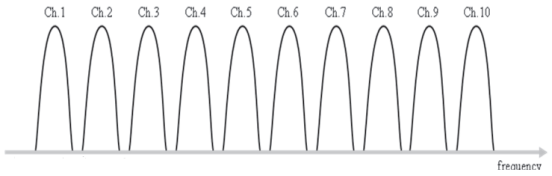

Figure. 1(a) Conventional Multi carrier technique

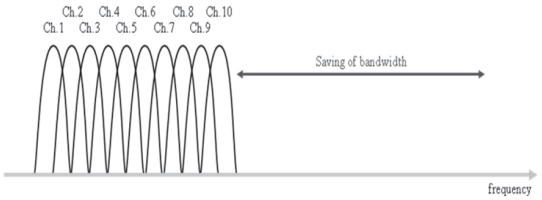

Figure. 1(b) Orthogonal Multi carrier technique

The Fig.2 shows block diagram of OFDM transmission system. The design consists of OFDM transmitter and receiver with different sub blocks. The OFDM transmitter accepts the serial data and this data is grouped in to n-bits and applied to IFFT through a bulk modulator like QPSK. The IFFT converts frequency domain signals into time domain signals and these signals are transmitted to receiver through parallel in serial out shift register with I (real) and Q (imaginary) channel data. At the receiver the received time domain data symbols are grouped with serial in parallel out and converted into frequency domain by using FFT with QPSK demodulation. The parallel frequency domain data is recovered in serial order using parallel in serial out shifter.

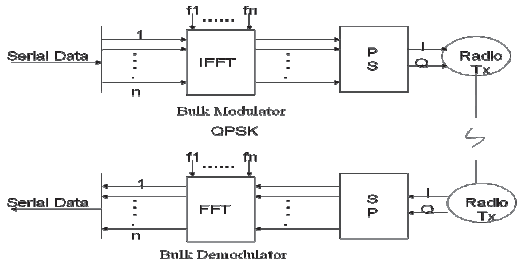

Figure.2 Block diagram of OFDM transmission system.

The objective of this paper is to develop the single FPGA based OFDM transceiver using bulk modulator and demodulator for high speed data transmission on

wireless media. The modulation is with QPSK and 8 sub carriers are used.

The 8-point IFFT/FFT is designed by using the fast implementation of IDFT/DFT equations using butterfly diagrams. The equation for DFT is given by [3].

$$X(k) = \sum_{n=0}^{N-1} x(n)\, W_N^{nk}$$

Where X(k) indicates the DFT of x(n) sequence and W_N^{nk} is the twiddle factor of the transform. The equation for IDFT is given by [3].

$$x(n) = 1/N \sum_{k=0}^{N-1} X(k)\, W_N^{-nk}$$

Where the x(n) is the inverse DFT of X(k), here n=8 and k=8.

The FPGA implementation of OFDM test set up with synthesis is explained in section II and Simulation results of each block is explained in section III. The FPGA implementation results are explained in section IV then conclusion in section V and references.

II. The FPGA Implementation of OFDM Test Setup

The FPGA implementation of OFDM needs a test setup. To provide the test set up the Fig.1 can be modified by removing two radios channels and directly connect the I/Q output values of transmitter to 1/Q input values of receiver. This setup will provide a back to back connected OFDM transmitter and receiver namely OFDM transceiver. This OFDM transceiver FPGA implementation test setup is shown in the Fig.3. The design is tested for 8, 16, 32 Mbit by using proper selection of input switches of FPGA.

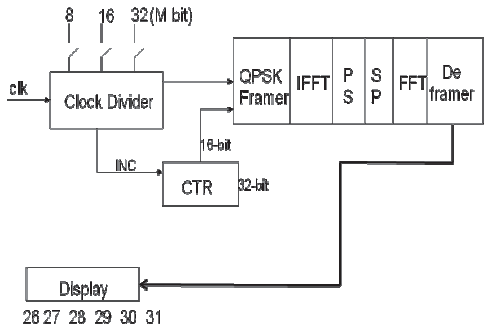

Figure.3 FPGA Implementation of OFDM transceiver test setup

The FPGA implementation of OFDM transceiver can be designed by using following blocks.

A. Counter

The serial I/P data to the OFDM transmitter can be applied by using a 16-bit counter. The 16-bit data is applied to QPSK framer.

B. QPSK framer

The QPSK framer accepts 16-bit data and converts every two bits data in to real and imaginary of constellation mapping as shown in Table 1. This QPSK framer block produces eight real and eight imaginary data values.

TABLE I
QPSK mapping

Input data	Output
00	1+j0
01	0+j1
10	-1+j0
11	0+j(-1)

C. IFFT

The eight complex pair outputs of QPSK framer is connected to the IFFT and the conversion from frequency domain to time domain can be done by using IEEE 754 floating point arithmetic operations on data and twiddle factors.

*D. PS and SP (**P**arallel in **S**erial out and **S**erial in **P**arallel out)*

The eight complex pair time domain IFFT output data (i.e. OFDM frame) is applied to PS and the output is taken serially and transmitted directly to the receiver first stage i.e. SP. The SP accepts serial input data from PS one after another and generates eight complex pair data as output (i.e. OFDM frame).

E.FFT

The eight complex pair outputs of SP (i.e. OFDM frame) is connected to the FFT and the conversion from time domain to frequency domain can be done by using IEEE 754 floating point arithmetic.

F. De framer

The De framer accepts eight complex pair data values and converts each pair of data in to two bit digital data according to de framer logic and produces 16-bit digital data as the output. This received 16-bit data should be same as the transmitted input data which is the output of 16- bit counter.

G. Clock Divider

The FPGA implementation of OFDM requires a clock signal frequency. The OFDM design frequency can be generated by converting the FPGA on-board clock frequency (i.e. 33Mhz) into different required frequencies by using the below formula.

$$\text{Required frequency} = \text{On-board frequency}/2^n$$

Where ‘n’ indicates the bit position in counter of frequency divider. Here the OFDM transceiver is running with three different frequencies of 0.5 MHz, 1 MHz and

2 MHz by using proper selection of input switches available on FPGA board.

H. Display

The eight Most Significant output bits of the OFDM transceiver is connected to the eight LED indicators of Xilinx Virtex-5 LX110T FPGA board.

III. Simulation Results

The total OFDM transceiver blocks are designed and simulated and implemented by using Xilinx ISE 12.4 design suite with the sub tools listed in Table 2.

TABLE 2
List of Tools under Xilinx ISE design suite

Design Action	Name of the Tool
Design Entry	HDL Editor (Verilog)
Synthesis	Xilinx Synthesis Tool(XST)
Simulator	ISim Simulator
Implementation	FPGA Editor, Plan Ahead
Device Configuration	iMPACT

The OFDM transceiver has back to back connected transmitter and receiver blocks. The QPSK framer, IFFT and PS blocks forms OFDM transmitter.

The OFDM transceiver is designed by using Verilog Hardware Description Language. The design is synthesized for generating the net list from the given specifications for the target FPGA board. The output of synthesis i.e. RTL schematic view of OFDM transceiver is shown in Fig.4.

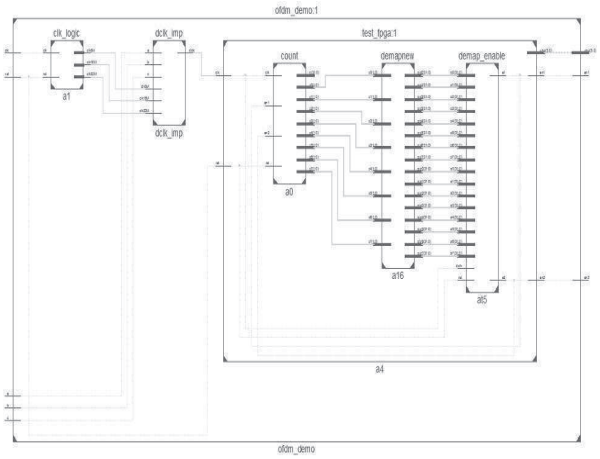

Figure.4 RTL Schematic of OFDM transceiver

The simulation results of all these blocks are shown in below figures. The Fig.5 shows the simulation results of OFDM transceiver data input counter.

The Fig.6 shows the simulation results of QPSK framer by accepting 16-bit input data from counter. This block generates eight real and eight imaginary modulated time domain signals.

The Fig.7 shows the simulation results of IFFT of QPSK framer output and generates eight real and eight imaginary frequency domain signals.

The IFFT output is connected to parallel in serial out shift register of transmitter. Since the design is back to back connected transceiver the parallel in serial out shift register output is directly connected to the first stage of receiver i.e. serial in parallel out shift register.

The SP, FFT and deframer forms OFDM receiver. The SP output is applied to FFT. The Fig.8 shows the simulation results of FFT. The FFT block generates eight real and eight imaginary frequency domain signals.

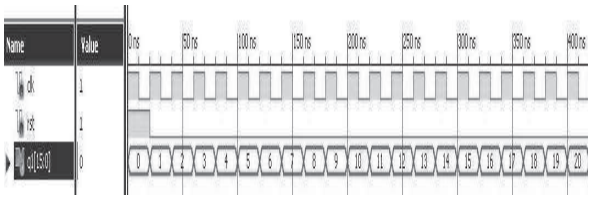

Figure.5 Counter simulation results

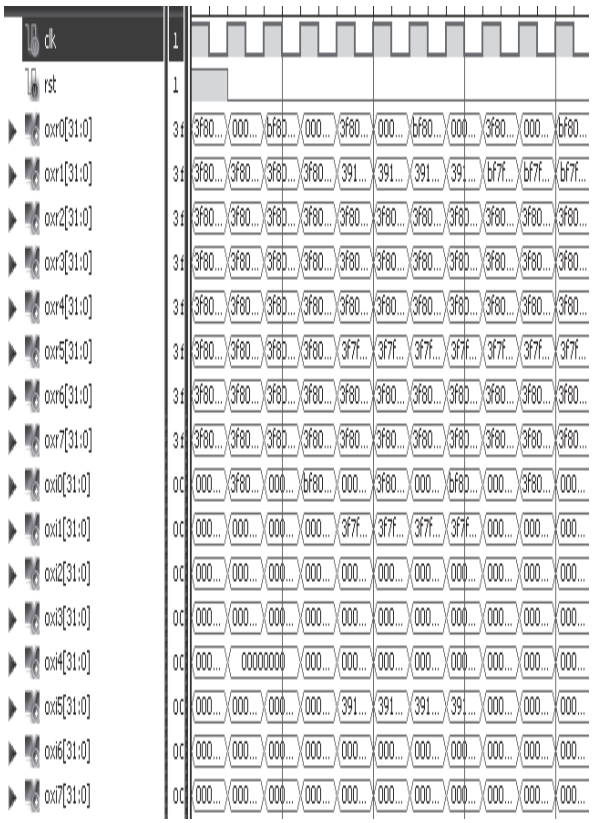

Figure.6 QPSK framer simulation

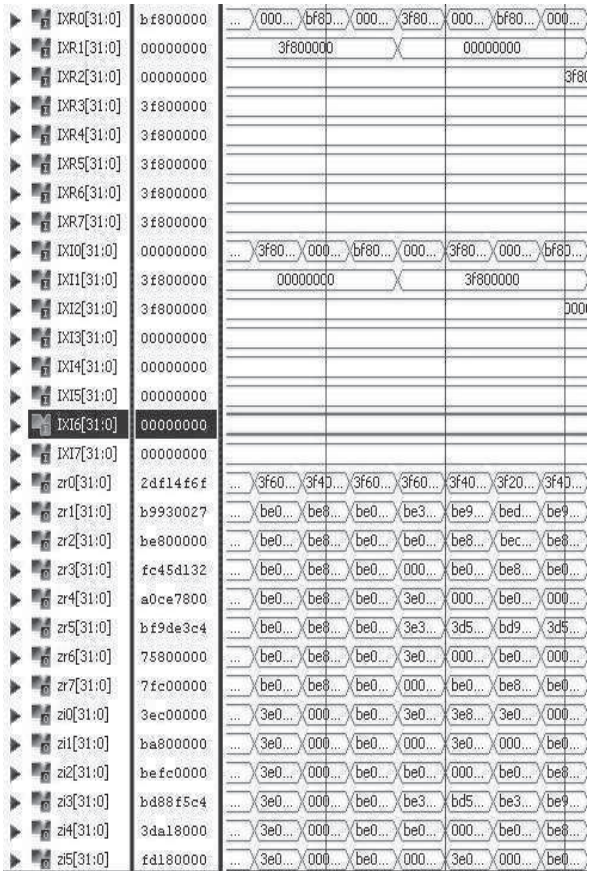

Figure.7 IFFT simulation results

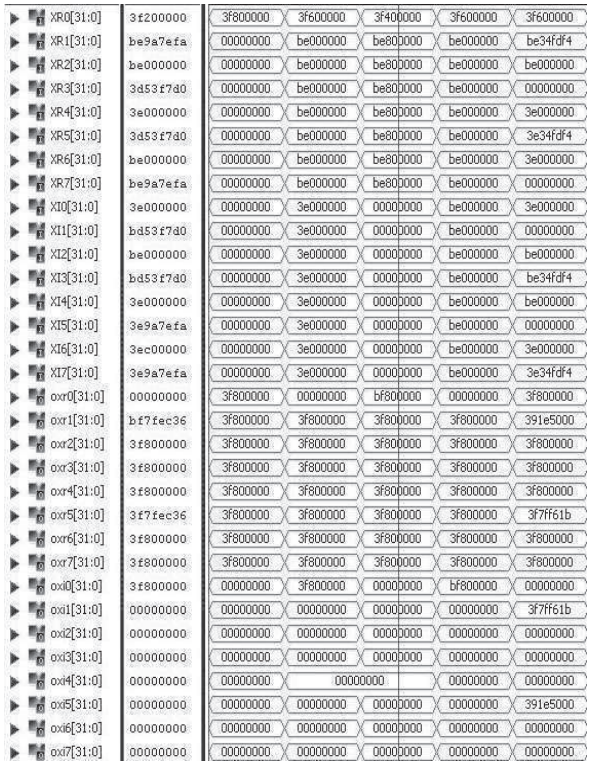

Figure.8 FFT simulation results

The FFT output is demodulated by using QPSK with the help of demapping logic by using deframer. The simulation result of deframer logic is shown in Fig.9. The simulation results guarantees that the functionality of OFDM transceiver is correct and the design can be used for FPGA prototyping for real time functional checking.

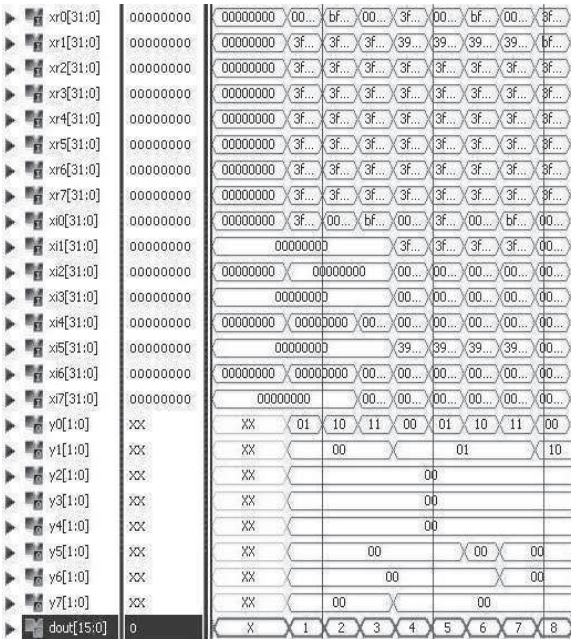

Figure.9 Defframer simulation results

IV. FPGA IMPLEMENTATION OF OFDM TRANSCEIVER

After the functional verification of the OFDM transceiver this design is used for implementation by using Xilinx Virtex 5 XC5VLX110T.The FPGA implementation of OFDM transceiver result is shown in Fig.10.

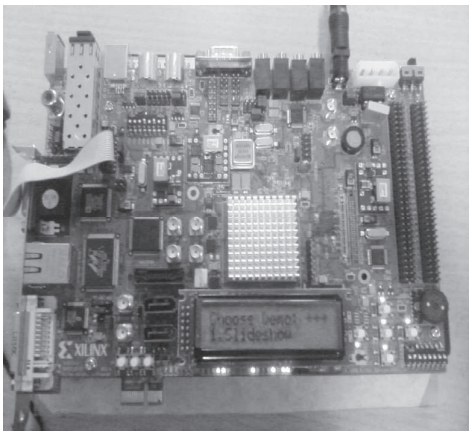

Figure.10 FPGA Implementation of OFDM Transceiver

CONCLUSIONS

The main focus of this work is to design 8-point IFFT/FFT based back to back connected OFDM transceiver using single FPGA. In this work the design, simulation and implementation of OFDM transceiver using Xilinx ISE Design suite for Virtex 5 FPGA is completed. The design functionality is verified for 8, 16, and 32 Mbit data rates.

The design can be extended by isolating OFDM transmitter and receiver using two FPGA boards.

REFERENCES

[1] Atul Govindrao Pawar,*"Wireless Communication in Missiles: Challenges"*, Hyderabad, DRDO Science Spectrum, March 2009, pp.230-235.

[2] Hemant Kumar Sharma, Sanjay P. Sood, Balwinder Singh, *"Design of COFDM Transceiver Using VHDL",* International Journal of Computer Applications (0975 – 8887), Volume 5– No.7, August 2010.

[3] Poonam Agrawal, Vikas Gupta*,"Enhanced Core Processor Blocks of OFDM System",* International Journal of Electronics Communication and Computer Engineering, Volume 1, Issue 2, 10/09/2011.

[4] Dr. Miguel Rodrigues*,"Orthogonal Frequency Division Multiplexing: (OFDM A Primer)",* Laboratory for Communication Engineering, University of Cambridge.

[5] Klaus Witrisal, *"Presentation on OFDM Concept and System-Modeling",* Technical University Graz, Austria, VL: Mobile Radio Systems, Ch. 5: Wideband Systems, 24-Nov-05.

Transmission of Message between PC and ARM9 Board with Digital Signature using Touch Screen

R.R. Dhruva[1] and V.V.N.S. Sudha[2]
[1] CVR College of Engineering, Hyderabad, India.
Email: rinkudhruva.ravi@gmail.com
[2] Aurora's Technological and Research Institute, Hyderabad, India.
Email: vedantam_sudha@yahoo.com

***Abstract*—This paper deals with the Transmission of message between ARM9 board and Personal Computer. This system can be used as a paperless fax machine. The main advantage of this paper is to create a paperless office and to store the fax for future references. Here, a PC is used as first fax machine and ARM9 board is used as second fax machine. The message is typed in the System and sent to ARM9 board. The user can read the message on the touch-screen and do the digital Signature using Stylus, if required and send back to the PC. A copy of the message as well as the Signature is stored in the pen-drive connected to USB of ARM9 board for future references. The processor used is S3C2440 and Qtopia is the cross-compiler used. Various widgets are created in Qtopia using CPP as the programming language. Firstly, Porting is done in order to load the Bootloader, Kernel and Root File System. Then various widgets are created in Qtopia. Ethernet cable is used to connect the PC and the ARM9 board. Linux Operating System is used.**

***Index Terms*—ARM9, Qtopia, Porting**

I. INTRODUCTION

Samsung S3C2440A is a 16/32-bit RISC microprocessor. Samsung S3C2440A is designed to provide hand-held devices and general applications with low-power, and high-performance micro-controller solution in small die size. The ARM processor is a Reduced Instruction Set Computer (RISC). The S3C2440 is a 32 bit microcontroller that internally integrates ARM920T of the ARM Company [9]. ARM920T implements 5-stage pipeline architecture and separate 16KB Instruction cache and 16KB Data cache which are used for faster performance. The S3C2440 have some integrated on-chip functions such as LCD controller, RAM controller, 3 paths UART, 4 paths DMA, 4 path with PWM of Timer, parallel I/O port, 8 channels of 10-bit ADC, the interface of touch screen, I2C interface, two USB interface controllers, two channels SPI, the main frequency of S3C2440 up to 400MHz [4]. The Figure below shows the MINI2440 on-board peripherals layout. The Transmission of Message with Digital Signature on Touch Screen using ARM9 application is implemented in ARM9 board using QT.

The proposed model consists of S3C2440, PC, Touch Screen and Ethernet cable. The transmission of data between S3C2440 and PC is done through this Ethernet cable.

ARM9 board is considered as one fax machine and PC as another. The message or fax is sent from PC to board. The user can do the signature on touch screen of the board and should click on the save option. A copy of the message as well as the signature is saved in the pen-drive for future reference. Single touch panel added to conventional fax machine-replaces the scanning and printing units. Touch panel acts as an input device as well as displaying device, which can detect the location being touched. Handwriting reconstruction algorithm is used internally in the board itself to turn a user's signing act into a digital signature, close to the original as much as possible. The document containing the message as well as the signature is sent back to PC and is seen by typing the IP address of the board in URL of the web-browser.

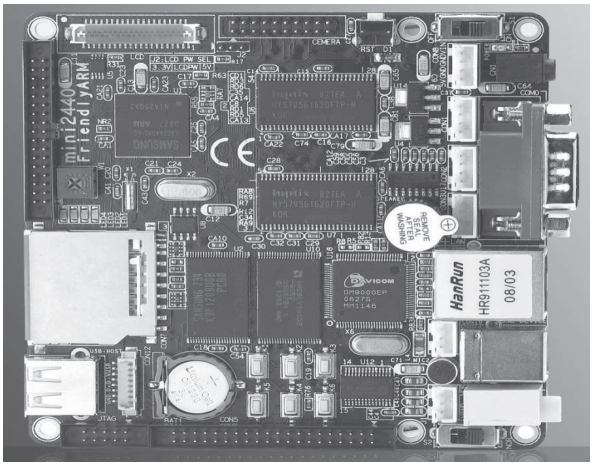

Figure 1: Mini2440 Development Board

Qtopia is used to create various components on the touch screen such as widgets. The operating System used is Linux and programming is done using CPP.

The procedure for implementing this project is as follows:

- The First step is porting of boot loader , kernel , root file system into S3C2440 board.
- The next step is to develop the application in QT using CPP.
- Then the output can be seen by typing the message to be transmitted in hyper terminal of personal computer. Then the message is displayed on the

Touch Screen of ARM9 board. Digital Signature is done using Stylus and a copy of Signature and message is stored in the pen drive.

- The message is again sent back and retrieved on PC by giving the IP address of board in the URL of web-browser.

Qtopia is used for set of applications with GUI running on desktop environment and general application based on interface. It supports cross compilation for all multiple boards (open source GUI environment). Qtopia 2.2.0 controls embedded related devices on target board and compatible with Fedora 9 and ubuntu.

- Qt_Embedded is a C++ toolkit for GUI and application development for embedded devices. It runs on a variety of processors, usually with Embedded Linux.
- Qt_Embedded based applications write to the Linux frame buffer directly and includes several tools to speedup and ease in development in testing and debugging of applications.
- Applications targeted for Embedded Linux can be developed using standard Qt tools, including Qt Designer for visual form design, and with tools specifically tailored to the embedded environment.

II. RESULTS

1) Load the files of bootloader, kernel and file system into the board by switching the board on, in NOR flash.

2) After loading the above files switch to NAND flash mode.

3) Restart the board and calibrate the touch screen.

4) Open the port terminal using Debug Port.

5) Open the hyperterminal. Select com1 Port and set the Baud rate to 115200.

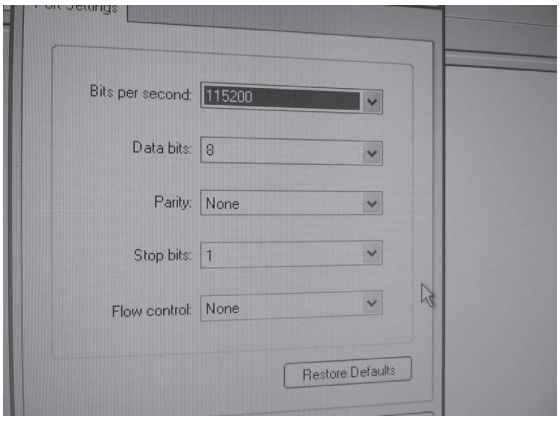

Figure 2: Entering 11,5200 as baud rate

On the Personal Computer we need to enter the message which has to be transferred to the board.

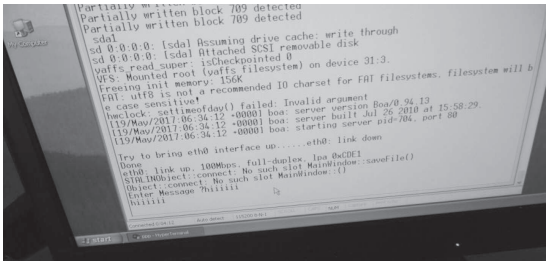

Figure 3: Entering message on PC
Digital signature is done in the space provided

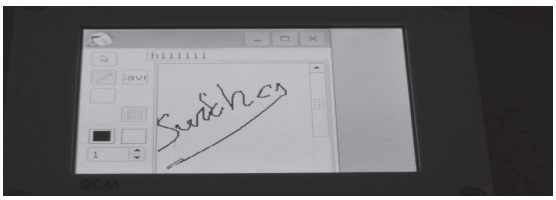

Figure 4 : Digital Signature done in widget provided
Saving the message as well as the signature by pressing save on widget in the touch screen.

Figure 5 : Clicking the save option to save a copy of image in the pen drive

The message as well as the signature is sent back to the PC. It is observed by typing the IP address of the kit in the URL of the web-browser.

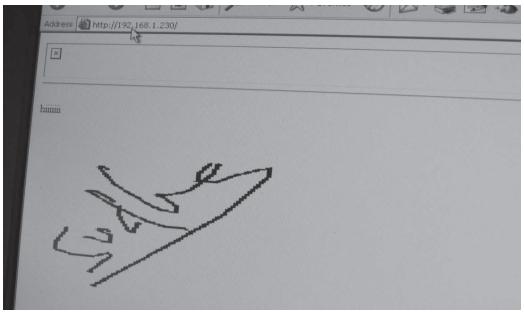

Figure 6: Retrieval of message as well as digital signature on PC

III. Conclusion

The model "Transmission of Message with Digital Signature on Touch Screen using ARM9" has been successfully designed and tested.

It has been developed by integrating features of all the hardware components and software used. Presence of every module has been reasoned out and placed carefully thus contributing to the best working of the unit.

Secondly, using highly advanced ARM9 board and with the help of growing technology the project has been successfully implemented.

IV. Future Scope

In the future scope we can go with the usage of touch screen monitor PC's where the ARM board can be directly interfaced to the PC's. Here in this we are going to reduce the extra touch screen panel connected to the ARM board by using touch screen monitors where we can read the received data and we can do the necessary modifications require and can send the modified data and keep the copy of the data inside the memory.

We can also have alert message to your mobiles whenever a new fax is received and also can have alert message with voice by using voice play back recorder circuit like "You received a new FAX ". In this way we are reducing the cost and complexity of the circuit. Here in this concept we are totally eradicating the usage of paper which reduces the environmental pollution.

References

[1] "Linux transplantation based on the processor S3C2440" by Sun Yanpeng,peng peng,Zhang Yuan, 2009.
[2] Beginning Linux Programming, Third Edition, Neil Matthew and Richard Stones.
[3] http://www.friendlyarm.net
[4] www.kernel.org
[5] www.linuxjournal.com/magazine
[6] http://www.arm.com/
[7] http://www.w3schools.com/php
[8] http://www.datasheetcatalog.com
[9] ITU-T.37: Procedures for the Transfer of Facsimile Data via Store-and forward on the Internet, 1998.
[10] ITU-T.38: Procedures for Real-time Group 3 Facsimile Communication over IP Networks, Amendment 1, 1999.
[11] Handwriting Recognition Group, <hwr.nici.kun.nl>, May, 2008.
[12] ITU-T.4: Standardization of Group 3 facsimile terminals for document transmission, 1996
[13] ITU-T.30: Procedures for document facsimile transmission in the general switched telephone network, 1996
[14] http://en.wikibooks.org/wiki/C++_Programming

A Novel Source Based Min-Max Battery Cost Routing Protocol for Mobile Ad Hoc Networks

Humaira Nishat[1]
[1] CVR College of Engineering/ECE Department, Hyderabad, India
Email: huma_nisha@yahoo.com

Abstract—**In the existing energy efficient routing protocols for mobile ad hoc networks such as minimum battery cost routing (MBCR) and min-max battery cost routing (MMBCR) the cost functions are calculated in the route request phase and the decision of selecting a route is taken by the destination node. It is more cost effective and energy efficient if the cost functions are calculated in the route reply phase and the decision of selecting a route for data transmission is taken by the source node. In this paper I propose a novel routing algorithm for mobile ad hoc networks called Source based min-max battery cost routing (SBMMBCR) protocol wherein the routing decision is taken by the source node considering the changes in energy levels during the route reply phase. The performance of the proposed protocol is compared with the existing MMBCR protocol based on application oriented metrics such as throughput, packet delivery ratio, end-to-end delay, normalized routing load and residual energy. Simulation is carried out using NS2. From the simulation results it is observed that the proposed protocol SBMMBCR outperforms MMBCR by giving more network lifetime as well as better throughput, packet delivery ration. Average end-to-end delay is less and the residual energy is also more for SBMMBCR as compared to MMBCR protocol.**

Index Terms—**Cost function, Energy level, Routing protocols, MANETs, Network lifetime, Throughput, Packet delivery ratio, Delay, Residual energy, Normalized routing load.**

I. INTRODUCTION

Mobile ad hoc networks [MANETS] [10], have gained significant attention in the past several years due to the characteristics of being infrastructureless, mobile and robust. Nodes in MANETS generally rely on batteries for their operation [4]. Due to the limited lifetime of these energy sources, battery power [1], [3] is one of the most important constraints for the operation of the ad hoc network. Extensive research efforts have been dedicated to both developing energy efficient protocols and improving the throughput of a MANET [5], [6], [7]. In this paper I have considered the problem of routing in an ad hoc network from energy efficiency point of view. Other quality of service parameters like throughput, delay, packet delivery ratio, residual energy and routing overhead are also evaluated and compared with the existing routing protocol.

The rest of the paper is organized as follows. In section 2 we present the theoretical analysis of existing energy efficient protocols. The concept of designing the proposed SBMMBCR protocol is described in section 3. The simulation scenario is presented in section 4 followed by the simulation results in section 5. Finally, section 6 concludes the paper.

II. THEORETICAL ANALYSIS OF EXISTING ENERGY EFFICIENT ROUTING PROTOCOLS

Here I present a brief description of the existing energy efficient routing protocols-MBCR and MMBCR [2]. In minimum battery cost routing (MBCR), individual battery costs are taken into consideration while selecting the route i.e., the path selected must not contain the nodes that have less remaining battery capacity. The route cost function is the sum of the individual cost functions of the nodes and a route with less energized node may be selected which is a demerit. Whereas min-max battery cost routing (MMBCR) selects a route based on the battery capacity of all the individual nodes. The cost functions are calculated during the route request phase and the decision of selecting a route is taken by the destination node. But the main disadvantage is that once a route with minimum cost function is selected; same route is used unless the data transmission is completed or unless the network fails due to exhaustion of less energy nodes in that route. Also since the cost functions are calculated in route request phase there are chances of changes in energy levels of nodes during route reply which are not considered in MMBCR. In order to overcome the above mentioned problems a new mechanism is proposed and is implemented in MMBCR. This new protocol is named Source based min-max battery cost routing (SBMMBCR) protocol.

III. PROPOSED ROUTING PROTOCOL-SBMMBCR

The proposed routing algorithm aims to increase the network lifetime by considering the changes in the battery cost functions during the route reply phase thereby making the protocol more energy efficient. The basic idea used in this protocol is described below.

In the existing MMBCR protocol, the cost functions are computed and stored in route request (RREQ) packet header while these packets are sent from source to destination. The selection of a route for data transmission is done by the destination by calculating the cost functions stored in the route request (RREQ) packets. It actually takes some time for the route reply (RREP) packet to reach the source. The energy levels of the nodes

in the network may change during this period. Thus, the protocol does not consider these changes in energies while selecting a route. The proposed source-based MMBCR protocol overcomes this problem by calculating the cost functions in the route reply phase i.e., after receiving the RREP packets from each route; the source node selects a route for data packet transmission. The destination node receives RREQ packets through various routes and then replies to the source node immediately through the corresponding routes with RREP packets. During the process, the intermediate nodes calculate their cost functions, record the value in the RREP packet and follow the same process as was in MMBCR protocol. The source node waits for some time, receives the RREP packets and finally makes a decision of selecting the route with maximum lifetime. The route selected is used for sending the data packets. Another advantage of this SBMMBCR is that the source node receives all possible routes, stores it in the routing cache for future use. This feature is not available in MMBCR protocol.

IV. SIMULATION SETUP

The proposed algorithm is implemented using NS2 simulator [11], [12]. Fedora version 8 is used as operating system. The parameters used for carrying out simulation are summarized in table1 below.

TABLE I.
SIMULATION PARAMETERS

Parameter	Value
Routing Protocol	MMBCR & SBMMBCR
MAC layer	IEEE 802.11
Terrain Size	1000m*1000m
Number of nodes	10,20,30,40,50
Packet size	512 KB
Initial Energy	1.5 Joules
Idle power consumption	0.1W
T^x power consumption	0.1W
R^x power consumption	0.1W
Simulation time	100 seconds
Traffic source	UDP

V. SIMULATION RESULTS

A network scenario is created as an example network and is developed in Network Animator as shown in figure1 with Tool Command Language.

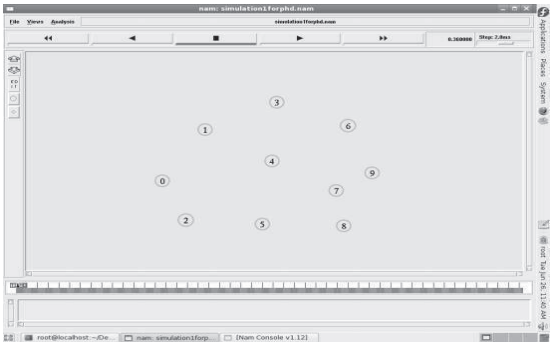

Figure 1. Screenshot showing a network scenario of 10 nodes

The network scenario shown in fig. 1 above consists of 10 nodes. For comparing the behavior of the two protocols, the positions of nodes in the network is fixed. Each node is assigned an initial energy of 1.5W. The TCL script is written in such a way that initially node 4 sends data packets to node 1 after initializing route discovery process at 0.5 seconds. By the end of simulation i.e., at 10 seconds node 4 has energy level of 1.046582W and node 1 has energy level 1.360537W. The neighboring nodes which have not contributed in data transmission process but were active during this period have their residual energies more than nodes 1 and 4. At 11 seconds, node 4 is made to transmit data to node 6 after initiating route discovery process and the simulation stops at 20 seconds. At 21 seconds, node 4 is made to transmit data packets to node 7 after reinitiating route discovery process. The simulation stops at 30 seconds. The main idea behind the above three simulations is to drain the energy of node 4 and it should be easy to observe the behavior of the two routing protocols as each node has a different energy level at a certain period. Consider another data transmission between node 0 and node 9 i.e., node 0 is the source node and node 9 is the destination node. The route discovery process is initialized at 31 seconds.

A. Route selection by MMBCR

MMBCR finds the maximum battery cost (i.e., minimum battery capacity) in a route, stores the value and then selects the route with minimum total cost function (i.e., the maximum battery capacity) during the route request phase. The destination node selects that route with the minimum value of the total cost among all the routes that exists between the source and the destination and sends it to the source node through route reply.

The routing protocol considers the individual node battery capacity apart from the total cost function in the selected route. The routes available between node 0 and node 9 are 0-1-3-6-9, 0-4-9, 0-5-7-9, 0-2-5-7-9, 0-5-8-9, etc. with respective cost functions 4.4145326, 6.298343, 3.507176, 4.38851, 3.505405, etc. Hence the route 0-5-8-9 is selected as it has the minimum cost function (i.e., maximum battery capacity) among all the routes mentioned above. Also each of the nodes in this route has maximum battery capacity compared to other nodes in other routes. For example 0-5-7-9 and 0-5-8-9 has almost same cost function but node 8 has more battery capacity and minimum cost function as compared to node 7. Thus, the route 0-5-8-9 is selected by the route discovery process. The advantage of MMBCR is that it avoids the route that has minimum battery capacity leading to enhancing the network lifetime. But the main disadvantage is that once a route with minimum cost function is selected; same route is used unless the data transmission is completed or unless the network fails due to exhaustion of less energy nodes in that route. The protocol does not monitor the individual node battery once a route is selected and does not consider the changes in energy levels during the route reply phase. At 47.9 seconds, node 5 dies due to exhaustion of its battery power resulting in route failure and partitioning of network. Node 5 as such was only an intermediate node in the data transmission process from 0 to 9.

B. Route selection by proposed protocol SBMMBCR

In case of SBMMBCR protocol, the route selection decision is taken by the source node after receiving the RREP packets from the destination node. At 31 seconds, route discovery process is initiated and after receiving the RREP packets with the updated cost functions in the route reply phase stored in it, the source node decides which route to be selected for transmission of data packets. This gives more accurate information of the energy levels of each node. The route failure time for the proposed SBMMBCR protocol is found to be 50.1 seconds which is much better compared to the existing MMBCR protocol. Fig. 2 below shows the network failure time of both MMBCR and SBMMBCR routing protocols.

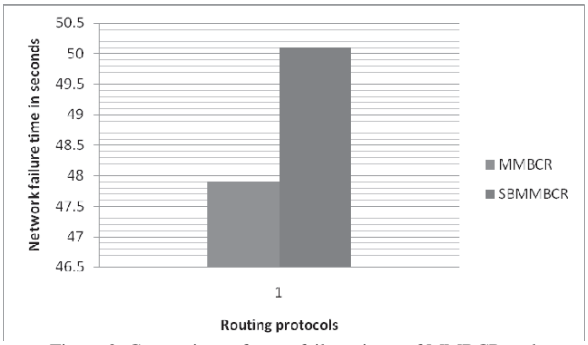

Figure 2. Comparison of route failure times of MMBCR and SBMMBCR

The following figures from 3 to 7 gives the performance comparison of both the routing protocols- MMBCR and SBMMBCR using UDP as the traffic source by varying the number of nodes. The performance comparison is based on residual energies of nodes, delay, packet delivery ratio, throughput and normalized routing load.

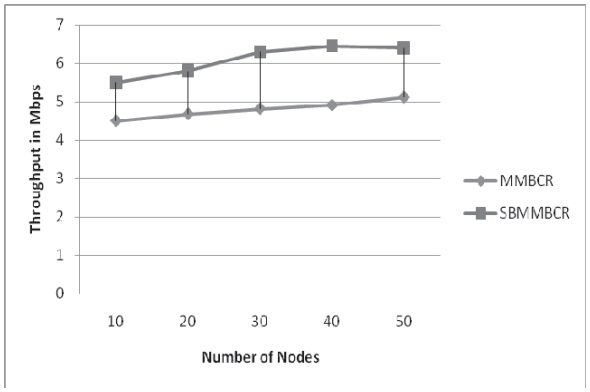

Figure 3. Throughput versus number of nodes

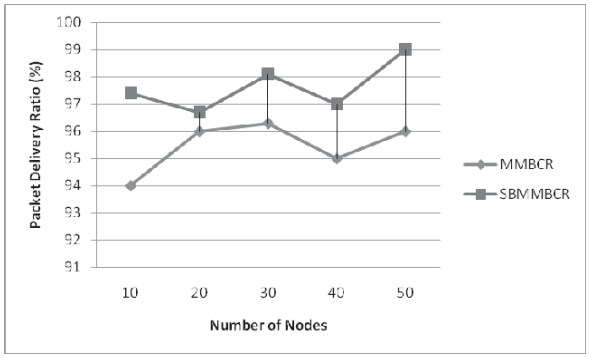

Figure 4. Packet delivery ratio versus number of nodes

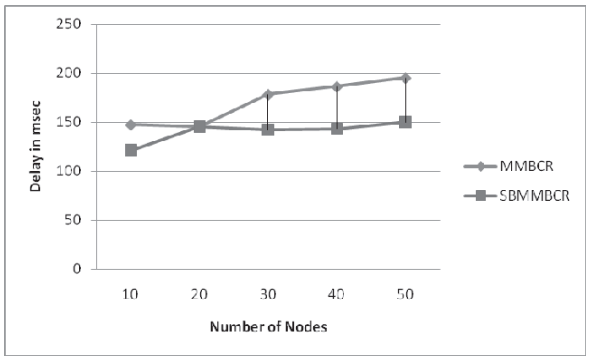

Figure 5. Delay versus number of nodes

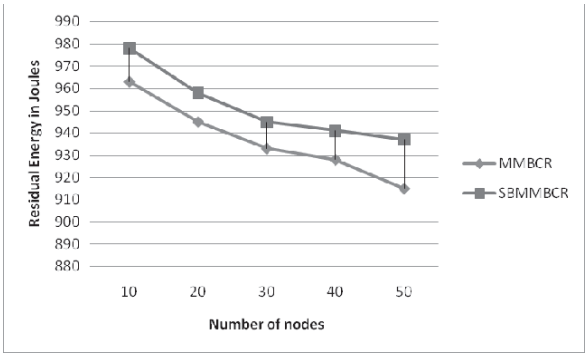

Figure 6. Residual energy versus number of nodes

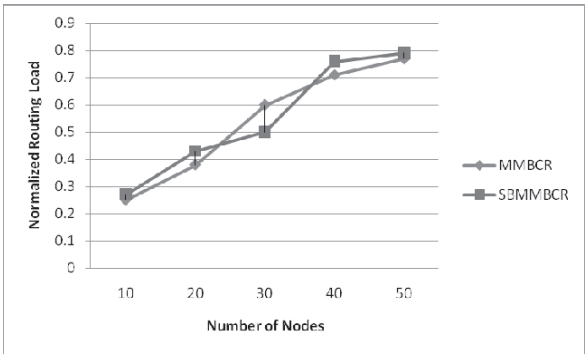

Figure 7. Normalized routing load versus number of nodes

CONCLUSIONS

In this paper, the existing MMBCR protocol is analyzed where the cost functions are calculated in the route request phase and the decision of selecting a route is taken by the destination node. A novel routing algorithm for mobile ad hoc networks called Source based min-max battery cost routing (SBMMBCR) protocol is proposed wherein the routing decision is taken by the source node instead of destination node considering the changes in energy levels during the route reply phase. The performance of the proposed SBMMBCR protocol is compared with the existing MMBCR protocol based on application oriented metrics such as throughput, packet delivery ratio, end-to-end delay, normalized routing load and residual energy. From the simulation results it is observed that the proposed protocol SBMMBCR outperforms MMBCR by giving more throughput and packet delivery ratio due to extended network lifetime. The network lifetime for a 10 node network with UDP as traffic source is found to be 47.9 seconds whereas for the proposed protocol it is 50.1 seconds. Delay and normalized routing load is also comparatively less for SBMMBCR as compared to MMBCR. Residual energy though decreases with time is more for SBMMBCR as compared to MMBCR protocol.

REFERENCES

[1] Samir R. Das, Charles E. Perkins and Elizabeth M. Royer, "Performance Comparison of Two On-Demand Routing Protocols for Ad Hoc Networks", *Proceedings of IEEE INFOCOM 2001* , pp. 3-12, March 2001.

[2] C. K. Toh, "Maximum Battery life Routing to Support Ubiquitous Mobile Computing in Wireless Ad Hoc Networks", *IEEE Communications Magazine*, vol. 39, no. 6, pp. 138-147, June 2001.

[3] C. F. Chiasserini and R. Ramesh Rao, "Improving Battery Performance by Using Traffic- Shaping Techniques", *IEEE Journal on Selected Areas in Communications,* vol.19, no. 7, pp. 1385-1394, July 2001.

[4] C. F. Chiasserini and R.Ramesh Rao, "Energy-Efficient Battery Management", *Proceedings of IEEE INFOCOM 2000,* vol. 2, pp.396-403, March 2000.

[5] L. M. Freeney, "An Energy Consumption Model for Performance Analysis of Routing Protocols for Mobile Ad Hoc Networks"*, Mobile Networks and Applications,* vol. 6, pp. 239-249, 2001. J. Clerk Maxwell, *A Treatise on Electricity and Magnetism*, 3rd ed., vol. 2. Oxford: Clarendon, 1892, pp.68–73.

[6] L.M.Feeney and M. Nilsson, "Investigating the Energy Consumption of a Wireless Interface in an AD Hoc Networking Environment", Proceedings of IEEE INFOCOM 2001, Volume 3, Anchorage A.K. April 2001, pages 1548-1557.

[7] Marwan Krunz, Alaa Muqattash and Lee, "Transmission Power Control in Wireless Ad Hoc Networks: Challenges, Solutions and Open Issues", *Proceedings of IEEE INFOCOM 2003*, vol.1, 2003.

[8] Sharad Agarwal, R. H. Katz, V. Krishnamurthy and S. K. Dao, "Distributed Power Control in Ad Hoc Wireless Networks", *Proceedings of IEEE PIMRC 2001*, vol.2, pp. 59-66, October 2001.

[9] Vikas Kawadia and P. R. Kumar, "Power Control and Clustering in Ad Hoc Networks", *Proceedings of IEEE INFOCOM 2003*, vol.1, pp. 459-469, April 2003.

[10] M. Adamou, S. Sarkar, "A Framework for Optimal Battery Management for Wireless Nodes", *Proceedings of IEEE INFOCOM 2002*, pp. 1783-1792, June 2002.

[11] UCB/LBNL/VINT Network Simulator http://www.mash.cs.berkeley.edu/ns/referred on March 2010.

[12] "The Network Simulator–ns-2", available at http://www.isi.edu/nsnam/ns/referred on march 2010

Design of Static Random Access Memory for Minimum Leakage using MTCMOS Technique

T. Esther Rani [1] and Dr. Rameshwar Rao [2]
[1] CVR College of Engineering, Dept of ECE, Hyderabad, India
estherlawrenc@gmail.com
[2] Hon'ble VC, JNT University, Hyderabad, India
Rameshwar_rao@hotmail.com

Abstract—**This work involves implementation of 8x8 SRAM using Multi Threshold CMOS (MTCMOS) technique which reduces the leakage power by placing sleep transistor either between ground and pull-down network or V_{DD} and pull up network. SRAM is designed using D-Latch. As reduction in the leakage power is more by using PMOS sleep transistor compared to NMOS sleep transistor, this design is implemented using MTCMOS technique with PMOS as sleep transistor. The design can be used where low power is the constraint, as it offers 86% of power savings.**

Index Terms—**SRAM, leakage power, MTCMOS, sleep transistor.**

I. INTRODUCTION

Memory refers to bits that are stored in a structured manner. In a two dimensional array, a row of bits are accessed at a time. Some kinds of memory may be integrated along with the logic in VLSI chips. Memory can be a primary memory or memory for other purposes in computers and digital electronic devices. Generally in CPU, Read Only Memories (ROM) are used to store complex instruction set; Static Memory is used to hold recently used instructions and data and Dynamic Memory for complete operating system, programs and data. DRAM is volatile and SRAM is fast cache memory used in CPU. SRAM is faster but energy-consuming and offers lower memory capacity per unit area than DRAM and non-volatile like flash memory, ROM, PROM, EPROM and EEPROM. SRAM does not require periodical refreshing and is faster than DRAM, the access time is very less and consumes less power compared to DRAM[1].

SRAM operates in three modes. They are standby mode or idle mode, Read mode and Write mode[2]. In idle mode, the SRAM is disabled. In read mode the data is read from a selected address location. In write mode the data is written into a particular address location. SRAM is used in many embedded applications. SRAM is also used in different industrial and scientific subsystems and automotive electronics. There are design tradeoffs like, density, speed, volatility, cost, and features. Suitable SRAM is selected based on these parameters. Applications of Static Random Access Memories include the revolutionary Quad Data Rate, NoBL and MoBL SRAMs from Cypress required for communications in the networks.

II. MTCMOS TECHNIQUE

In MTCMOS technique, low-V_t transistors are employed for the implementation of the logic block and high-V_t transistors for gating the logic block from the power supply. For this purpose, virtual power supply rails are placed rather than direct connection from the real power supply. By placing high-V_t transistors in this manner, leakage power is very much reduced. During active mode, the normal operation of the circuit is performed and during standby mode high-V_t transistors called sleep transistors are switched off by enabling an input to the sleep transistor. Sleep device can be a PMOS transistor which will be placed in between pull up network and V_{DD} or an NMOS transistor which will be placed in between pull down network and ground.

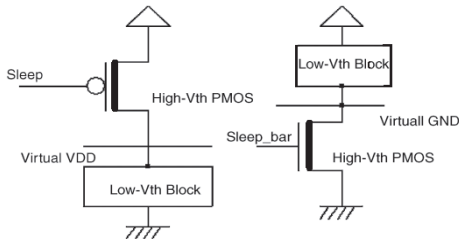

Figure 1: MTCMOS method

Effectiveness of MTCMOS in reducing power dissipation has been verified by implementing SRAM and the author observed great power savings as discussed.

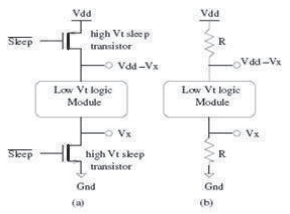

Figure2 : Sleep Transistors in MTCMOS circuits

MTCMOS circuit with both PMOS and NMOS as sleep devices is shown in figure 2.

Performance of a system can be improved by reducing leakage current. Sub-threshold leakage current is reduced by the sleep transistor with high Vt and performance loss is controlled. In MTCMOS Technique, there a disadvantage that, in sleep mode, the data that is stored in latches and flip-flops of logic blocks cannot be preserved when the power supply is turned off [3].

III. IMPLEMENTATION OF SRAM USING MTCMOS DESIGN WITH PMOS AS SLEEP TRANSISTOR

A high V_{th} PMOS transistor placed between V_{dd} and the logic block results in the MTCMOS design with PMOS sleep control transistor as shown in figure3.

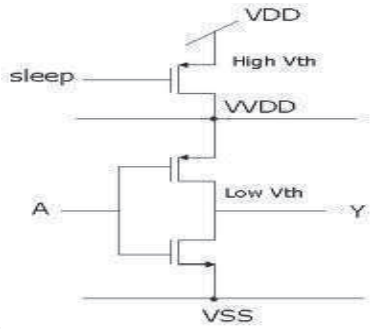

Figure 3 : MTCMOS design with PMOS sleep transistor for an inverter

The work involves in the implementation of SRAM using MTCMOS technique in Cadence Virtuoso Analog Design Environment. The design flow of SRAM is shown in figure 4[4,6].

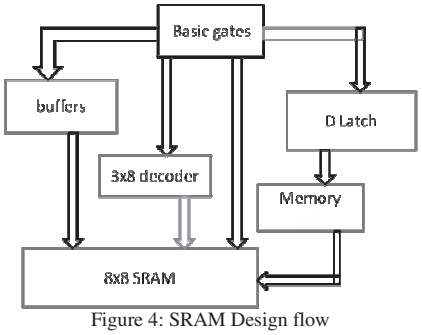

Figure 4: SRAM Design flow

A. D-LATCH WITH ENABLE

When an input of E is made '1', then the output of Q is same as the value on D. Now, the latch is said to be "open" and the path from D to Q is "transparent". So, this is called as a *transparent latch*. When the input E is made '0', then the latch "closes" and the output of Q retains as previous value and the changes made on D do not appear on Q. Figure [5] shows the circuit of D-Latch with enable.

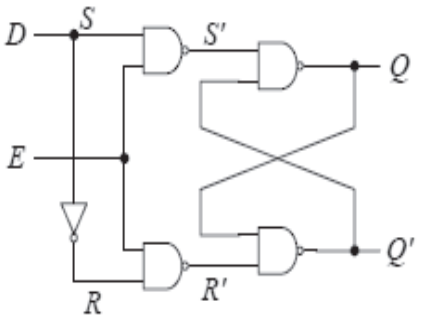

Figure5: D-Latch with enable

B. TRISTATE BUFFER

A tri-state buffer has three states. They are 0, 1, and *Z*. The value *Z* represents a high-impedance state, which acts like an open switch. The symbol, truth table and gate level circuit of tri state buffer is shown in figure 6 [5].

When *E* is made '0', the tri-state buffer is disabled, and the output *y* is high-impedance *Z* state. When *E* is made ' 1', the buffer is enabled, and the output *y* follows the input *d*.

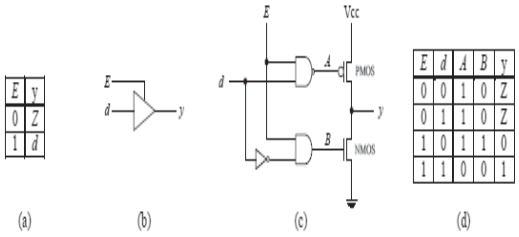

Figure 6: Tri-state buffer
(a) truth table (b) logic symbol (c) circuit (d) truth table

C. MEMORY CELL

A single bit memory cell of a SRAM chip is shown in Figure 7.

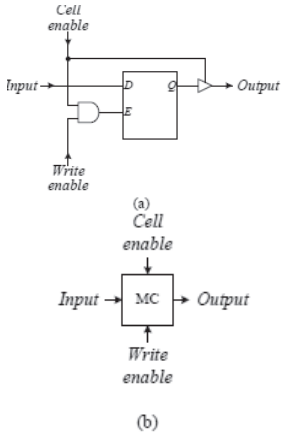

Figure 7: Memory cell (a) circuit; (b) logic symbol.

D latch with enable is used as a building block of SRAM. When read operation is selected, a tri-state buffer is connected to the output of the D latch. For reading, only the *Cell enable* signal is enabled. For writing, the *Cell enable along* with the *Write enable* signals are used to enable the D latch. Now, the data on the *Input* line is latched into the memory cell[1].

D. MEMORY TIMING DIAGRAM

During write operation, a suitable address on the address lines and suitable data on the data lines is specified and *CE* is enabled. When the *WR* line is asserted, the data here on the data lines is written into the memory location pointed by the address lines. Memory Timing Diagram with read and write operations is in Figure 8.

Suitable address on the address lines and *CE* to high make read operation begins. The *WR* is made low and suitable data from the addressed memory location is accessible on the data lines.

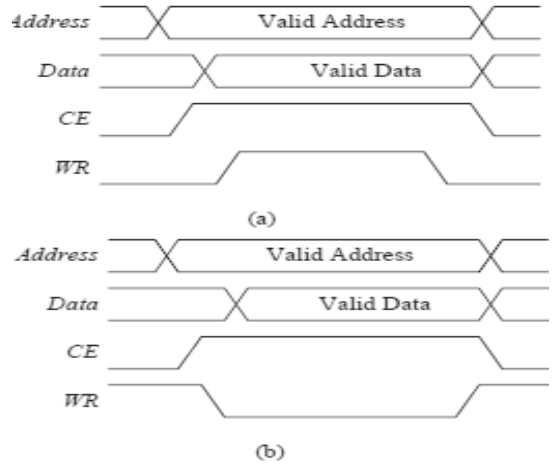

Figure 8: Memory Timing Diagram (a) read operation (b) write operation.

E. STATIC RANDOM ACCESS MEMORY

SRAM has data lines, *Di*, and address lines, *Ai*. Address lines specify the address and corresponding data on either input or output can be read or written into. Depending on the number of bits in the data, number of data lines are decided. Depending on the number of locations, the number of address lines are decided.

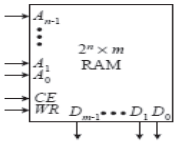

(a)

Figure 9: A 2^n x *m* RAM chip: (a) logic symbol

CE	*WR*	Operation
0	×	None
1	0	Read from memory location selected by address lines
1	1	Write to memory location selected by address lines

(b)

Figure 9: A 2^n x *m* RAM chip: (b) operation table.

Along with the data and address lines, two control lines called chip enable (*CE*) and write enable (*WR*) are also used as shown in figure9. For accessing memory of a microprocessor, either with read or write operation, the active-high *CE* line is enabled. The entire memory chip can be enabled by making CE high. The active-high *WR* line selects memory operation to be performed. For read operation, 0 is applied to *WR*, and data from the memory is retrieved. For write operation, 1 is applied to *WR* and microprocessor data is written into the memory. Some memory chips have separate read enable and write enable. The memory location in which the read and write operations are to be done, is selected by the corresponding address. The RAM chip designed in this work does not require a clock signal and is shown in figure 10. Here, the data operations are synchronized to the two control lines, CE and WR [5].

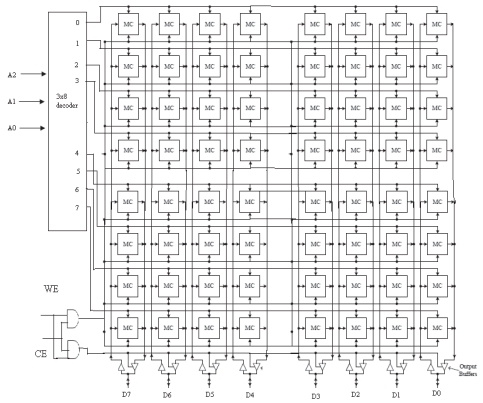

Figure 10: A 8X8 SRAM chip circuit.

To design 8X8 static RAM chip, 64 memory cells are required to form a 8X8 grid, as shown in Figure10.

Each row of the memory represents a single storage location. Number of bits in the data represents the number of memory cells in a row. By using the same address, all the memory cells of a row are enabled. A decoder is used to decode the address lines. Here, a 3 to 8 decoder is used to point to eight address locations. The *CE* signal enables the chip, and specific enabling of the read and write functions is through the two AND gates.

The external data bus, *Di*, gives data through the input buffer to the *Input* line of each memory cell. Depending on the given address, the data is written in to the memory cells. For read operation to be performed, *CE is* enabled and *WR is* disabled. This enables the internal *RE* signal, which in turn enables the eight output tri-state buffers. The location that is read from is selected by the address lines. Figure 11 and 12 shows the schematic of the

SRAM with PMOS MTCMOS cell and without the cell respectively.

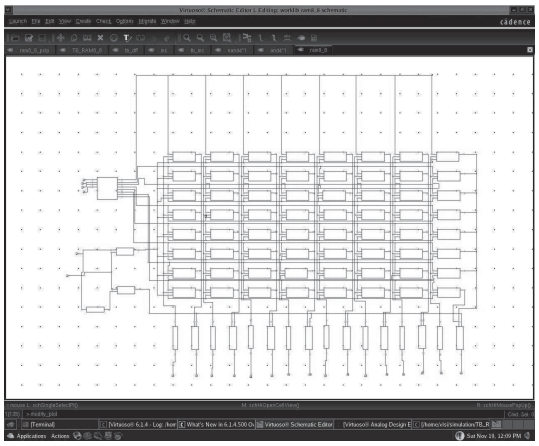

Figure 11:SRAM without MTCMOS

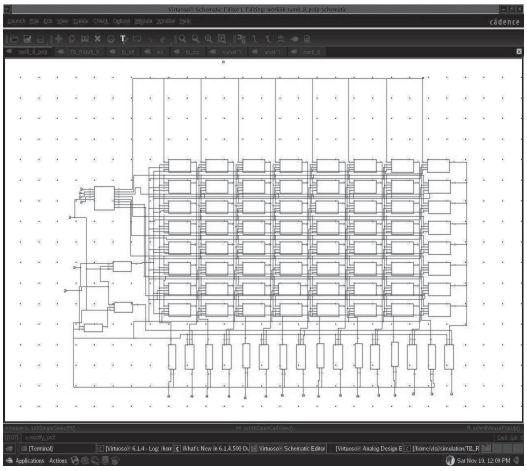

Figure 12: SRAM with MTCMOS

V. RESULTS

The operation of SRAM is verified and the average power is also calculated. Data is written into SRAM by using chip enable and write enable. The written data is read from SRAM chip. The results of read operation and write operation are shown in figure 13 and 14 with and without MTCMOS cell respectively. Power savings is observed to be 86% with the PMOS transistor used as sleep transistor.

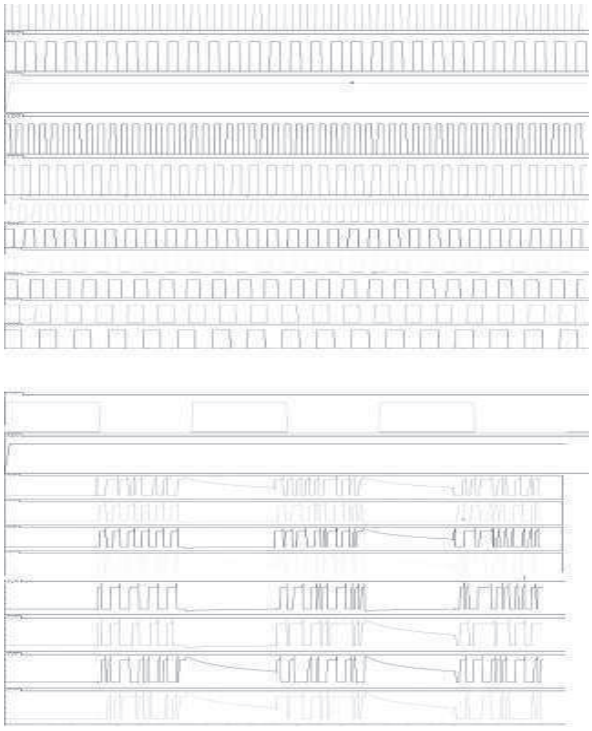

Figure 13: Output waveforms of SRAM without MTCMOS

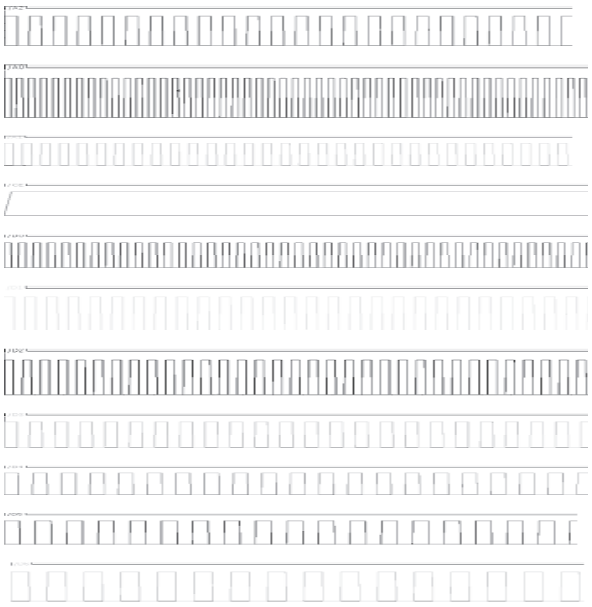

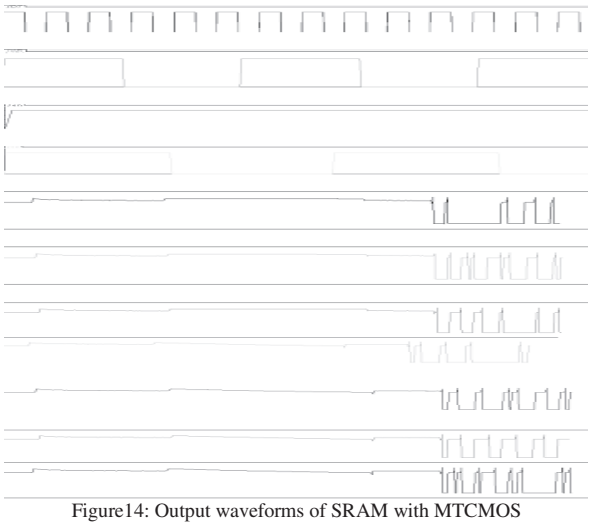

Figure14: Output waveforms of SRAM with MTCMOS

Table1
Comparison of power consumed with and without MTCMOS

S.NO	COMPONENT	WITHOUT MTCMOS	WITH MTCMOS
1	INVERTER	117.5nW	71.53nW
2	NAND GATE	248.9nw	98.12nW
3	D-LATCH	1.507uW	0.6268uW
4	TRI-STATE BUFFER	1.216uW	0.801uW
5	3x8 DECODER	9.47uW	2.113uW
6	MEMORY CELL	1.559uW	0.368uW
7	8x8 SRAM	97.92uW	13.11uW

CONCLUSIONS

In this work, SRAM is implemented for minimum leakage power dissipation with overall 86% of power savings. The SRAM operating in read mode and write mode should have "readability" and "write stability" respectively. SRAM has been verified for *reading* the data that is requested and *writing* the data or updating the contents. When the sleep enable is not active, SRAM will be in standby mode. There is tradeoff between area and power as PMOS takes more space on silicon but with much better savings in power dissipation.

REFERENCES

[1] Digital Design Principles & Practices- John F. Wakerly, PHI/ Pearson Education Asia, 3rd Ed., 2005

[2] Essentials of VLSI circuits and systems by Kamran Eshraghain, Eshraghian Dougles and A. Pucknell, PHI, 2005 Edition

[3] M. Anis, S. Areibi, and M. Elmasry, "Design and Optimization of Multithreshold CMOS (MTCMOS) Circuits," *IEEE Transaction on Computer-Aided Design of Integrated Circuits and Systems*,vol. 22, no. 10, pp. 1324- 1342, Oct. 2003.

[4] Cadence, "Cadence Low Power Design Flow" Cadence, "Low Power Application Note for RC 4.1 and SoCE 4.1 USR3", Version 1.0,1/14/2005

[5] Digital Logic and Microprocessor Design With VHDL by Enoch O. Hwang

[6] S. Sirichotiyakul and et al., "Stand-by Power Minimization through Simultaneous Threshold Voltage Selection and Circuit Sizing," *Proc. of the DAC*, pp. 436-441, 1999.

Design of a Portable Functional Electrical System for Foot Drop Patients

Harivardhagini S[1]
[1]CVR College of Engineering, Department of EIE, Ibrahimpatan, R.R.District, A.P., India
Email: harivardhagini@gmail.com

Abstract- **A portable functional electrical stimulation system has been designed using embedded systems technology. The system, which was applied to patients suffering from foot drop, uses sensors to monitor foot movement and orientation in a unique way, uses sophisticated algorithms for feedback, and drives an array of surface electrodes for stimulation. A new technique was invented based on using the twitch response of muscles to optimize the configuration of the electrode array. This reduces the setup time in the clinic. The feedback is used from the sensors and the optimum configuration of electrodes is chosen to produce correct stimulation and movement in real time. The instrument presents the patient with a ranked list of electrode combinations that are likely to be optimum, the patient can then choose a combination that is both effective and comfortable. The system can change the pattern of electrodes and also the stimulation signal during the process of stimulation. This may enable some problems associated with fatigue and skin irritation to be reduced. Trials were carried on 10 controls and 2 patients to test the instrument and study and develop the system optimization and control algorithms. These preliminary clinical trials showed that control of the stimulation during walking, based on the optimization algorithms developed in this work, gives high quality correction of foot drop. This was shown by gait assessment analysis by the physiotherapists earlier in the project. These trials prove that the concept of using the electrode array for stimulation has advantages over using a conventional 2-electrode system. The system has been designed and developed for the mentioned problem and has been tested for its efficacy.**

Index Terms— **Embedded systems technology, foot drop , functional electrical stimulation system**

I. INTRODUCTION

When the dropping of the forefoot occurs due to weakness, damage of the peroneal nerve or paralysis of the muscles in the anterior portion of the lower leg, such condition is called FOOT DROP. Though it is not a disease, it serves as a symptom for a bigger problem. Foot drop is characterized by the difficulty or the inability in moving the ankle and toes upward (dorsiflexion). Foot drop condition, can be temporary or permanent depending upon the weakness state of the muscle or paralysis. It can occur unilaterally or bilaterally. While stepping forward during walking, the knees are bent slightly so that the front of the foot can be lifted higher than usual to prevent the foot from dragging along the ground. Another cause of foot drop is the nerve damage. Multiple Sclerosis (MS) or Spinal Cord Injury (SCI) can produce partial or total paralysis. A person suffering from any one of the above conditions may not be able to move his or her body parts. Other factors that may get affected includes problems in breathing, blood circulation, bladder and bowel function. Over the last 30 years several methods and devices are invented by scientists and engineers to assist these problems. One such technique is called Functional Electrical Stimulation (FES). Any person suffering from MS or SCI can try FES as a treatment option as it can be applied to many different physical problems.

FES is a method of application of low level electrical currents to certain body parts to restore or improve its function. One example of FES system is a pacemaker. Some other types of FES may help to restore lost abilities such as standing or grasping. Also, FES may assist with some secondary problems of paralysis such as slow wound healing or poor blood circulation. In such treatments the term used is general called as Electrical Stimulation or ES. Some drawbacks of FES systems are found especially with people having complete spinal lesion, in such cases it provides benefits only when the system is operating. The benefits disappear when the system is turned OFF. So FES is an assistive device. In cases where patients suffer from incomplete spinal lesion or multiple sclerosis the usage of FES may help to recall some amount of voluntary muscle function. In such cases benefits are present even when the system is turned OFF. This is a restorative benefit of FES. FES itself does not reverse paralysis. People of any age or any level of injury can undergo this technique. This makes FES technology far more superior than many other similar techniques.

II. FES TECHNOLOGY

The main components of an FES system are the electrodes**,** the stimulator**,** and sensors or switches. When FES is being used to move muscles, current

pulses in the electrodes cause the weakened or paralyzed muscles to contract. In other applications, currents in the electrodes may simply produce electrical currents in the tissues without moving any muscles. The stimulator controls the strength and timing of the low-level pulses that flow to the electrodes. The sensors or switches control the starting and stopping of the pulses supplied by the stimulator. The FES simulator unit is shown in figure 1 and the parts of it are explained as follows.

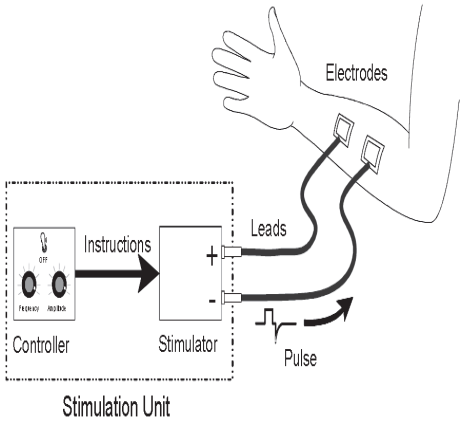

Figure 1. FES Simulator unit

A. Electrodes

Skin Surface electrodes may be attached to the skin daily. Several other types of electrodes are available that can also be implanted within the body. Skin surface electrodes are generally made of a flexible material such as rubber that has the ability to conduct electricity. Tiny electrical currents are sent through the electrode to the skin and the tissues beneath the skin. Generally surface electrodes are attached with a conductive gel while others are self adhesive. The electrodes of either type may be reusable. It is convenient to simply apply electrodes to the skin surface. Examples are plate electrodes, suction type electrodes, floating electrodes etc.

B. Leads and Stimulators

Leads are used to connect the electrodes to a stimulator. The leads are insulated wires. The electrical charge is delivered to the nerve, muscle or other tissue through the leads from the simulator. Stimulators mostly are external units. The size of a stimulator can be as small as a calculator or as large as a computer workstation. A stimulator usually has a computer controller unit built into it. Each stimulation channel sends pulses to one or more electrodes.

C. Sensors

Sensors are electronic or mechanical devices that measure some feature of the environment and send information about it back to the stimulator-controller. This information is used by the controller to adjust the stimulation. Sensors may include switches that the FES user can use to start and stop the system. Also some systems have switches that allow the user to select from a menu of choices. Certain sensors are built into shoes or braces to detect the angle at a joint or the pressure when weight transfers onto a foot. All the sensors used are man-made or artificial sensors.

III. HARDWARE MODEL

The basic hardware is divided into two parts Required Voltage Supplier and the Controller part

A. Required Voltage Supplier

The Required Voltage Supplier is shown in Figure 2 It supplies around 200 Volts to the body surface electrodes which are used to stimulate the inactive nerves. It contains the following parts

- Astable multi vibrator
- Centre tapped transformer
- Bridge rectifier

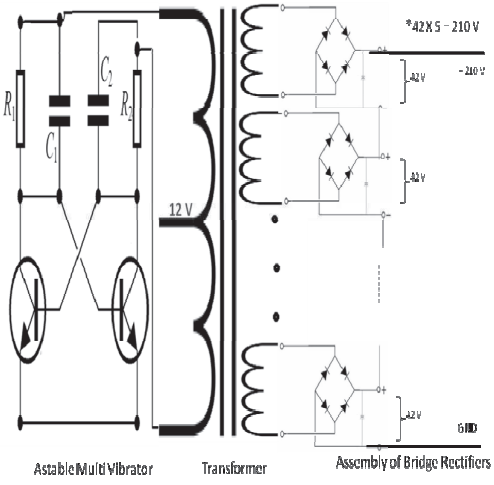

Figure 2. Required Voltage Supplier

An Astable Multivibrator is also known as a FREE-RUNNING MULTIVIBRATOR. When the time is ON it alternates between two different output voltage levels

hence it is also called free-running. The output remains at each voltage level for a definite time period. The output of the astable multivibrator is a continuous square or rectangular waveforms. There is no input for an Astable Multivibrator but has two outputs.

A Centre tapped transformer is a transformer with a tap in the middle of the secondary winding, usually used as a grounded neutral connection, intended to provide an option for the secondary side to use the full available voltage output or just half of it according to need.

A diode bridge is an arrangement of four diodes in a bridge configuration. For either polarity of the input it provides the same polarity of output. A diode bridge is commonly called as a bridge rectifier when used for conversion of an alternating current (AC) input into direct current (DC) output. A bridge rectifier provides full-wave rectification from a two-wire AC input. This results in lower cost and weight as compared to a rectifier with a 3-wire input from atransformer with a center-tapped secondary winding.

B. The Controller

The major components in this half of the hardware are

- Micro controller
- Opto isolator
- IGBT
- Sensor

If the first part helps in giving high voltage to the body surface, this part helps in regulating that potential in such a way that, it doesn't cause any kind of damage to the body. Here, the 210 V potential is always supplied to the positive electrode, but the negative electrode is grounded based on the regulation of the micro controller. Whenever a high pulse is supplied from the MC to the opto isolator, 12 V is given to the IGBTs. When the IGBTs are given a 12 V potential, they ground the negative electrode and thus 210 V is supplied to the body surface. This helps in activating the inactive nerves. Here the major problem is, if this high potential is supplied for a long time of 5-10 secs continuously to the body, it may affect the particular nerves. For this reason, we use a MC to control in such a way that the duration of the applied potential does not become greater than 2-3 mill seconds. The pulse width starts initially at 0.05 ms and is incremented in terms of 0.05 till the foot position reaches the required height. Figure 3 shows the parts of controller.

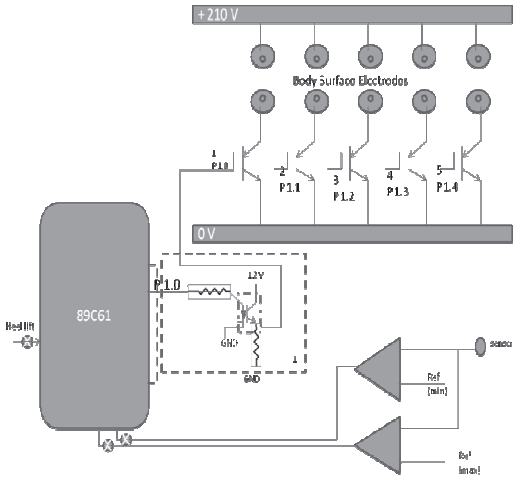

Figure 3. The Controller

During testing the hardware for accurate results, the presence of leakage currents was detected. To reduce these leakage currents, the following circuit was used in place of electrodes. Instead of attaching electrodes directly to 210V, we use the following design, which will help in eliminating unnecessary leakage currents.

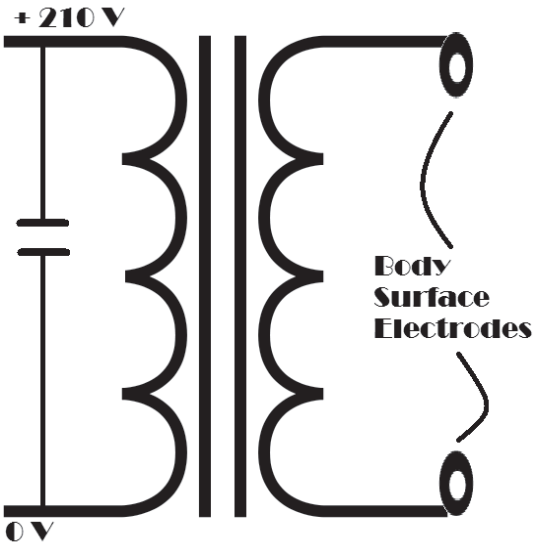

Figure 4. Solution for leakage currents

IV. CONCLUSION

The benefits of FES begin with improved walking:

- Provide close to natural movement while walking
- Increase speed and improve steadiness while walking
- Increase social participation
- Re-educates the muscles to function without the need of the system
- Prevents loss of muscle
- The range of motion in the ankle and foot is maintained or increased
- Increase in local blood flow

V. REFERENCES

[1] Acimovic R, Gros N, Malezic M, Strojnik P, Kljajic M, Stanic U, and Simic V, "A comparative study of the functionality of the second generation of peroneal stimulators", Proc. 10th RESNA Conf, (PP: 621–623), 1987.

[2] http://feswww.fes.cwru.edu/info/

[3] Alon G, Kantor G, Ho HS, "The effects of selected stimulus waveforms on pulse and phase characteristics at sensory and motor thresholds", Phys Ther, (Vol: 74, PP: 951-962), 1994.

[4] Brandell H. B. R, "Study and Correction of Human Gait by Electrical Stimulation", The American Surgeon, (Vol:52, No:5), 1986.

[5] "Biomedical instrumentation and Measurements" by Leslie Cromwell.

[6] "The Handbook of Biomedical Instrumentation" by R.S Khandpur, Second Edition.

[7] "Medical Instrumentation" by John Webster, Third Edition.

Low-Power Successive Approximation ADC with 0.5 V Supply for Medical Implantable Devices

O. Venkata Krishna [1] and B. Janardhana Rao [2]
[1] CVR College of Engineering/EIE, Hyderabad, India
Email: venkatakrishna.odugu@gmail.com
[2] CVR College of Engineering/ECE, Hyderabad, India
Email: janardhan.bitra@gmail.com

Abstract- **In this paper the design and implementation of very low-power Analog to Digital converter, which is used in medical implantable devices like pacemakers et al. The ADC uses a successive approximation architecture and operates with a low supply voltage is 0.5 V. A suitable dynamic two-stage comparator is selected due to its energy efficiency and capability of working in low supply voltages. This ultra-low power 10-bit ADC is Implemented in a 90nm Complimentary Metal-Oxide semiconductor (CMOS) technology, this ADC consumes 12nW at supply voltage of 0.5V and sampling frequency of 1kS/s with figure of merit 0.14pJ/Conversion. It has a signal-to-noise-and-distortion (SINAD) ratio of 60.29dB and effective-number-of-bits (ENOB) of 9.72 bits.**

Index terms— **Pacemaker, Analog-to-digital conversion, CMOS, low power, low voltage, two stage dynamic latched comparator, binary search algorithm for successive approximation.**

I. INTRODUCTION

Successive approximation analog-to-digital converters have recently become very attractive in low-power moderate-resolution/ moderate-speed applications such as implantable bio-medical devices or wireless sensor nodes due to their minimal active analog circuit requirements and low power consumption. As an integral part of the medical implantable devices like the Pacemaker, a moderate resolution) with low power dissipation Analog-to-Digital Converter is required[1].The converter should also operate from a low power supply to drive its integration with low-power digital circuitry. In this paper, we present an analog-to-digital converter (ADC) that satisfies requirements of Pacemakers. The Architecture of a Successive Approximation ADC is shown in Figure.1, It consists of a sample-and-hold (S/H) circuit, a Comparator, a Successive Approximation Register (SAR), and a digital-to- analog converter (DAC). The operation of the Successive Approximation-ADC starts with the sampling phase, the analog input signal is sampled by the S/H circuit and this sample is given to comparator. During the conversion phase, the SAR and control logic perform a binary search algorithm, which constructs the binary word. This binary word is fed through the DAC; then DAC produced value is an equivalent analog value which is exactly half of the DAC reference value. This is compared with the sampled analog input signal by the comparator. The comparator gives either VDD or Zero, if $V_H > V_A$ or $V_H < V_A$ respectively. The same procedure is repeated for generating the reference voltage and it is compared with the sampled value and finally set the input Digital data for Successive Approximation Register in N clock cycles. For entire conversion of ADC N+1 clock cycles are required.

This paper proposes a new 10-bit ADC fabricated in the 90nm CMOS technology. Section II explains about the proposed SAR individual blocks. Various analyses about switching power and Implementation results are presented in section III. Finally, section VI draws our conclusions.

II. ARCHITECTURE DESIGN

The architecture of Successive approximation Analogto-Digital converter is shown in Figure 2. It mainly consists of Sample & hold circuit, Comparator, digital to analog converter and successive approximation register.

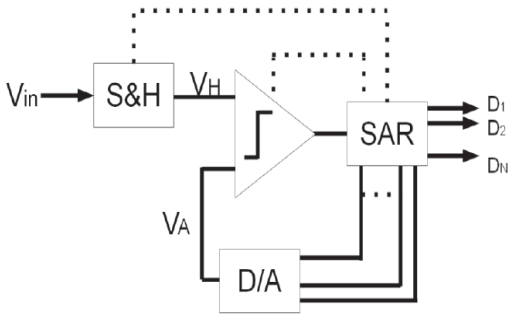

Figure 1. The Architecture of A Successive Approximation ADC.

A. *Sampling Network Design*

The Sampler takes the varying input Analog signal and converts it to a fixed voltage or current or electrical charge. The signal is sampled at Nyquist rate i.e. a frequency rate more than double the maximum

frequency of the input analog signal. The Sampled signal has to be held constant while conversion is taking place in A/D Converter. This requires that an ADC should be preceded by a Sample & Hold circuit.

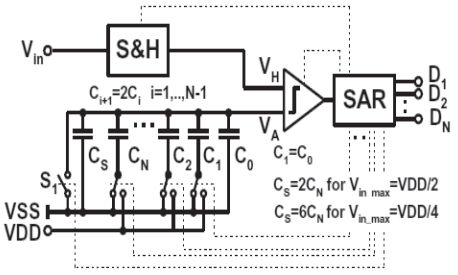

Figure 2. Overall Architecture of the ADC .

For Sample & Hold circuit, the important two basic elements needed in a sampling circuit are the switch and a memory element. The switch allows the S/H circuit to be configured into one of its two operating modes: one is Sample mode and other one is Hold mode. In CMOS technology, the MOS transistor is used as switch. For the storage purpose either voltage sampling or current sampling methods can be used. The voltage sampling method employs capacitors; the current sampling method employs inductors. However, in Integrated Circuit technology, the fabrication of capacitors is easier than fabrication of inductors. The reason for which all S/H circuits are done with voltage sampling only.

Next, the operation of the MOS transistor as a switch and its important limitations are discussed. When a voltage large enough is applied to the gate terminal of the MOS transistor, then the formation of the channel between its source and drain terminals allows the transistor to transmit any signal through that channel. The removal of a voltage at the gate follows the same operation principle of an ideal switch. When the transistor is turned "on" a signal path is present. If the transistor is turned off the channel vanishes and no signal path exists.

One of the main differences between an ideal switch and a transistor is that when the transistor is "on", a small on-resistance (i.e.0.5 - 2 kΩ) is present where as in ideal switch zero resistance is present, in the signal path between the drain and source terminals. Similarly, in the "off" state there is a resistance large enough to prevent signals from passing between the drain and source terminals.

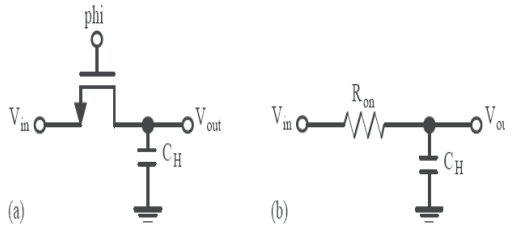

Figure. 3 (a) MOS-based S/H circuit (b) equivalent circuit during sampling phase.

Figure.3. (a) and (b), respectively, shows the basic sampling circuit using an MOS switch and its equivalent circuit during Sampling mode. When operated in the *triode* or linear region, the on-resistance of a NMOS transistor can be approximated as

$$\varepsilon_{settling} = e^{-t/R_{on}C_S} < \frac{1}{2^{N+1}} \quad \textbf{(1)}$$

B. Comparator Design

Latch only comparators are clocked comparators. They operate based on amplification and positive feedback. Figure.4 shows the Dynamic Latched Comparator circuit.

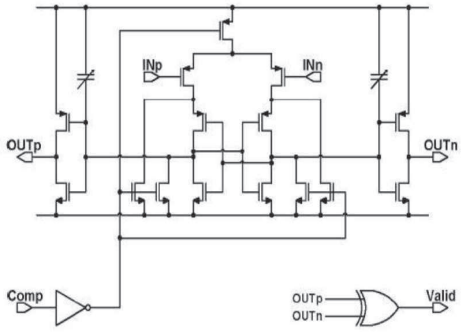

Figure 4. Dynamic-Latched Comparator circuit.

The figure 5. shows the operation of the comparator circuit. There are two operation phases, reset phase and regeneration or evaluation phase. In the reset phase, the output nodes are charged to supply voltage or discharged to the ground depending on the architecture of comparator. During the reset phase, the comparator tracks the input, and then in the regeneration phase the positive feedback produces a digital value at the comparator output. One of the advantages of dynamic-latched comparators is their power efficiency since they only consume power in the regeneration phase and there is no static power consumption in the reset phase.

Dynamic latched architecture is the most power efficient comparator. However, it introduces large input referred offset which makes it unappealing for high resolution ADCs. This effect can be reduced by increasing the width of input transistors in the differential pair. Employing offset cancelation techniques in the comparator implementation is also an effective approach to mitigate this problem. Furthermore, the offset voltage can be reduced by using a pre-amplifier which is previously described as a latched comparator with preamplifier. However, in all the mentioned methods, offset reduction is achieved at the cost of more power consumption. Latched comparators are fast and are suited to be used in high speed ADCs. In order to derive the

delay equation, the latched comparator can be modeled as a single pole comparator with positive feedback. The delay time of this comparator is calculated as below [3].

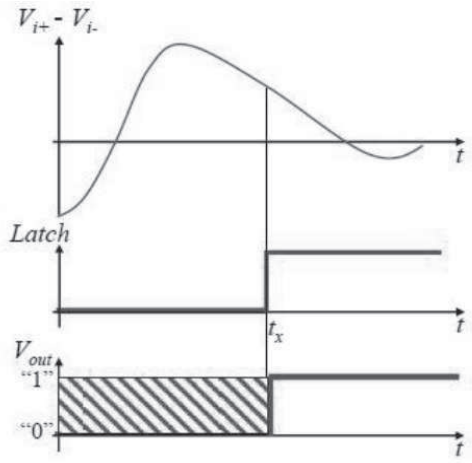

Figure 5. Latched Comparator Operation

C. Design of Digital-to-Analog Converter.

The digital to analog converter (DAC) converts the digital word at the output of SAR logic to an analog value. Then in the comparator, this value is compared to the input signal. In the capacitive DAC with inherent Sample and hold, the sampling operation is performed by DAC. This type of DAC is called charge redistribution DAC. Nowadays, charge redistribution DACs are commonly used. They consume less power and induce less mismatch errors compared to the resistive-based DAC. Charge redistribution DAC has fast conversion time. Moreover, they are fabricated easily [4], [5].

In this paper a 10-bit charge-redistribution DAC with the Binary weighted Capacitor (BWC) array was implemented in 90nm CMOS technology. Figure 6. shows the block diagram of the 10-bit DAC. There are three phases of the operation to perform a conversion: First, in the sampling phase switch S1 connects the top plats of all capacitors to the VCM and the bottom plates are connected to VIN. Thus, the input voltage is sampled on the capacitor array. During the hold phase, S1 is opened and the rest of switches connect the bottom plates to the ground therefore a charge of –VIN + VCM is stored in the capacitor array.

In the redistribution phase, the digital code determines the status of the switches and the actual conversion is performed in this phase. In the beginning of the conversion, D9 is high so the MSB capacitor is connected to V_{REF}. At this step the output voltage of the DAC is equal to $-V_{IN} + V_{CM} + 0.5V_{REF}$ and is compared to V_{CM}. Based on the comparator result, D_9 remains connected to V_{REF} if the comparator output is one, or change the connection to ground when the result of the comparator is zero. Thus, the MSB is defined. Next, D_8 is connected to V_{REF}. Depending on the value of D_9, Vout-DAC is $-VIN + V_{CM} + 0.5D_9.V_{REF} + 0.25V_{REF}$ and is compared to V_{CM}.

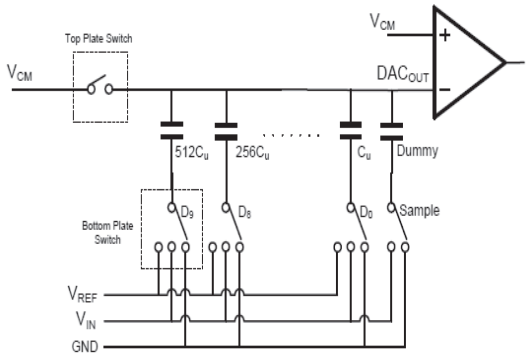

Figure 6.The schematic view of DAC

The linearity of ADC is restricted by the linearity of the DAC, which is caused by the capacitor mismatch. Therefore, choosing an appropriate value for the unit capacitance is vital. Reducing the unit capacitance value improves the linearity but deteriorates the noise performance at the same time due to thermal noise. The minimum required value of the unit capacitor is limited by several factors, including KT/C thermal noise, capacitor matching and the value of the parasitic capacitances [6]. A unit capacitance of 20fF is chosen in this design. The values of the other capacitors in the capacitor array are defined based on the unit capacitance.

The diagram of the bottom plate switches are presented In figure.7(a) NMOS switches can properly pass a zero while PMOS switches can pass a strong one. On the other hand, CMOS transmission gate combined both features of the NMOS and PMOS switch and is capable of properly passing both zero and one. It also benefits from low on-resistance [13]. In this design, VREF is set to VDD; therefore the PMOS switch is used for VREF. NMOS switch is employed to ground the bottom plate. Since Vin varies from 0 to 1, CMOS TG is chosen for Vin. Figure 7.2 (a) shows the block diagram of the bottom plate switches [7].

The leakage current contribution of the top plate switch is significant in this low speed design since most of the time this switch is off and it only turns on during the sampling phase. The leakage-current in the top plate switch adversely affects the linearity of the DAC and consequently the linearity of ADC [8]. In order to alleviate this problem, a stack of two PMOS switches are used in series form, this switch is depicted in Figure (b).

D. Successive approximation register

The successive approximation register (SAR) is realized in static CMOS logic. The circuit also generates the clock signals for the comparator and the sample-and

hold circuit. All clock signals are derived from an externally provided master clock.

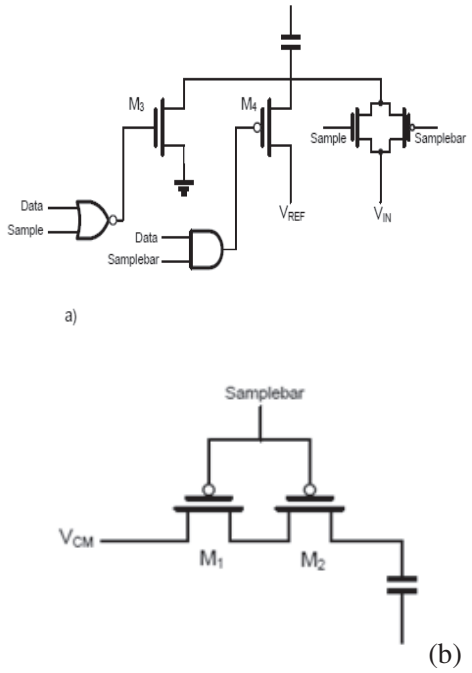

Figure 7.Schematic views of a) bottom plate switch and b) top plate switch.

Successive approximation register ADC implements the binary search algorithm using SAR digital control logic. In general, there are two fundamentally different approaches to designing the SAR logic. The first one is proposed by Anderson consists of a ring counter and a shift register. At least 2N Flip-flops are employed in this kind of SAR [9]. The other, which is proposed by Rossi, contains N flip flops and some combinational logic [10].

The SAR control logic determines the value of bits sequentially based on the result of the comparator. Each conversion takes 12 clock cycles. In the first clock cycle, SAR is in the reset mode and all the remaining outputs are zero. In the next ten clock cycles, data is converted and each bit is determined sequentially. The last cycle is for storing the results of the complete conversion.

The SAR architecture shown in Figure 8. is presented in [9], and is commonly used in SAR ADCs due to its straightforward design technique. This control logic encompasses a ring counter and a code register. The ring counter is in fact a shift register. For each conversion, in clock cycle 0, the EOC signal is high and all Flip Flops outputs reset to zero, and for the rest of cycles EOC is low. In the next clock cycle, the most significant Flip Flop is set to one which corresponds to MSB of the digital word to DAC. Then the counter shifts '1' through the Flip-Flops from MSB to LSB.

In each clock cycle, one of the outputs in the ring counter sets a Flip-Flop in the code register. The output of this Flip-Flop, which is set by the ring counter is used as the clock signal for the previous Flip Flop. At rising edge of the clock, this Flip-Flop loads the result from the comparator. This type of SAR logic requires 12 clock cycles to convert each sample.

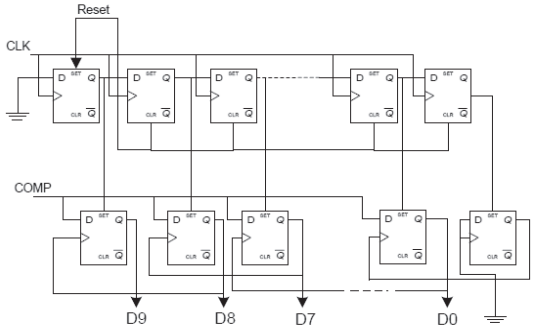

Figure 8. The SAR block diagram

The Flip-Flops which are employed in this structure are set-reset D-FFs. For the low power purpose, transmission gate based Flip Flops are used [11]. Minimum size transistors with double length are chosen for improving the power performance. In order to decrease the leakage power even more while simultaneously maintaining the speed, high threshold voltage transistors are used in the non- critical paths and low-VT transistors in the critical path. Thus, this dual threshold approach provides high performance Flip-Flops [12].

III. Simulation Results

The Low power 10-bit ADC is fabricated in a 90nm *n-well* CMOS process technology with single poly, four metal layers and a MIMCAP (Metal-Insulator-Metal) capacitor option. The threshold voltages are 0.43V for the n-MOS and -0.38V for the p-MOS device. Simulation results for the low supply voltage as well as high temperature are presented to evaluate their influence on power consumption.

The ADC is simulated with VDD= VREF = 1,VCM = 0.5V, and sampling frequency of 1kS/s. The input signal is an full swing sinusoidal with fin= 450Hz. The simulation results under 27ºC and 80ºC temperatures are presented in the Table 1.

The total power consumption of the implemented SAR ADC, including the clock power is almost 12.4nW. The distribution of power consumption between different blocks of ADC is shown in figure 9.

As shown in the Figure 9, DAC consumes the largest amount of power among other blocks which is 84%. As discussed above, the unit capacitance in the DAC is chosen to be 20fF. After DAC, SAR control logic with 12%, clock power and comparator both with 2% consumes the largest amount of power respectively.

A. Dynamic Performance Evaluation

The dynamic performance is evaluated by calculating the SFDR, SINAD, and ENOB of ADC. For this purpose, a full swing sinusoidal wave with fin = 30.273438 Hz which is based on coherent sampling is applied to the input of ADC. The simulation is performed to achieve 1024 samples with sampling frequency of 1kS/s. Then, Fast Fourier Transform of the stored output data is executed in MATLAB and by performing some post processing of the SFDR, SINAD, and ENOB are measured.

Table I.
Power consumption of different blocks of ADC

Block	Power Consumption at 27ºC (nW)	Power Consumption at 80ºC (nW)
DAC	10.4	11.1
SAR	1.54	2.028
Comparator	0.26	0.620
Clock Power	0.208	0.224
Total	12.408	13.97

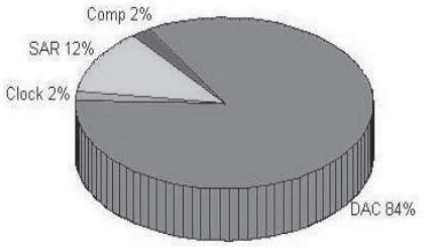

Figure 9. The Power distribution of ADC

The FFT of 10-bit ADC output is shown in Figure10. The simulation results predict that the ADC have SINAD=60.29, SFDR=79.89, and achieves 9.72 of ENOB which are reasonable for schematic level simulation. Energy per conversion-step can be calculated using the FOM definition of ADC which is given by Equation (2) [16].

$$FOM = \frac{P}{2^{ENOB} \cdot F_S} \text{ (fJ/conversion-step)} \quad (2)$$

Table II Summarize the performance parameters of the designed SAR ADC.

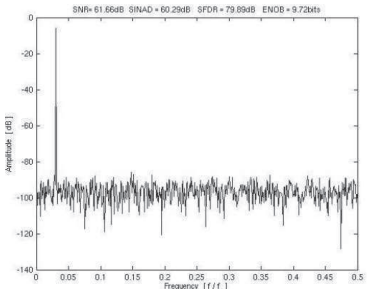

Figure 10. FFT of the ADC output for Fin=30.273438Hz

Table II.
Performance summarize for ADC

Items	Result	Unit
Technology	90nm	-
Supply Voltage	0.5	V
Resolution	10	bits
Sampling Frequency	1	KS/s
Power Consumption	6.8	nW
Conversion Time	167	ns
SINAD	60.29	dB
SFDR	79.89	dB
FOM	14.7	pJ/Conversion

CONCLUSION

This paper presented implementation of a 10-bit SAR ADC operating at 1kS/s and the supply voltage of 0.5 V in 90nm CMOS technology. The power consumption of 12.4nW is achieved. The ADC used a charge-redistribution DAC, a dynamic two-stage comparator, and a SAR control logic containing a sequencer and a ring counter. The ADC exhibited good performance and achieves a FOM of 14.7fJ/conversion-step with ENOB of 9.72 bit.

The SAR logic is implemented as a conventional SAR logic with a sequencer and a ring counter, consumes the lowest power of 1.2nW at 1kS/s. Thus the power consumption of SAR control logic is significantly reduced and consumes only 12% of the total power.

The Design of the comparator is a crucial part of ADC design. In this work, comparator performance metrics is studied and the two-stage dynamic comparator is designed. Dynamic comparators consume lower power compared to the other approaches. Therefore, the Architectures of dynamic comparators are implemented and compared regarding power consumption, speed, and accuracy.

This Very Low power ADC with moderate resolution and low sampling frequency is suited for biomedical applications such as Pacemakers. These results make SAR ADC is the suitable choice for biomedical application. It consumes low power due to its simple structure.

REFERENCES

[1] Dai Zhang," Design and Evaluation of an Ultra-Low Power Successive Approximation ADC ", *LiTH-ISY-EX*--09/4176—SE, March 2009.

[2] J. Sauerbrey, D. Schmitt-Landsiedel, and R. Thewes, "A 0.5-v 1-μW Successive Approximation ADC," *IEEE Journal of Solid-State Circuits,* vol. 38, no. 7, July 2003

[3] H. Khurramabadi *ADC Converters (Lecture 21).* UC Berkeley Course, *Analog-Digital Interfaces in VLSI Technology EE247*. 2006

[4] B. Razavi, *Principles of Data Conversion System Design*, IEEE Press, 1995.

[5] J. L. McCreary and P. R. Gray, "All-MOS Charge Redistribution Analog-to-Digital Conversion Techniques-Part I," *IEEE Journal of Solid-State Circuits*, vol. SC-10, no. 6, December 1975.

[6] M. Saberi, R. Lotfi, K. Mafinezhad, W. A. Serdijn, "Analysis of Power Consumption and Lineary in Capacitive Digital-to-Analog Converters Used in Successive Approximation ADCs," *IEEE Transactions on Circuits and Systems,* vol. 58, no. 8, August 2011.

[7] D. Zhang, "Design and Evaluation of an Ultra-Low Power Successive Approximation ADC," *Master thesis, Linkoping University*, 2009.

[8] A. K. Bhide, D. Zhang and A. Alvandpour, "Design of CMOS Sampling Switch for Ultra-Low Power ADCs in Biomedical Application," *in proceedings of the 28th Norchip conference IEEE,*Nov.2010.

[9] T.O. Anderson, "Optimum Control Logic for Successive Approximation Analog-to-Digital Converters," *Computer Design*, vol. 11, no. 7, pp. 81-86, 1972.

[10] A. Rossi and G. Fucili, "Nonredundant successive approximation register for A/D converter," *Electronics Letters*, vol.32, no.12, pp.1055-1057,1996

[11] S. T. Oskuii, "Comparative Study on Low-Power High-Performance Flip-Flops," Master thesis, Linkoping University, 2003.

[12] Joao C. Vital andPedro M. Figueiredo, "Kickback Noise Reduction Techniques for CMOS Latched Comparators," *IEEE Transactions on Circuits and Systems,* vol.53, no.7, July 2006.

[13] J. M Rabaey, A. Chandrakasan , and B. Nikolic, *Digital Integrated Circuits – A Desigsn Perspective,* Prentice Hall, 2nd edition, 2003.

PC Based Wave Form Generator Using Labview

Mahammad D V[1], Dr B V S Goud[1] and Dr D Linga Reddy[2]
[1]Dept. of Electronics & Instrumentation Tech. Acharya Nagarjuna Uni., Nagarjuna Nagar – 522510, A.P. India.
E mail : goudbvs@yahoo.com
[2]CVR College of Engineering, Vastunagar, Mangalpalli (V), Ibrahimpatnam (M), R R Dist., 501 510, A P India.
E mail : dlreddy_phy@yahoo.com

***Abstract*--A Personal Computer (PC) based wave form generator for laboratory applications has been thought and developed which is generating Sine, Square and Triangular waves in the range of 1 Hz to 20 MHz. The generation, recording and monitoring of wave forms, controlled through USB Data Acquisition system (DAS) connected to computer which is having 14-bit ADC, 10-bit DAC and 12-I/O lines. In the present work National Instrument's USB DAS 6009, Maxim Company's Max038 waveform generator are used for Hardware development. Higher level Graphical language such as 'LabVIEW' is used to develop the software. The experimental study reveals that the developed system is quite suitable to perform laboratory applications accurately. The results obtained from system are in agreement with results of standard instruments.**

***Index Terms*-- Wave Form, LabVIEW, DAS, FLC**.

I. INTRODUCTION

A Waveform generator is widely used for experimental work in all electronics labs [1,2,3]. It generates various types of wave forms like sine, square, triangle, etc., with a particular frequency, amplitude and duty-cycle. Currently, most waveform generators in the laboratory made use of manual control and these are not programmable. Usually, the manual function generators do not provide feedback to the user regarding the condition of the output. Therefore, the user will never know whether the required waveform is available at the output or not unless they measure it by suitable equipment. Although software controlled waveform generators are available in the market, they are not widely used, because of their high cost. To overcome this problem, A Low cost PC based wave form generator for laboratory application has been thought and developed in our lab. This is generating sine, square and triangle wave forms in the range from 1Hz to 20 MHz. The present work deal with designing and building a programmable waveform generator in LabVIEW plot form. The block diagram of the system is shown in figure-1.

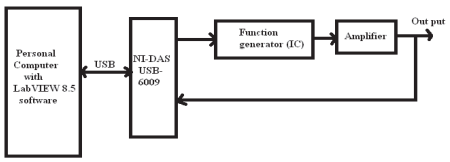

Figure 1. Block diagram of PC based waveform generator system.

II THE DESIGN OF PC BASED WAVEFORM GENERATOR

A. Personal Computer

Computer plays a pivotal role in instrumentation in field of data acquisition; instrument control and data processing [4]. To measure and control any instrument it is to be interfaced with a personal computer. For this we need interface ports like Serial, Parallel and Universal Serial Bus (USB) ports. In present study, a powerful 32-bit Intel® core™2 Duo CPU processor based Acer personal computer is used. It consists of a system unit of CPU, clock speed 2.80 GHz, 360 GB hard disk, internal memory 2GB RAM, 105 key-full function keyboard and color monitor. The mother board consists of two PCI slots, four USB ports, two serial and one parallel ports to interface Data Acquisition Systems (DAS). The system is compatible to Windows-7, Unix Operating System and Linux OS etc. also compatible to a vast variety of popular application PC software packages and all language compilers. However, the software and the interface are designed such that it can work in any advanced computer environment.

B. NI DAS USB-6009

To measure and control the hardware frequency of the output of Max-038 function generator, it is to be interfaced with a PC. It requires one ADC Input channel, one DAC output channel, four I/O lines. The DIOT/DAS card provides these requirements. In present study, DAS of National instruments USB-6009 is used. It is having 14-bit ADC with 8-single ended or 4-dual ended channels, two 10-bit DAC channels, 12-I/O lines and two counter/timers [5]. This fulfils the present system requirements.

C. Max038 Waveform Generator IC

Advancement in Integrated Chip technology brings tremendous changes in simplification of hardware design. Single chip incorporating much integration of required tasks. Maxim has produced a family of high quality and reliable one-chip waveform generator ICs. The IC MAX-038 is one best among them [6], with accurate, high frequency, precision function generator producing triangle, sine, square, and pulse waveforms with a minimum of external components. It generates 0.1Hz to 20 MHz range of Independent frequency and Duty-Cycle adjustments with 15% to 85% Variable Duty Cycle.. are some of the important features. It is a 20-pin IC, works with +5V supply and features a parallel digital interface that connects easily to most systems like Microprocessors/microcontrollers or PCs.

The desired output wave form is selected under logic control by setting the appropriate code at the A0 and A1 inputs. The wave form selection table is shown in table-1. The basic oscillator is a relaxation type. The operates by alternately charging and discharging a capacitor, 'CF' with constant current, simultaneously producing a triangle wave and a square wave.

TABLE 1.
Waveform Selection

A0	A1	Waveform
X	1	Sine wave
0	0	Square wave
1	0	Triangle wave

D. BB PGA103

The PGA 103 is a Programmable gain amplifier having gains of 1, 10 and 100 which are digitally selected by two compatible inputs. It is high speed circuitry provides fast settling time. It operating voltage is +/_ 4v to +/_18v, available in 8 pin DIP package [7]. The digital inputs, A0 and A1, select the gain according to the logic table, table-2.

TABLE 2.
PGA103 gain selection

Gain	A1	A0
1	0	0
10	0	1
100	1	0
Not valid	1	1

.

E. Interface Circuit

The Max-038 IC's I/O can easily be interfaced with a PC. IIN pin is connected to DAC output.. A0, A1 pins are connected to P0.0, P0.1 port lines of DAS. Frequency adjustment is accomplished with a capacitor C2 and variable resistor, R1. I in current is drive from DAS's DAC. Amplitude, offset, and duty-cycle adjustments are performed via variable resistors. Switches A0 and A1 select the waveform type, to be generated. The frequency range decides the capacitor C2 value (in present work C2 is fixed for particular range). The F*adj* pin of U1 is tied to ground through a 12k resistor, so the frequency of the waveform at U1-19 is f = 2(IIN/C2), where IIN = VREF/R, and VREF = 2.5 V. The output at U1-19 is 2 V p-p, centred around zero, for all waveforms. For amplitude adjustment, The portion of U1-19 fed to the programmable gain amplifier BB PGA103. The gain varies from 1, 10 and 100 times in fixed 3 - steps. This gain is digitally selected from PGA's

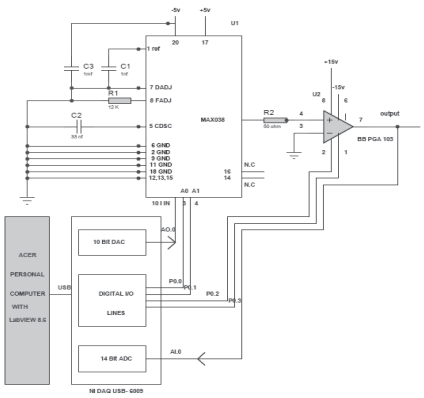

Figure 2. Schematic Diagram of PC Based Waveform Generator.

A0, A1 pins which are connected to P0.2, P0.3 port line of DAS. The duty cycle adjustment is fixed at 50% in present work for constant output. The schematic diagram is in figure-2.

F. Software requirement

Software plays very important role in any PC based instrumentation system, as it includes all tools which a developer needs to build and execute applications. In the present work National Instruments' LabVIEW 8.5 version is used for development of application software like C/C++, Java. It is Graphical programming language, so called 'G' language [8]. It has back panel where we write programming code in form of icons and front panel indicators, controls for display and control purpose. The programs written in LabVIEW are called "Virtual Instruments" or VI's due to their instrument related origin. The programs created are portable of the type of machine and operating system. It has a built-in mathematical function, graphical data display objects and data input objects. LabVIEW has many features some them are.. data flow controlled execution, real time debugging features, data base (SQL) interfacing for industrial PLC's, and add-on software packages for specific extension of the program features, etc.

The software control program is written in LabVIEW 8.5.

Figure-3a shows the program of front and back panels of present developed setup system.

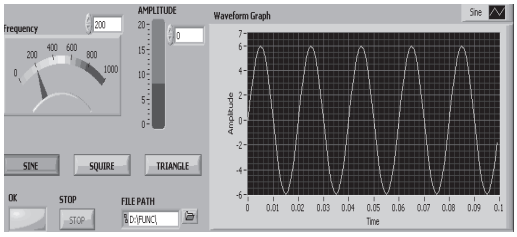

Figure 3a. Show a front and back panel of waveform generator in LabVIEW.

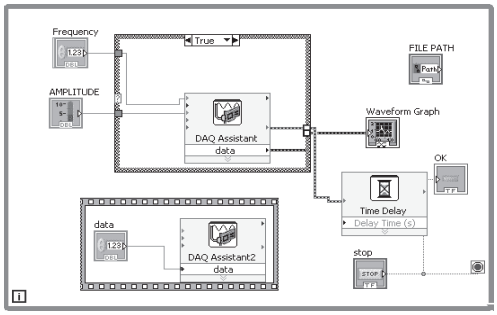

Figure 3b. LabVIEW Program for PC based waveform generator.

III. EXPERIMENTAL

The prototype of the PC based waveform generator is successfully designed and tested in the laboratory. The photograph in figure-3 b, shows the prototype used in the present experiment. The performance of the present design system is evaluated by comparing with standard reported instrument [9]. The response time (τ) of Ferroelectric Liquid Crystal (FLC) compounds 2CI.BAAP.120-BBP and 2CI.BAAP.180-BBP, with temperature variation is calculated in present work. To determine the response times (in SC* phase) also by the measurement of shift (frequency dependent) of the peaks due to polarization reversal in the current signal (converted in to voltage) as reported [10] by Bawa et.al. . Plotting the current peaks measured at double the frequencies (viz., 100Hz and 200Hz) reduces the pulse gaps to half in the time axis 10. The scanning time of the oscilloscope is to be halved, while plotting the higher frequency signal (to obtain the same abscissa length) and the slope of the applied triangular pulse. By doing so (i.e., doubling the frequency), one actually shifts the event (occurrence of peak of the polarization reversal current) by the same time corresponds to the response time of the device. The response time is directly measured by the difference of the occurrence of peaks in lower frequency (i.e., 100Hz) time scale. The reported values are tabulated in table-3. Then the experiment (for two compounds) is performed by substituting the function generator with developed waveform generator and the calculated values are tabulated in the same table.

IV. RESULTS AND DISCUSSION

The temperature variation of response time is measured by following the reported double frequency technique [10]. The observed variation of switching times with temperature in Smectic-C* phase is given in Tables-3,4,5,6 for the compounds 2Cl.BAAP.12O-BBP and 2Cl.BAAP.18O-BBP respectively. It is also observed that the range of switching times exhibited by the present compounds with developed setup are found to agree with the reported [9] values of same FLC compounds.

TABLE 3.
Response time of FLC compound 2CI.BAAP.120-BBP

S.No.	Temperature°/C	Reported values (T/μs)	Instrument measured values(T/μs)
1	35	77	77
2	36	74	75
3	37	71	71
4	38	69	70
5	39	67	67
6	40	65	64
7	41	*63*	62
8	42	60	60
9	43	58	58
10	44	55	54
11	45	53	53
12	46	48	48
13	47	45	45
14	48	40	42

Table 4
Response time of FLC compound 2CI.BAAP.120-BBP

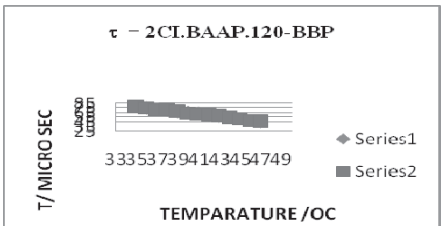

TABLE 5
Response time of FLC compound 2CI.BAAP.180- BBP

S.No.	**Temperature °C**	**Reported values (T/μs)**	**Instrument measured values (T/μs)**
1	32	90	90
2	33	90	89
3	34	88	87
4	35	78	78
5	36	75	75
6	37	71	70
7	38	66	66
8	39	60	61
9	40	57	57
10	41	49	48
11	42	38	36
12	43	33	30
13	44	22	21

TABLE 6
Response time of FLC compound 2CI.BAAP.180-BBP

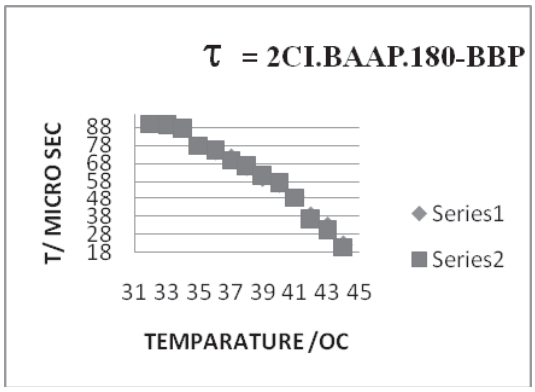

CONCLUSION

PC based wave form generator which was built and tested for its functionality with standard instruments capable to generate sine, square and triangular waves with accurate frequency and amplitude had been built and tested for its functionality with standard instruments.

REFERENCES

[1] T.J. Byers, "PC Based Test Equipment," Electronics Now. 1993.
[2] R.C. Chua, J.A. Cu, E.M. Diaz, S.I. Kung, and A.N. Santos, " Design of a Function Generator Plus an MCU-Based Pulse Generator," Electronics and Communications Engineering Department of De La Salle University - Manila. 2003
[3] Nguyễn Trường An and PhạmThị Thu Phương, Converting PC into two channel digital oscilloscope, presented at the same ISEE05.
[4] Shanley, Tom and Anderson, Don. PCI System Architecture (4thEd.). Mindshare, Inc. Addison-Wesley Professional. 1999.
[5] www.ni.com
[6] Data sheet and application notes of MAX038, www.MAXIM.com .
[7] Data sheet and application notes of PGA103,Burr-Brown.
[8] S. Sumathi, P. Surekha, LabVIEW based Advanced Instrumentation systems, Springer, (2007).
[9] Madhu Mohan M. L. N., Goud B. V. S., Kumar P. A. and Pisipati V. G. K. M., Mater.Res.Bullett., 34, 2167 (1999).
[10] Bawa S. S., Biradar A. M. and Chandra S., Jpn.J.Appl.Phys., 25, L446 (1986).

A Simple Laboratory Demonstrate Pacemaker

Mahammad D V[1], Dr B.V.S. Goud[1] and Dr D Linga Reddy[2]
[1]Dept. of Electronics & Instrumentation Tech. Acharya Nagarjuna Uni., Nagarjuna Nagar – 522510, A.P. India.
E mail : goudbvs@yahoo.com
[2]CVR College of Engineering, Vastunagar, Mangalpalli (V), Ibrahimpatnam (M), R R Dist., 501 510, A P India.
E mail : dlreddy_phy@yahoo.com

***Abstract*--A simple pacemaker circuit has been designed, fabricated and tested. The circuit consists of Signal Generator, Amplifier, Filters and Noise reduction circuits. The pulse signals generated from an operational amplifier circuit and fed to monostable 555 timer circuit. The pulses are acquired with Digital Storage Oscilloscope (DSO). The performance of the developed system is evaluated by recording the pulses of people having different heart beats, wave forms recorded are compared with standard pulse wave forms e.g. frequency, amplitude, pulse duration, shape etc. The accuracy of the diagnosis presently depends on the expertise of the physician.**

***Index Terms*-- Pacemaker, Monostable, Pulse duration.**

I. INTRODUCTION

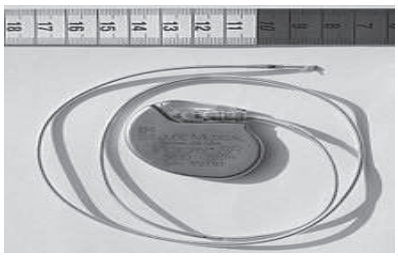

Picture 1(a) 1(b) Pacemaker model.

A pacemaker is a device that placed in chest or abdomen to help abnormal heart rhythms. This device uses electronic pulse to promote the heart beat at a normal rate. In 1958, Arne Larsson became the first to receive an implantable pacemaker [1,2]. He had a total of 26 devices during his life and campaigned for other patients needing Pacemaker In 1899, J A McWilliams reported in the British Medical Journal of his experiments in which application of an electrical impulse to the human heart in a systole caused a ventricular contraction and that a heart rhythm of 60-70 beats per minute could be evoked by impulses applied at pacing equal to 60–70/minute. Picture-1a,1b shows the pace maker model.

A. Need of Pacemaker

Doctors recommend pacemaker for a number of reason. The most common reason is bradycardia and heart block. BRADYCARDIA is a slower than normal heart beat. HERT BLOCK is problem with hearts electrical system. The disorder occurs when an electrical signal is slowed or disrupted as it moves through the beat [3]. Heart block can happen as a result of aging damage to heart from heart attack or other condition that interface with heart electrical activity. Certain nerve and muscle disorder can also cause heart block, including muscular dystrophy. Aging or heart disease damages your sinus node's ability to set the correct pace for your heart beat. Such damage can cause slower than normal heart beat or long pause between heart beats. The damage also can cause your heart to alternate between slow and fast rhythms. This condition is called "sick sinus syndrome". You have had a medical procedure to treat an arrhythmia called atrial fibrillation. A pacemaker can help regulate your heart beat too much. You faint or have some other symptoms of a slow heartbeat. You have heart muscle problem that causes electrical signal to travel too slowly through your heart beat muscle. You have long QT syndrome which puts you at risk for dangerous arrhythmias.

B. Energy Requirement to Excite Heart Muscle

To overcome of these all some of the measures are taken like all muscles tissues. The heart can be simulated with an electric shock. The minimum energy required for excite the heart muscle is about 10 µj. For safety purpose, a pulse of energy 100 µj is applied on heart muscle. A pulse of 5V, 10mA and 2mS duration is used

[4]. Ventricular fibrillation is a dangerous condition. This occurs due to a too high pulse. A patient loses consciousness in 10 to 15 sec and the brain cell dead within a few minutes from oxygen deficiency in the brain. This is caused by pulse of 400 µj. These pulses should have the pulse to the ratio of 1:1000 and that should be negatively going pulse to avoid ionization of the muscle. Pulse voltage is allowed to adjust in such a way that the energy is delivered by the pacemaker to the heart during each pulse. The pulse rate is 70 pulse/min but many pacemakers are adjusted in the range of 50 to 150 pulse/min. The duration of each pulse is between 1 to 2 ms, shown in figure-1.

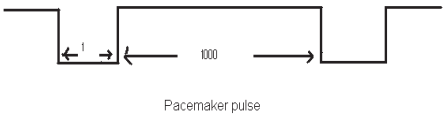

Figure 1. Duration of each pulse of Pacemaker.

II. METHODS OF SIMULATION

There are two types of simulations or pacing [3]

- External simulation
- Internal simulation

A. External Simulation

This simulation is used to restart the normal rhythm of heart. In this case the cardiac stands still. This occur during open heart surgery or whenever there is sudden physical shocks or accidents. The paddle shaped electrode is applied on the surface of the chest and current of 20 to 150 mA are employed. Picture-2a, 2b shows the model of external simulation.

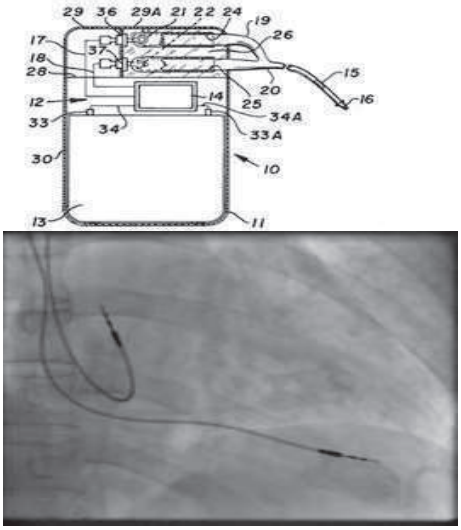

Pictures 2(a), 2(b). The model of external simulation of Pacemaker model.

B. Internal Simulation

This simulation is employed in case where long term pacing is required because of permanent damage. The electrodes are in the form of fine wires coated with Teflon coated stainless steel. During restarting heart after open heart surgery a spoon like electrode is used with current range of 2 to 15 mA.

C. Different Types of Pacemakers

Based on modes of operation of pacemaker is divided into five types

- Ventricular Asynchronous Pacemaker (Fixed rate pacemaker)
- Ventricular synchronous pacemaker
- Ventricular Inhibited Pacemaker (Demand Pacemaker)
- Atrial synchronous Pacemaker
- Atrial Sequential ventricular inhibited Pacemaker

III. VENTRICULAR ASYNCHRONOUS PACEMAKER

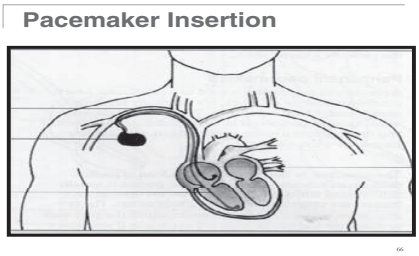

Picture 3. Shows pacemaker insertion model

It is the first type of pacing can be used in atrium or ventricle. It has a simplest mechanism and longest battery life. It is so cheap and easy to check and least sensitive device to outside interference. This pacemaker is suitable for patient with a stable, total Atrioventricular (AV) block, a slow rate atrial rate or arterial arrhythmia. It is basically a simple astable multivibrator .this produces a stimulus at a fixed rate irrespective of behaviour of heart rhytms. It is possible that such an event can be dangerous because if pacemaker impulse reaches heart during a certain vulnerable period, the ventricular fibrillation may occur. Picture-3 shows pacemaker insertion model.

A. *Block Diagram of Pacemaker*

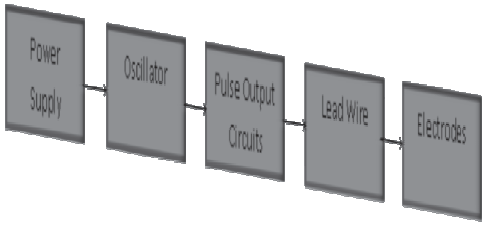

Figure 2. Block diagram of asynchronous pacemaker.

- Power supply – provides energy
- Oscillator – controls pulse rate
- Pulse output – produces stimuli
- Lead wires – conduct stimuli
- Electrodes – transmit stimuli to the tissue

Output circuit produces the electrical stimuli to be applied to the heart [4]. Stimulus generation is triggered by the timing circuit. Constant voltage pulses typically rated at 5.0 to 5.5V for 500 to 600μs Constant current pulses typically rated at 8 to 10mA for 1.0 to 1.2ms. Asynchronous pacing rates 70 to 90 beats per min. Figure-3 Realistic depiction of waveform appearing across heart emitted from capacitor discharge output circuit.

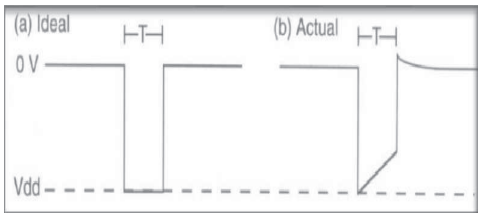

Figure 3. The Ideal and Realistic waveforms of O/P of pacemaker.

B. *Schematic diagram*

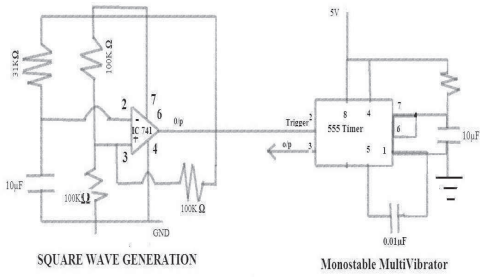

Figure 4. The schematic diagram of pacemaker

Figure-4 shows the schematic diagram of pacemaker. It consist of an integrated chip (IC) 741 and IC 555 timer. IC 741 acts as a square wave generator which generates square wave and its square wave o/p is fed to as trigger of 555 timer than IC 555 timer produce the required pulse width. IC 741, 555 timer, Resistors (100k-4, 10k, 31 k, 22k-1), Capacitors (10 μF-2, 0.01 μF-1), DSO A Square wave generator is obtained by connecting a capacitor of 10μ and resistors of 32kΩ to a voltage detector circuit [5]. The output of this combination will provide a positively and negatively going square waves with a equal duration of positive and negative pulses. The period of square wave generator is given by

$$T = -2RC \ln 1-\alpha / 1+\alpha \qquad (1)$$

Where α is feedback voltage fraction such that
$\alpha = R2/R1+R2$, T=0.8589 Sec.

The period of this oscillator can be changed by changing α or Time constant RC

The Square wave generator is nothing but astable multivibrator. Which periodically switches between | vsat | and -|vsat|. Now the output of the square wave generator is coupled to the positive edge triggered monostable multivibrater circuit. A positive Step at trigger circuit will pass through the capacitor CC . The capacitor CC is chosen so as to make 5time constant equal to the pulse duration TD. Otherwise trigger will still represent after TD has passed and a second would be wrongly generated

$$TD = 5C_C [R4\ R3/R3+R4] = -R5Cm \ln R3/R3+R4$$
$$= 5x0.16x10^{-6} [1200 / 2.2]$$
$$= -721(10^{-6}) \ln 1.2/2.2 = 0.437\ \mu sec$$

A pacemaker should deliver the pulse with period of T=0.8589 Sec and duration = 0.437 μsec

IV. ELECTRICAL CONDUCTION SYSTEM OF THE HEART

A. *Principle of ECG formation*

The normal intrinsic electrical conduction of the heart allows electrical propagation to be transmitted from the Sinoatrial Node through both atria and forward to the Atrioventricular Node. Normal/baseline physiology allows further propagation from the AV node to the ventricle or Purkinje Fibers and respective bundle branches and subdivisions/fascicles. Both the Sinoatrial node (SA) and AV nodes stimulate the Myocardium. Time ordered stimulation of the myocardium allows efficient contraction of all

four chambers of the heart, thereby allowing selective blood perfusion through both the lungs and systemic circulation [6]. Picture-4 shows the Electrical conduction system of the heart

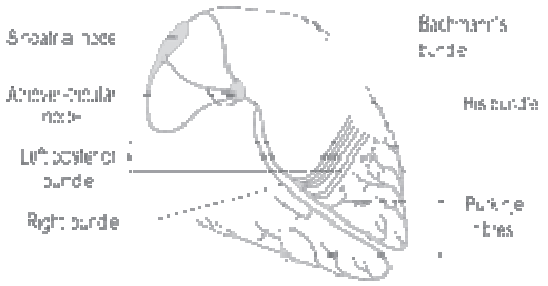

Picture 4. Electrical conduction system of the heart

B. Conduction Pathway

Action potentials arising in the SA node (and propagating to the left atrium via Bachmann's bundle) cause the atria to contract. Simultaneously, action potentials travel to the AV node via three internodal pathways. After a delay, the stimulus is conducted through the bundle of His branches and then to the purkinje fibers and the endocardium at the apex of the heart, then finally to the ventricular myocardium. The pathway can be summarized as: SA node → anterior, middle, and posterior internodal tracts → transitional fibers → AV node → penetrating fibers → distal fibers → Bundle of His (AV bundle) → right and left bundle branches → Purkinje fibers → myocardium [7]. The total time taken by the nerve impulse to travel from the SA node to the ventricular myocardium is 0.19 seconds. Microscopically, the wave of depolarization propagates to adjacent cells via gap junctions located on the intercalated disk. The heart is a functional syncytium. In a functional syncytium, electrical impulses propagate freely between communicating cells via gap junctions, so that the myocardium functions as a single contractile unit. This property allows rapid, synchronous depolarization of the myocardium. While normally advantageous, this property can be detrimental as it potentially allows the propagation of incorrect electrical signals (e.g., via an ectopic pacemaker). Gap junctions can close, e.g., after a cardiac ischemic event such as myocardial infarction, thus isolating damaged or dying tissue in the myocardium, which then no longer participate in synchronous myocardial contractility.

V. RESULTS AND CONCLUSION

A Brief overview of the history and development of the circuit design applied in pacemakers has been presented and successfully developed and demonstrated in our lab with Tektronix DSO model TDS 1012B. And we found that the designed system performance is satisfactory. The advances in integrated circuit designs have resulted in increasingly sophisticated pacing circuitry, providing, for instance, for diagnostic analysis, adaptive rate response and programmability Using fixed rate pacemaker, the heart rate cannot be increased to generate physical effort. Simulation with fixed impulse frequency results in ventricles area beating at different rates. This varies the stroke volume of the Heart Causes some loss in Cardiac Output Possibility for ventricular fibrillation will be more, when we use it for the patient with unstable block, due to interference between the ventricular contracts evoked by the pacemaker and the Atria. The present developed system is only for students practice to analyse and understanding of working conditions of pacemaker in their laboratory.

REFERENCES

[1] Ouellette, S. Anesthetic considerations in patients with cardiac assist devices. CNRA, 23(2), 9-20. (2000).

[2] Roth, J. Programmable and dual chamber pacemakers: An update. Progress in anes thesiology, 8, chapter 17. WB Saunders. (1994).

[3] Michael M. Domach, " Introduction to Biomedical engineering" pearson education Inc, 2005.

[4] S. R. Khandpur, " Handbook of Bio-medical instrumentation" second edition, Tata McGraw-hill professional press, 2006.

[5] Ramakantht A. gayakwad " Op-Amps and linear Integrated circuits" 4th edition, pearson prentice hall, 2006.

[6] Anesthesia. Philadelphia: Saunders.1997

[8] Moser SA, Crawford D, Thomas A. AICDs, CC Nurse;62-73, 1993.

MHD Free Convection Effects of Radiating Memory Flow

Syed Amanullah Hussaini [1] M.V Ramana Murthy [2] and Rafiuddin [3]
[1]M J College of Engineering & Technology, Department of Mathematics, Hyderabad, India
Email: amanullahsd@gmail.com
[2]Osmania University, Department of Mathematics, Hyderabad, India
Email: mv_rm@rediffmail.com
[3]CVR College of Engineering, Department of H & S, Ibrahimpatam (M), R.R.District, A.P., India
Email: rafiuddin2008@gmail.com

***Abstract* – Two dimensional unsteady radiating oscillatory memory flow past an infinite plane porous wall is investigated. Expressions for the mean velocity and the mean temperature are obtained. The effects of various parameters such as Permeability parameter (K), Grashoff number (G_r), Hartmann number (M), Radiation parameter (N), Prandle number (P_r) are depicted graphically. Nusselt number (Nu) and Skin friction (C_f) are discussed by tables.**

***Index Terms* – Suction, Porous medium, Walter's liquid- B and Rosseland's approximation.**

I. INTRODUCTION

The study of flow of electrically conducting fluid, the so-called magneto-hydrodynamics (MHD) has a lot of attention due to its diverse applications in astrophysics and geophysics. It is important to study the effect of the interaction of magnetic field on the temperature distribution and heat transfer when the fluid is not only electrically conducting but also when it is capable of emitting and absorbing thermal radiation. Heat transfer by thermal radiation is important when we are concerned with space technology applications and in power engineering. Seddeek [3] studied the effects of radiation and variable viscosity on a MHD free convection flow past an semi-infinite flat plate with an aligned magnetic field in the case of unsteady flow. Mazumdar and Deka [4] investigated MHD flow past an impulsively started infinite vertical plate in presence of thermal radiation. Analytical closed-form solution of the unsteady hydro-magnetic natural convection heat and mass transfer flow of a rotating, incompressible, viscous Boussinesq fluid was presented by Mbeledogu and Ogulu [5]. Mbeledogu et al. [6] also studied the free convection flow of a compressible Boussinesq fluid under the simultaneous action of buoyancy and transverse magnetic field. Mohamed and Abo- Dahab [7] analysis, the effects of chemical reaction and thermal radiation on hydromagnetic free convection heat and mass transfer for a micropolar fluid via a porous medium bounded by a semi-infinite vertical porous plate in the presence of heat generation. Natural convection of an electrically conducting and radiating fluid in the presence of an external magnetic field is investigated numerically by Young [8]. Zueco and Anwar [9] studied the steady-state, magneto hydrodynamic, optically thick, dissipative gas boundary layer flow and heat transfer past a non-isothermal porous wedge embedded in a scattering, homogenous, isotropic Darcy_Forchheimer porous medium, with significant thermal radiation effects in the presence of heat sink/sources and surface transpiration, in a (x, y) coordinate system. Ahmed and Sarmah [10] analyzed the joint effect of thermal radiation and transverse magnetic field on an unsteady convection and mass transfer flow of an incompressible viscous electrically conducting fluid past a suddenly fixed vertical plate. Ishak [11] worked mixed convection boundary layer flow over a horizontal plate with thermal radiation. Soret and Dufour effects on free convection flow of non-Newtonian fluids along a vertical plate embedded in a porous medium with thermal radiation were studied by Tai and Char [12]. Israel – Cookey and Nwaigwe [13] considered unsteady MHD flow of a radiating fluid over a vertical moving heated porous plate with time – dependent suction. Narahari [14] studied the effects of thermal radiation and free convection currents on the unsteady Couette flow between two vertical parallel plates with constant heat flux at one boundary. Israel – Cookey et al. [15] investigated the combined effects of radiative heat transfer and a transverse magnetic field on steady flow of an electrically conducting optically thin fluid through a horizontal channel filled with porous medium and non- uniform temperatures at the walls. Singh et al. [16] studied the effect of surface mass transfer on MHD mixed convection flow past a heated vertical flat permeable surface in the presence of thermophoresis, radiative heat flux and heat source/sink. Ahmed [17] given the exact solution to the problem of MHD transient free convection and mass

transfer flow of a viscous, incompressible, and electrically conducting fluid past a suddenly started infinite vertical plate taking into account the thermal diffusion as well as the thermal radiation was presented. The heat and mass transfer characteristics of the unsteady electrically conducting fluid flow past a suddenly started vertical infinite flat plate studied by Turkyilmazoglu and Pop [18]. Free convective heat and mass transfer flow over a moving permeable flat vertical stretching sheet in the presence of non-uniform magnetic field is numerically investigated by Ferdows et al. [19].

Now we study the free convection effects on the fluctuating flow of radiating memory flow past an infinite porous wall with constant suction through porous medium.

II. FORMULATION OF PROBLEM

We consider the free convective flow due to fluctuating mean stream of memory fluid (Walter's Liquid Model-B) flow past an infinite plane, porous wall with constant suction at the surface. Let y=0 be the wall in the presence of magnetic field normal to the direction of flow. Let u and v be the velocity components along and normal to the wall.

We make the following assumptions:

1) That all the fluid properties are constant except the density in the buoyancy force term;
2) That the term due to the electrically dissipation is neglected in energy equation (2.2) as the magnetic field is not strong enough to cause Joule heating (electrical dissipation)
3) That the Eckert number E_c and the magnetic Renold's numbers are small so that the induced magnetic field can be neglected. The x-axis is taken along the surface in the upwards direction and y-axis is taken normal to it.

As the bounding surface is infinite in length, all the variables are functions of y alone. By the usual boundary layer approximation the basic equation for unsteady flow are

$$v = -v_0 \tag{2.1}$$

$$\frac{\partial u}{\partial t} - v_0 \frac{\partial u}{\partial y} = \frac{dU}{dt} + g\beta_1(T - T_\infty) + \vartheta \frac{\partial^2 u}{\partial y^2} - \frac{\beta}{\rho}\left[\frac{\partial^3 u}{\partial t\, \partial y^2} - v_0 \frac{\partial^3 u}{\partial y^3}\right] - \frac{\vartheta u}{K} - \left(\frac{\sigma \mu_e^2 H_0^2}{\rho}\right) u \tag{2.2}$$

$$\frac{\partial T}{\partial t} - v_0 \frac{\partial T}{\partial y} = \frac{\kappa}{\rho C_p}\frac{\partial^2 T}{\partial y^2} + \frac{\vartheta}{C_p}\left(\frac{\partial u}{\partial y}\right)^2 - \frac{1}{\rho C_p}\left(\frac{\partial q_r}{\partial y}\right) \tag{2.3}$$

where the Rosseland's approximation (Brewster[2]) is used, which leads to

$$q_r = \frac{-4\sigma^*}{3k^*}\frac{\partial T^4}{\partial y} \tag{2.4}$$

The boundary conditions are:

$$u(0,t) = 0, T(0,t) = T_w, T(\infty, t) = T_\infty$$

$$u(y,t) = U = U_0(1 + \varepsilon e^{i\omega t}) \text{ as } y \to \infty \tag{2.5}$$

We assumed that the temperature differences within the flow are sufficiently small such that T^4 may be expressed as a linear function of the temperature. This was accomplished by expanding T^4 in a Taylor series about T_∞ and neglecting higher-order terms. Thus,

$$T^4 \cong 4T_\infty^3 T - 3T_\infty^4 \tag{2.6}$$

Using (2.4) and (2.6) in (2.3) gives

$$\frac{\partial T}{\partial t} - v_0 \frac{\partial T}{\partial y} = \frac{\kappa}{\rho C_p}\frac{\partial^2 T}{\partial y^2} + \frac{\vartheta}{C_p}\left(\frac{\partial u}{\partial y}\right)^2 + \frac{1}{\rho C_p}\left(\frac{16\sigma^* T_\infty^3}{3\kappa k^*}\right) \tag{2.7}$$

Introducing the following non-dimensional quantities:

$$\bar{y} = \frac{y v_0}{\vartheta}, \quad \bar{t} = \frac{t v_0^2}{\vartheta}, \bar{K} = \frac{K v_0^2}{\vartheta^2}, \bar{\omega} = \frac{\vartheta \omega}{v_0^2},$$

$$M = \frac{\sigma \vartheta H_0^2 \mu_e^2}{\rho v_0^2}, \quad N = \frac{16\sigma^* T_\infty^3}{3\kappa k^*}, \quad \bar{u} = \frac{u}{U_0},$$

$$W = \frac{u(t)}{U_0}, \quad G_r = \frac{g\beta_1(T_w - T_\infty)}{U_0 v_0^4},$$

$$R_m = \frac{\beta v_0^2}{\vartheta^2}, \qquad E = \frac{u_0^2}{C_p(T_w - T_\infty)}$$

$$P_r = \frac{\vartheta \rho C_p}{\kappa}, \qquad \theta = \frac{T - T_\infty}{T_w - T_\infty} \tag{2.8}$$

Using equation (2.2) into (2.3), then with the help of (2.8), the following equations are obtained

$$\frac{\partial u}{\partial t}-\frac{\partial u}{\partial y}=\frac{dW}{dt}+G_r\theta+\frac{\partial^2 u}{\partial y^2}-R_m\left(\frac{\partial^3 u}{\partial t\,\partial y^2}-\frac{\partial^3 u}{\partial y^3}\right)$$

$$-u\left(\frac{1}{K}+M\right) \qquad (2.9)$$

$$\frac{\partial\theta}{\partial t}-E\left(\frac{\partial u}{\partial y}\right)^2=\left(\frac{1+N}{P_r}\right)\frac{\partial^2\theta}{\partial y^2}+\frac{\partial\theta}{\partial y} \qquad (2.10)$$

The corresponding boundary conditions becomes

$$\theta=1,\qquad u=0\quad at\quad y=0$$

$$\theta\to 0,\qquad w\to W(t)\ \ as\ \ y\to\infty$$

Free-stream boundary condition

$$W(t)=(1+\varepsilon e^{i\omega t})\quad as\ y\to\infty \qquad (2.11)$$

Where

ρ Density of fluid,
β Kinematic visco-elasticity,
β_1 Coefficient of volume expansion,
H_o Magnetic intensity,
μ_e Magnetic permeability,
R_m Magnetic Renolds number,
ϑ Kinematic viscosity,
K Permeability parameter,
C_p Specific heat at constant pressure,
N Thermal radiation parameter,
K Thermal conductivity,
G_r Grashoff number,
P_r Prandtl number,
M Hartmann number,
E Eckert number,
q Heat flux,
σ Electric conductivity,
σ^* Stephan-Boltzman constant,
k^* Mean absorption coefficient,
$f_1=\left(\frac{P_r}{1+N}\right)$

III. SOLUTION OF THE PROBLEM

Following Lighthill, [1] we put velocity and temperature field as

$$u=u_0+\varepsilon e^{i\omega t}u_1 \qquad (3.1)$$

$$\theta=\theta_0+\varepsilon e^{i\omega t}\theta_1 \qquad (3.2)$$

since free stream velocity fluctuates, we may take

$$W(t)=(1+\varepsilon e^{i\omega t}) \qquad (3.3)$$

Where 'ω' is the frequency and 'ε' is very small quantity $<<1$.

Now making use of (3.1) and (3.2) into the equations (2.9) and (2.10), equating harmonic and non-harmonic terms, we get

Zeroth order

$$R_m u_0'''+u_0''+u_0'=-M_1u_0=-G_r\theta_0 \qquad (3.4)$$

$$\left(\frac{1+N}{P_r}\right)\theta_0''+\theta_0'=-E(u_0')^2 \qquad (3.5)$$

First order

$$R_m u_1'''+(1-si\omega)u_1''+u_1'-(M_1+i\omega)u_1=-i\omega-u_0'-G_r\theta_1 \qquad (3.6)$$

$$\theta_1''+f_1\theta_1'-f_1 i\omega\theta_1=-f_1[\theta_0+2Eu_0'u_1'] \qquad (3.7)$$

Boundary conditions are

$$\theta_0=1,\theta_1=u_0=u_1=0\ \ as\ y=0$$

$$\theta_0=\theta_1=0,u_0=u_1=1\ as\ y\to\infty \qquad (3.8)$$

In equations (3.4) and (3.6), because of the presence of elasticity term, we get third order differential equation. To solve this, we need three boundary conditions but we have two. So following Beard and Walters (1964), we assume the solution as

$$F=F_1(y)+R_mF_2(y)+o(R_m^2) \qquad (3.9)$$

$$u_0(y)=u_{01}(y)+R_mu_{02}(y)+o(R_m^2)$$

$$\theta_0(y)=\theta_{01}(y)+R_m\theta_{02}(y)+o(R_m^2)$$

$$u_1(y)=u_{11}(y)+R_mu_{12}(y)+o(R_m^2)$$

$$\theta_1(y)=\theta_{11}(y)+R_m\theta_{12}(y)+o(R_m^2) \qquad (3.10)$$

Where u_0 and θ_0 are the mean velocity and mean temperature and u_1 and θ_1 are the fluctuating parts of the velocity and temperature respectively.

Using equations (3.10) into equations (3.4) – (3.7) equating the coefficients of different powers of R_m and neglecting those of R_m^2

Thereafter considering differential equations related to mean parts

$$u_{01}'' + u_{01}' - M_1 u_{01} = -G_r \theta_{01} \quad (3.11)$$

$$u_{01}''' + u_{02}'' + u_{02}' - M_1 u_{02} = -G_r \theta_{02} \quad (3.12)$$

$$\theta_{01}'' + f_1 \theta_{01}' = E f_1 (u_{01}')^2 \quad (3.13)$$

$$\theta_{02}'' + f_1 \theta_{02}' = E f_1 2 u_{01}' u_{02}' \quad (3.14)$$

Boundary conditions are

$$\theta_{01} = 1, \theta_{02} == u_{01} = u_{02} \to 0 \text{ as } y \to 0$$

$$\theta_{01} = \theta_{02} = 0, u_{01} = 1, u_{02} = 0 \text{ as } y \to \infty \quad (3.15)$$

We solve the equations (3.11) – (3.14), we expand u and θ in powers of E because of Eckert number E is very small (< < 1) for incompressible fluid

$$F = F_1 + EF_2 \quad (3.16)$$

Replacing F by $u_{01}, u_{02}, \theta_{01}, \theta_{02}$, we get

$$u_{011}'' + u_{011}' - M_1 u_{011} = -G_r \theta_{011} \quad (3.17)$$

$$u_{011}''' + u_{021}'' + u_{021}' - M_1 u_{021} = -G_r \theta_{021} \quad (3.18)$$

$$u_{012}'' + u_{012}' - M_1 u_{012} = -G_r \theta_{012} \quad (3.19)$$

$$u_{012}''' + u_{022}'' + u_{022}' - M_1 u_{022} = -G_r \theta_{022} \quad (3.20)$$

$$\theta_{011}'' + f_1 \theta_{011}' = 0 \quad (3.21)$$

$$\theta_{021}'' + f_1 \theta_{021}' = 0 \quad (3.22)$$

$$\theta_{012}'' + f_1 \theta_{012}' = f_1 (u_{011}')^2 \quad (3.23)$$

$$\theta_{022}'' + f_1 \theta_{022}' = 2 f_1 u_{011}' u_{021}' \quad (3.24)$$

Boundary conditions are

$$\theta_{011} = \theta_{012} = \theta_{021} = \theta_{022} = 0$$

$$u_{011} = u_{012} = u_{021} = u_{022} = 0 \text{ as } y \to 0$$

$$u_{011} = 1, u_{012} = u_{021} = u_{022} = 0$$

$$\theta_{011} = \theta_{012} = \theta_{021} = \theta_{022} = 0 \text{ as } y \to \infty \quad (3.25)$$

We get the following solutions for the mean temperature profiles as

$$\theta_{011} = e^{-f_1 y} \quad (3.26)$$

$$\theta_{012} = G_r^2 \left[b_2 e^{-f_1 y} + a_1^2 f_1 m_1 e^{-2my} + \frac{a_1^2 f_1 e^{-2f_1 y}}{2} - a_1^2 f_1 f_2 e^{-(m+f_1)y} \right] \quad (3.27)$$

$$\theta_{021} = 0 \quad (3.28)$$

$$\theta_{022} = 2G_r^2 a_1 f_1 \left[-\{m_4 + m_5 - m_6 + f_4\} e^{-f_1 y} + (m_5 - m_6) e^{-2my} + (m_4 - f_2 f_3) e^{-(m+f_1)y} + \frac{a_1^2 f_1^3 e^{-2f_1 y}}{2} - m_0 y e^{-2my} + m_3 y e^{-(m+f_1)y} \right] \quad (3.29)$$

$$\theta = \theta_0 + \varepsilon \theta_1 \quad (3.30)$$

$$\theta_0 = \theta_{01} + R_m \theta_{02} \quad (3.31)$$

$$\theta_0 = (\theta_{011} + E\theta_{012}) + R_m (\theta_{021} + E\theta_{022}) \quad (3.32)$$

Mean dimensionless coefficient of heat transfer i.e., Nusselt's number is given by

$$Nu = \theta_0'|_{y=0} = -f_1 + E[G_r^2 \{-b_2 f_1 - 2m a_1^2 f_1 m_1 - a_1^2 f_1^2 + a_1^2 f_1 f_2 (m + f_6)\}] + R_m E \begin{bmatrix} 2G_r^2 a_1 f_1 \{m_4 + m_5 - m_6 + f_4\} f_1 \\ -2m(m_5 - m_6) - \\ (m + f_1)(m_4 - f_2 f_3) - \\ a_1^2 f_1^4 - m_0 + m_3 \end{bmatrix} \quad (3.33)$$

Now we get the following solutions for the mean velocity profiles.

$$u_{011} = G_r a_1 \left[e^{-my} - e^{-f_1 y} \right] \quad (3.34)$$

$$u_{021} = G_r \left[f_1^3 a_1^2 e^{-my} - a_1 b_1 y e^{-my} - a_1^2 f_1^3 e^{-f_1 y} \right] \quad (3.35)$$

$$u_{012} = \frac{G_r^2}{b_1}[(a_8 + a_9 + a_{10} - a_{11})e^{-my}] - \frac{G_r^3}{b_1}\left[\left(a_8 e^{-f_1 y} + a_9 e^{-2f_1 y} + a_{10} e^{-2my} - a_{11} e^{-(m+f_1)y}\right)\right] \quad (3.36)$$

$$u_{022} = G_r^3\left[(2f_1 a_7 + a_{16})e^{-my} + (2f_1 a_3 - a_{12})e^{-f_1 y} - (2f_1 a_4 + 2f_1 a_1 m_{10} + a_{14})e^{-2my} - (2f_1 a_1 a_6 + a_{13})e^{-2f_1 y} - (2f_1 a_1 a_5 + 2f_1 a_1 m_3 f_6 - a_{15})e^{-(m+f_1)y} - (2f_1 a_1 m_9 + a_8 + a_9 + a_{10} - a_{11})ye^{-my} - (2f_1 a_1 m_3 f_5)ye^{-(m+f_1)y}\right] \quad (3.37)$$

$$u_0 = (u_{011} + Eu_{012}) + R_m(u_{021} + Eu_{022}) \quad (3.38)$$

Mean non-dimensional skin friction is given by

$$C_f = u_0'|_{y=0} = [G_r a_1(f_1 - m)] + E\left[\frac{G_r^2}{b_1}\{m(a_{11} - a_{10} - a_9 - a_8)\} - \frac{G_r^3}{b_1}\{a_{11}(m + f_1) - 2ma_{10} - 2a_9 f_1 - a_8 f_1\}\right] + R_m[\{G_r(a_1^2 f_1^4 - a_1^2 f_1^3 m - a_1 b_1)\} + EG_r^3\{-m(2f_1 a_7 + a_{16}) - f_1(2f_1 a_3 - a_{12}) + 2m(2f_1 a_4 + 2f_1 a_1 m_{10} + a_{14}) + 2f_1(2f_1 a_1 a_6 + a_{13}) + (m + f_1)(2f_1 a_1 a_5 + 2f_1 a_1 m_3 f_6 - a_{15}) - (2f_1 a_1 m_9 + a_8 + a_9 + a_{10} - a_{11}) - 2f_1 a_1 m_3 f_5\}] \quad (3.39)$$

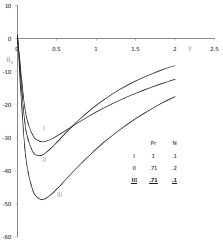

figure-1
Mean temperature distribution θ_0 versus y for fixed values of M=5,K=0.1 , G_r=5, E=0.01and R_m=0.4

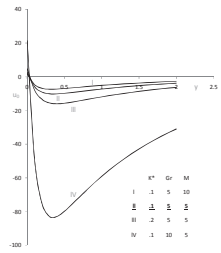

figure-2
Mean velocity distribution $u_0$versus y for fixed values of f=0.1,E=0.01 and R_m=0.4

NUSSELT'S NUMBER TABLE 1

K	Nusselt's Number	Pr	Nusselt's Number	Gr	Nusselt's Number	M	Nusselt's Number	N	Nusselt's Number
0.2	12136.7	0.2	23105.0	2	19196.8	2	14873.3	0.2	19889.8
0.4	8915.03	0.4	22848.7	4	19210.2	4	17740.4	0.4	20997.3
0.6	7894.28	0.6	20488.8	6	19232.5	6	20729.7	0.6	21844.3
0.8	7394.51	0.8	18269.2	8	19263.8	8	23834.5	0.8	22480.3
1.0	7098.13	1.0	16459.3	10	19304.1	10	27048.8	1.0	22945.5

For fixed values of K=0.1,Pr=0.71,Gr=5,M=5, N=0.1and Rm = 0.4

SKIN FRICTION TABLE 2

K	Skin Friction	Pr	Skin Friction	Gr	Skin Friction	M	Skin Friction	N	Skin Friction
0.2	11.182	0.2	26.9039	2	3.6201	2	12.9959	0.2	16.1654
0.4	6.0182	0.4	20.3494	4	9.5948	4	13.9239	0.4	18.5692
0.6	2.7696	0.6	17.5894	6	20.2742	6	14.3923	0.6	19.7510
0.8	0.6292	0.8	10.6247	8	38.0083	8	14.6059	0.8	20.2481
1.0	-0.8731	1.0	0.41004	10	65.1472	10	14.6717	1.0	20.3468

For fixed values of K=0.1,Pr=0.71,Gr=5,M=5, N=0.1and Rm = 0.4

CONCLUSIONS

We observe that as permeability parameter K and Groshoff number G_r suppress velocity distribution it is due to the fact that in Rosseland's approximation the temperature differences are very small, that is why adverse trend is noted. In general permeability parameter K and Groshoff number G_r influence velocity distribution, whereas Lorentz force influences the velocity distribution because of the Roseland's approximation refer fig-2

We see that temperature is in direct proportion to radiation parameter N from (2.8), so the effect of radiation parameter N is to influence the temperature distribution and also we note that as Prandle number P_r increases temperature distribution increases refer fig-1

The effect of K (Permeability parameter) and P_r (Prandle number) is to decrease the heat transfer whereas G_r (Grashoff number), M (Hartmann number) and N (Radiation parameter) is to influence the heat transfer. The above parameters have the same effect on skin friction refer table 1 & 2.

REFERENCES

[1] M.J. Lighthill "The response of laminar skin friction and heat transfer to fluctuation in the stream velocity" Proceedings of the Royal Society, A 224,1. (1954)

[2] M.Q. Brewester, "Thermal radiative transfer and properties" New York, John Wiley and Sons Inc. (1992)

[3] M.A. Seddeek, "Effects of radiation and variable viscosity on a MHD free convection flow past a semi-infinite flat plate with an aligned magnetic field in the case of unsteady flow" International Journal of Heat and Mass transfer 45 (2002) 931-935

[4] M.K. Mazumdar and R.K. Deka, "MHD flow past an impulsively started infinite vertical plate in presence of thermal radiation", Romanian Journal of Physics, 52(5-7), (2007) 565-573

[5] I.U. Mbeledogu and A. Ogulu, "Heat and mass transfer of an unsteady MHD natural convection flow of a rotating fluid past a vertical porous flat plate in the presence of radiative heat transfer" International Journal of Heat and Mass Transfer 50 (2007) 1902–1908

[6] I.U. Mbeledogu, A.R.C. Amakiri and A. Ogulu, "Unsteady MHD free convective flow of a compressible fluid past a moving vertical plate in the presence of radiative heat transfer" International Journal of Heat and Mass Transfer 50 (2007) 1668–1674

[7] R.A. Mohamed and S.M. Abo-Dahab, "Influence of chemical reaction and thermal radiation on the heat and mass transfer in MHD micro polar flow over a vertical moving porous plate in a porous medium with heat generation" International Journal of Thermal Sciences 48 (2009) 1800–1813

[8] C. Y. Han, "Hydromagnetic free convection of a radiating fluid" International Journal of Heat and Mass Transfer 52 (2009) 5895–5908

[9] J. Zueco and O. A. Beg "Network simulation solutions for laminar radiating dissipative magneto-gas dynamic heat transfer over a wedge in non-Darcian porous regime" Mathematical and Computer Modelling 50 (2009) 439 - 452

[10] N. Ahmed and H.K. Sarmah, "Thermal radiation effect on a transient MHD flow with mass transfer past an impulsively fixed infinite vertical plate", International Journal of Applied Mathematics and Mechanics 5 (2009) 8798.

[11] A. Ishak, "Mixed convection boundary layer flow over a horizontal plate with thermal radiation" Heat Mass Transfer 46 (2009) 147–151.

[12] Bo-C. Tai and M.-I. Char, "Soret and Dufour effects on free convection flow of non- Newtonian fluids along a vertical plate embedded in a porous medium with thermal radiation" International Communications in Heat Mass Transfer 37 (2010) 480–483.

[13] C.I.Cookey and C. Nwaigwe, "Unsteady MHD flow of a radiating fluid over a moving heated porous plate with time – dependent suction", American Journal of Scientific and Industrial Research, (2010) 1(1): 88 – 95.

[14] M. Narahari, "Effects of thermal radiation and free convection currents on the unsteady Couette flow between two vertical parallel plates with constant heat flux at one boundary", World Scientific and Engineering Academy and Society Transactions on Heat and Mass Transfer, (2010) 1(5): 21 – 30.

[15] C.I Cookey, V. B. O. Pepple and I. Tamunobereton-ari "On steady hydromagnetic flow of a radiating viscous fluid through a horizontal channel in a porous medium" American Journal of Scientific and Industrial Research, (2010), 1(2): 303-308

[16] N.P. Singh, A.K. Singh, A.K. Singh and P. Agnihotri, "Effects of thermophoresis on hydromagnetic mixed convection and mass transfer flow past a vertical permeable plate with variable suction and thermal radiation" Communications in Nonlinear Science and Numerical Simulation 16 (2011) 2519–2534

[17] N. Ahmed, "Soret and radiation effects on transient MHD free convection from an impulsively started infinite vertical plate" J. Heat Transfer 134 (2012) 062701-1–062701-9.

[18] M. Turkyilmazoglu and I. Pop, "Soret and heat source effects on the unsteady radiative MHD free convection flow from an impulsively started infinite vertical plate" International Journal of Heat and Mass Transfer 55 (2012) 7635–7644

[19] M. Ferdows, M.J. Uddin and A.A. Afify, "Scaling group transformation for MHD boundary layer free convective heat and mass transfer flow past a convectively heated nonlinear radiating stretching sheet" International Journal of Heat and Mass Transfer 56 (2013) 181–187

A Brief Overview of Some Environmental Problems in India

K.T. Padmapriya[1] and Dr. Vivekanada Kandarpa[2]
[1] CVR College of Engineering, Department of H&S, Ibrahimpatan, R.R.District, A.P., India
Email:ktpadmapriya@gmail.com
[2] Professor, University of Phoenix, USA.
Email: kandarpav@gmail.com

Abstract- **The current article is a brief discussion of the enormity of environmental problems facing India. The problems are in the form of pollution of air, water, and land resources. High concentrations of pollutants of various kinds are directly linked with the health of the people, and in some cases they result in premature deaths. It is extremely important for engineers of the current and next generation to be cognizant of this situation in their future developments. Environmental laws exist, and every effort should be made to keep this in mind in all new developments.**

Index Terms- **Environment, Atmospheric pollution, pollutant, Environmental laws.**

I. INTRODUCTION

There is a preponderance of evidence that the majority of the respiratory and cardiovascular maladies, cancer and other serious diseases, and even premature death of millions of infants are due to very high level of the pollution of the air, water, and land. The sources for the pollution are many, and they include various industries, electric power plants, different modes of transportation, and waste disposal of various kinds (medical, industrial, radioactive, etc.,). In spite of the promulgation of many government regulations to combat the degradation of the environment, very little progress is being made and even the little progress made to date is too slow, especially in the developing countries. This is in spite of the global alarm expressed in the United Nations sponsored GEO-4 [1]: "Tipping points occur when the cumulative effects of steady environmental changes reach the thresholds that result in dramatic and often rapid changes. There is a concern that a number of environmental systems may be heading towards tipping points."

Most of the well developed countries are making much better progress at the local level in reducing harmful pollution, but many of them are reluctant to take full measures to reduce green house gas (GHG) emissions. Their main reasons expressed by the developed countries for the resistance to fully implement any reduction in GHG emissions are: (1) economic impact of such measures on the industry and (2) the lack of general belief on the GHG impact on global warming. On the other hand, the developing countries are reluctant to do anything regarding GHG emissions for a different set of reasons. They include: (1) the current urgent need of energy and other resource needs to support large populations, (2) a general lack of clean energy resources, and (3) the economic impact of importing advanced technologies to implement these reductions.

The purpose of this article is to educate the current generation of Engineers on the seriousness of the environmental problems currently facing India.

II. BRIEF HISTORICAL BACKGROUND

Historically speaking, the general concerns for the environment were expressed in Indian literature as far back as 300 BC in Kautilya's Arthasastra, where economic importance of forest administration is emphasized [2]. Following the ideas expressed in this document, Ashoka, in the early part of 1st Century implemented some concrete measures, as evident on the Ashoka Pillar, which expresses the necessity for biodiversity [3]:

"- - - - - Beloved-of-the-Gods, King PIYADASI (ASHOKA), speaks thus: Animals were declared to be protected – parrots, bats, - - - - and all four-footed creatures that are neither useful nor edible. Also protected were nanny goats, ewes and sows which are with young or giving milk to their young, and so are young ones less than six months old. Cocks are not to be caponized, husks hiding living beings are not to be burnt, and forests are not to be burnt either without reason or to kill creatures."

Additional evidence for the Indian society concern for environment can be found in the 5th Century document named "YAGNAVALKYA SMRITHI", which prohibited the cutting of trees and prescribed punishment for such acts.

These historical documents clearly demonstrated that the Indian society was implicitly conscious of the adverse environmental effects caused by deforestation and extinction of animal species (i.e. harmful effects of bio diversity). The latest GEO-4 [1] stresses the importance of biodiversity in preserving human and ecosystem welfare. However, over a period of several centuries, India lost this ideology and substantially deviated from its historic ethical philosophy and started embracing western utilitarian ethical philosophy. From the advent of industrial revolution, the utilitarian western ethical philosophy essentially dictated indiscriminate use of natural resources,

in the beginning in the western countries, and subsequently propagated throughout the world. According to utilitarian ethics, the right action is "the action that produces maximum happiness to man". It is generally accepted that "the main strands of Judeo-Christian thinking had encouraged the overexploitation of nature by maintaining the superiority of humans over all other forms of life on earth, and by depicting that all of nature as created for the use of humans"[4][5]. However, in the mid to late 20th century, many U.S. naturalists began to rethink some of these ethical viewpoints and started to voice concerns on the overuse of natural resources. They promoted the idea of conserving natural resources and eventually forced the legislative actions of the U.S. administration. The public awareness about the pollution and the degradation of the resource quality began to increase, in large part because of the publication of the book, *Silent Spring* by Rachel Carson [6]. Her book emphasized the harmful effects of DDT (dichlorodiphenyltrichloroethane) and other pesticides on birds as well as the contamination of human food supplies. Subsequently, further environmental movements followed throughout the U.S. and finally by 1970, the voices of the environmentalists were heard with the establishment of the first Earth Day by Gaylord Nelson, a former U.S. senator. Soon after, the US government formed Environmental Protection Agency (EPA) and established National Environmental Policy Act (NEPA). Now, most of the countries around the world have incorporated some form of environmental legislation to protect the environment. The EPA passed many environmental laws and regulations aimed at protecting the environment. However, it is not an easy task to implement the laws, especially when it comes to retrofitting changes to the already well established industries in the U.S. In spite of these difficulties, U.S. and many of the developed countries have been making substantial progress.

The developing countries, such as India, China, and other countries are facing similar environmental problems, but with more enhanced intensities due to relatively large populations using technologies. Before the problems get too severe, these developing countries should pay attention to the "lessons already learned" by the developed countries and implement the proper preventive measures at the inception of any new industrial developments. One of the crucial steps in this process is a general awareness of how natural environment functions.

III. WHAT IS ENVIRONMENTAL SCIENCE?

Environmental Science is the application of different sciences and non-sciences in understanding and managing or mismanaging the environment around us. It is not like other pure sciences. The goal of pure sciences is "to find how world works, to seek what regularities there may be, to penetrate to the connection of things – from sub-nuclear particles, which may be the constituents of all matter, to living organisms, the human social community, and thence to the cosmos as a whole" [7]. Science, especially physics attempts to understand the functioning of the universe, simply because it is there. In spite of the esoteric nature of sciences and its focus on fundamental research, humans benefited from the technologies they produced. However, some of the technological developments resulted in several unexpected consequences, such as "damages of various kinds" to the environment around us. There are many historical examples related to the "unexpected negative consequences" of useful technological products. Let us look at a recent example of a widely used pesticide which is banned subsequently because of the unexpected consequences.

NEONICOTINOID pesticides, a group of nicotine based chemicals, have been successfully helping in the control of pests of various kinds. Different research organizations, including the most recent work, hailed these pesticides to "have outstanding potency and systemic action for crop protection against piercing-sucking pests, and they are highly effective for flea control on cats and dogs. They generally have low toxicity to mammals (acute and chronic), birds, and fish."[8]. Since their registration in 1990's, these pesticides have been in use throughout the world. In recent research activities, a possible link between the use of NEONICOTINOID pesticides and drastic reduction in honey bees has been established. As the honey bees are considered the prime pollinators in agriculture, a majority of the countries in the European Union banned the use of NEONICTONOID pesticides. It is definite win for the bees and the environmentalists [9]. Further studies, probably, will ban the use of these pesticides in other countries. This example illustrates the relation among sciences, technologies, environmentalists, and government. Thus environmental science, unlike pure sciences is driven by humans for their need. Environmental Scientists are like "watchdogs" for the people and government agencies in proposing and implementing various environmental laws.

By its complex nature, environmental science handles many interconnected local as well as global issues involving human population, natural resources, and environmental pollution. It recognizes that whatever we do, that is going to alter the world's environment outside humans. The goal of environmental science is to encourage various governments, industries and people of the world to operate in an environmentally sustainable manner. Here, the environmental sustainability is defined as the ability to meet the current human needs for natural resources without compromising the ability of future generations to meet their needs, including minimum to the environment.

IV. ENVIRONMENT AS A SYSTEM: Natural Environment

As in Science and Engineering disciplines, it is convenient and useful to treat the environment as a system. The environmental system may be considered as made up four segments or individual sub-systems: Atmosphere, Hydrosphere, Geo-sphere or Lithosphere, and Biosphere. Fig.1 illustrates a schematic of natural environmental

system. Four segments or subsystems, namely, atmosphere, hydrosphere, lithosphere (or geo-sphere), and biosphere interact with one another. These interactions consist of energy and material transport among the segments, and ultimately they reach a dynamic equilibrium.

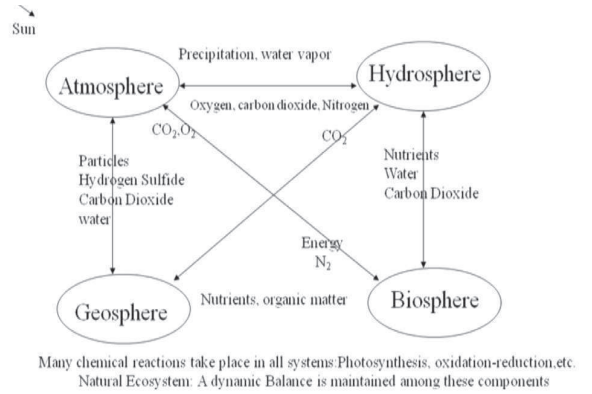

Figure 1: Schematic Representation of Natural Environment

Sun is the main source of energy in supporting life on earth. Earth's atmosphere provides radiation protection and molecular exchange needed to support life. Very high energy radiation from the sun is protected by the stratosphere (between about 11 km – 50 km above the earth's surface), where photochemical reaction creates a constant Ozone (O_3) content by an equilibrium reaction between oxygen and ozone. The ozone layer absorbs the majority of harmful ultraviolet radiation from the sun and prevents it from reaching the surface of the earth. The region from the surface of earth to about 11 km is called troposphere and is the most important zone for sustaining life on earth. The region is made up of nitrogen and oxygen, with minor amounts of carbon dioxide (about 0.03 percent of the atmosphere), and argon. Since the atmosphere is in equilibrium with the hydrosphere, varying concentrations of water vapor are also present in the atmosphere depending upon its location. The troposphere region provides the necessary molecular exchange between atmosphere and other subsystems of the environment needed. For example, the plants absorb radiation from the sun and the atmospheric carbon dioxide (CO_2) in utilizing the sun's energy through photosynthesis, and give off oxygen (O_2) as byproduct in respiration process. Humans and some animals breathe O_2 and give off CO_2. In addition to providing photosynthesis, CO_2 and water vapor help maintain a relatively comfortable temperature of earth around 15^{o}C by means of the greenhouse effect. Thus, life on earth is made possible by the energy from the sun and exchange of life supporting materials from atmosphere to other segments of the earth system.

In the hydrosphere (ocean and other surface waters), carbon dioxide dissolves in water. Carbonate minerals in the geo-sphere or lithosphere (land) also contain carbon. On land, carbon occurs as carbohydrates, proteins, and molecules essential for life in the biota, as fossil fuels from dead animals, and as carbonates in rocks. In ocean and other surface waters, carbon occurs as carbohydrates in the biota, as several forms of dissolved carbon dioxide, and as carbonates in the sediments. A schematic representation of a sustainable carbon cycle is shown Fig.2,. Through nitrogen cycle, the global circulation of nitrogen from the environment to living organisms and back to the environment are maintained. Similarly, hydrological cycle is maintained by global circulation of water from the environment to living organisms and back to the environment. A standard book on environmental science should be consulted for additional details on various cycles [10]. A dynamic balance of carbon, nitrogen, water, and other constituents are maintained in the natural environment, through carbon, nitrogen, phosphorus, sulfur, and water cycles.

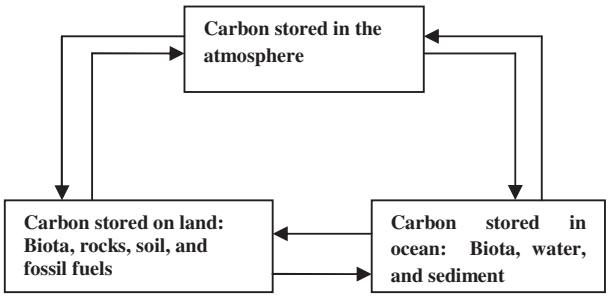

Figure 2: A schematic representation of Carbon Exchange in the Environment

V. TECHNOLOGICAL IMPACT ONNATURAL ENVIRONMENT

The dynamic equilibrium of the natural environment is impacted substantially by modern technological developments. Fig.3 schematically illustrates the impact of technology "currently" being used worldwide on the natural environment. All sub-systems of the environment see the impact of technology, either directly or indirectly through interaction among the sub-systems. Benign atmosphere becomes hostile due to harmful pollutant species, including especially dangerous particulate matter. These unnatural chemical pollutants and "their long-term exposure have serious health impacts for humans, ranging from minor eye irritation, respiratory symptoms to decreased lung and heart function, hospitalization, and even premature death." [11].

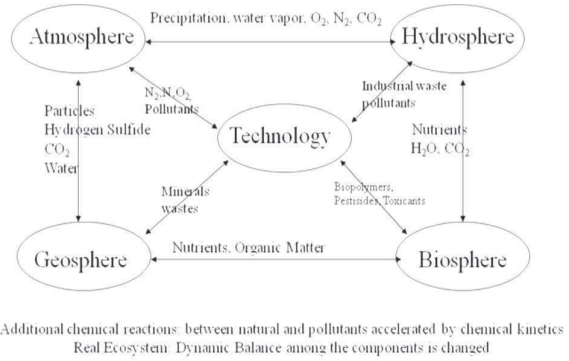

Figure 3: IMPACT OF TECHNOLOGY ON THE NATURAL ENVIRONMENT

The introduction of technology imparts additional constituents in all subsystems of the natural environment. Some of the technologies which directly impacted the natural environment include,

1) Energy production and utilization industries (fossil fuels including coal)
2) Transportation industries and private transportation (fossil fuels use)
3) Agriculture practices
4) Manufacture and utilization pesticides and insecticides
5) Manufacture of industrial products and various chemicals (Most of the Chlorine based chemicals)
6) Extraction and processing of mineral extraction (various acids, surfactants, etc.,)
7) Waste disposal (medical, radioactive, etc.)

These and many more modern developments contribute to the degradation of the environment. For example, coal mining industry and the burning of coal in the power generation industry cause serious environmental problems. Mining destroys existing vegetation and topsoil; the effluents in the mining operation generate pollutants in water and in the air (arsenic, lead, cadmium, particulate matter, etc.). Combustion of carbon produces several pollutants (CO_2, SO_2, etc). The GEO-4 of the UNEP emphasized that the energy, climate-change, industrial developments and environmental pollution are the main environmental concerns [1]. The report further reiterated that twenty years after the first report (UNEPT, 1998), factors such as population growth, and economic activities as well as consumption patterns have placed increased pressure on the environment. The population growth and increase in economic activities affect the environment negatively. The result is greater consumption of resources and higher pollution. However, by implementing improvement in technology, the negative effects of technology can be minimized or even eliminated.

VI. ATMOSPHERIC POLLUTION

The atmosphere, its pollutants and their associated issues are very complex. Here atmospheric pollution is defined as chemicals added to the "natural environment" in high enough concentrations to be harmful. The addition of these chemicals could occur by natural events (volcanic activity) or human activities (emissions from transportation and various industries). A given pollutant can have local or global effect depending upon the residence time of the pollutant in the atmosphere. The residence time of a pollutant is a measure of how long it stays in the atmosphere. The pollutants with short residence times affect local air quality. The pollutants that affect local air quality include particular matter (PM), gases such as SO_2, NO_2, NO, NH_3 and their ionic forms. All the gaseous species mentioned are called primary pollutants (emitted directly into atmosphere). The pollutants with residence time of days to weeks cause local and regional problems. The pollutants that belong to this category include, SO_4^{-2}, NO_3^-, NH_4^+, and particular matter having $PM_{2.5}$ (particulate matter with diameters less than or equal to 2.5 microns). The pollutants with residence time of weeks to months cause continental problems. The presence of Ozone in the troposphere belongs to this category. Ozone in the troposphere is formed as a result of secondary conversion of nitrogen oxides and some hydrocarbons in the presence of UV radiation. The pollutants with residence time from month to years result in global problems, including global warming. Pollutants that belong to this category are CO_2, CH_4, N_2, SF_6, HFCs, and PFCs.

The immediate effect of air pollution is its impact on human health. Evidence shows that many air pollutants suppress the immune system, cause respiratory illnesses, chronic respiratory diseases and premature death. The World Health Organization (WHO) uses six atmospheric pollutants in evaluating air quality. These include, Suspended Particular matter (SPM), Sulfur dioxide, Carbon monoxide, Ozone (troposphere), and lead. The particulate pollution in the atmosphere alone seems to be the leading cause of premature deaths in India and other Asian countries. In year 2000, over 500,000 premature deaths were reported as due to outdoor exposure to PM_{10} particulate materials. TABLE 1 lists the health effects of the WHO pollutants. If remedial effects are not implemented, the premature deaths could reach millions in future.

In addition to the atmospheric pollution, the land and water resources are also being degraded by various industries and people by improper discharge of harmful chemicals with consequences to the human and ecosystem health.

TABLE 1
HEALTH EFFECTS AND ATMOSPHERIC POLLUTION

POLLUTANT	SOURCE	HEALTH EFFECTS
Particulate	Motor vehicles, power plants, various industries, and construction	Respiratory illnesses, heart disease, suppresses immune system, some specific species may cause cancer.
Nitrogen Oxides	Motor vehicles, various industries, and fertilizer usage	Respiratory conditions
Sulfur Dioxide	Power plants and various industries	Same effects as particulate matter
Carbon Monoxide	Motor vehicles and various industries	Headache, fatigue and death when exposed to high level
Ozone	Secondary pollution in the troposphere	Aggravates respiratory conditions, irritation of eyes
Carbon dioxide	Fossil fuel use in power plants and various industries, transportation, and deforestation	Global warming and associated ill effects.

VII. ENVIRONMENTAL ISSUES IN INDIA

For the past fifty years, India has seen tremendous industrial and technological progress. This rapid growth is accompanied by innumerable environmental consequences. There is clear visible evidence of the pollution in many parts of India. A recent article in Slate Magazine reported that the air pollution in New Delhi is worse than the air pollution in Beijing, which itself made headlines around the world for its appalling air quality (Upton, 2013). The constituents of the pollution include particular matter, nitrogen oxides (NO_x), Carbon dioxide (CO_2), Ozone molecules, and many other hazardous chemicals. This is substantiated by a recent article on Delhi's particulate (PM) pollution in the Environmental Development magazine [11]. Other Indian cities have similar air pollution problems. Another news item reports pollution by high concentration of $PM_{2.5}$ [12]. The main sources of the pollutants are the vehicle exhaust, industries, waste burning, and construction. The paper reported that between 2008 and 2011, the particular pollution averaged $123 \pm 87\ \mu g/m^3$ for $PM_{2.5}$ and $208 \pm 137\ \mu g/m^3$, both exceeding the national standards of $40\ \mu g/m^3$ and $60\ \mu g/m^3$, respectively. Here, the $PM_{2.5}$ refers to the particular matter with diameters less than or equal to 2.5 microns and $\mu g/m^3$ refers to concentration in micrograms per cubic meter. Worldwide studies have consistently demonstrated that exposure to PM, NO_x, and Ozone pollution cause serious damage to respiratory and cardiovascular diseases, in some cases resulted in premature deaths [13] [14] [15] [16] [17].

A similar state of affairs exists in the case of water pollution. A recent study on the status of water quality in Delhi concluded that its surface water is highly polluted and groundwater is not fit for domestic and drinking purpose [18]. Other major cities in India face similar pollution problems, as evidenced by a brief stay in any of the larger cities. Besides air pollution and water pollution, India faces other major environmental issues on solid waste pollution, noise pollution, and land or soil pollution.

In 1997, the United National Environment program (UNEP) report published a report on global environmental outlook [19]. The report recognizes that Environmental problems are extremely complex as a result of interaction among the various components of the environment. For example, the emissions of greenhouse gases (CO_2, CH_4, etc.) and acidifying gases (SO_2, NO_2) have been shown to worsen the problem of ozone layer thinning.

VIII. GLOBAL ENVIRONMENTAL ISSUES

Various environmental problems exist in every corner of the world and most of them are attributed to the continuing progress or technological developments in different countries. Just from the point view of air pollution, based on the air monitoring data between 2003 and 2010, the world's worst pollution floats over Ahwaz, Iran followed by Ulaanbaatar, Mongolia [20]. Besides air pollution, other forms of environmental degradation exist throughout the world. According to a 1998 report by Canadian Scientists, the entire world is now polluted and even the most remote Polar Regions have substantial levels of toxic waste presence [21].

It is generally recognized that the environmental problems are extremely complex as a result of interaction among the various components of the environment. For example, the emissions of greenhouse gases (CO_2, CH_4, etc.) and acidifying gases (SO_2, NO_2) have been shown to worsen the problem of ozone layer thinning. However, the report issued specific recommendations for India (see Table 2). All these issues are associated with human health and natural ecological risks. To mitigate the problems listed in Table 1, a general understanding of some aspects of Environment Science is essential.

TABLE 2
RESOURCE AND ENVIRONMENTAL ISSUES

HIGH PRIORITY	MEDIUM PRIORITY	LOW PRIORITY
Land and Soil Resource	Pesticide and Fertilizer	Sea Level Rise
Deforestation	Acid Rain	Waste Disposal
Water Resources	Marine and Costal Degradation	
Industrial Pollution		
Urban Congestion and Pollution		

IX. CONCLUSION

The present article briefly describes the impact of technology on the natural environment. The impact is in the form of (1) pollution of the atmospheric air with toxic chemicals and particulate matter, (2) pollution of water resources with toxic chemicals, affluent disposals from industries, and sediments, and (3) pollution of land by waste disposals and spills. In the earth system, all the subsystems are interconnected and interact with one another, and as a result the pollution in one system goes to contaminate other systems. The effect of pollution of all systems contributes to millions of cases of pulmonary and other diseases. In many cases, they result in premature death, especially of infants.

The sources of pollutants are transportation, chemical, and power plant industries. It is extremely important to minimize the pollution through technological innovation of all industries. All nations have environmental regulations, and new generation of engineers should implement methods to follow these regulations in all future designs.

REFERENCES

[1]. UNEP, GEO -4, 2007. Global Environmental Outlook. http://www.unep.org/geo/geo4/report/GEO-4

[2]. Gosh Ray, R., 1996. The attitude of Kautilya to Aranya. Environment and History 2, no. 2, 221-229, http://www.environmentandsociety.org/node/2885.

[3]. Buddhist Publication Society, 1994. The Edicts of King ASHOKA.

[4]. White, 1967. White, L., 1967. "The Historical Roots of Our Ecological Crisis", *Science*, 155:1203-1207.

[5]. Bible, 2001.Genesis1:26. http://biblehub.com/genesis/1-26.htm

[6]. Rachel Carson, Author- Silent Spring, published by Houghton Mifflin on September 27, 1962.

[7]. Sagan, C. *Broca's Brain*. , Random House, Inc. See Ch.1 Can we know the Universe? Reflections on a Grain of Salt.

[8]. Motohiro Tomizawa and John E. Casida, Annual Review of Pharmacology and Toxicology, Vol. 45: 247-268 (Volume publication date February 2005).

[9]. Victory for the Bees, 2013. http://www.independent.co.uk/environment/nature/victory-for-bees-as-european-union-bans-neonicotinoid-pesticides-blamed-for-destroying-bee-population-8595408.html

[10]. Ahluwalia, V.K. and Malhotra, S., 2008. *Environmental Science.* Ane Books India, New Delhi, India.

[11]. Guttikunda, S.K. and Goel, R, 2013. Health impacts of particulate pollution in a megacity – Delhi, India, Environmental Development, Environmental Development, Volume 6, April 2013, Pages 8–20 Also see: http://dx.doi.org/10.1016/j.envdev.2012.12.002

[12]. Mascarenhas, A. Pune Air is more polluted now: New data shows. http://www.indianexpress.com/news/pune-air-more-polluted-now-new-data-shows/1082087/

[13]. Chhabra, S.K., Chhapra, P, Rajpal, S., Gupta, R., 2001. K. Ambient air pollution and chronic respiratory morbidity in Delhi. Archives of Environmental Health 56, 8.

[14]. Pande, J.N., Bhatta, N., Biswas, D., Pandey, R.M. Ahluwalia, G., Siddaramiah, N.H., et al., 2002. Outdoor air pollution and emergency room visits at a hospital in Delhi. The Indian Journal of Chest Diseases and Allied Sciences 44, 9.

[15]. Gupta, S.K., Gupta, S.C., Agarwal, R., Sushma, S., Agrawal, S.S., Saxena, R., 2007. A multicentric case-control study on the impact of air pollution on eyes in a metropolitan city of India. Indian Journal of Occupational Environmental Medicine 11, 37-40.

[16]. Siddique, S., Banerjee, M., Ray, M., Lahiri, T., 2010. Air pollution and its impact on lung function of children in Delhi, the capital city of India. Water, Air, and Soil Pollution 212, 89-100.

[17]. Balakrishnan, K., Ganguli, B., Ghosh, S., Sambandam, S., Roy, S., Chatterjee, A., 2011. A spatially disaggregated time-series analysis of the short-term effects of particular matter exposure on mortality in Chennai, India. Air Quality, Atmosphere and Health, 1-11Jones, J. "Entire World Polluted, Canadian Scientist Report." October 12, 1998, Reuters News Agency.

[18]. Abhay, R.K. Status of water quality and pollution aspect in Delhi. International Journal of Social Science Tomorrow, vol. 1, no. 5. Also see http://www.ijsst.com.

[19]. UNEP, GEO-1., 1997. Global Environmental Outlook. http://www.unep.org/geo/geo1

[20]. Upton, J., 2013. Slate Magazine article: Which City has the Worst Air Pollution in the World? http://www.slate.com/articles/health_and_science/medcal_examiner/2013/03/worst_air_pollution_in_the_world_beijing_delhi_ahwaz_and_ulaanbaatar.html

[21]. Jones, J. "Entire World Polluted, Canadian Scientist Report." October 12, 1998, Reuters News Agency.

Software Quality Estimation through Analytic Hierarchy Process Approach

B. B. Jayasingh, Professor, IT Dept., CVR College of Engineering, Ibrahimpatan, RR Dist-501510.
Email: bbjayasingh9@rediffmail.com
B. Rama Mohan, Associate Professor, CSE Dept., JNTUH College of Engineering, Hyderabad – 500085, (AP).
Email: b.ramamohan@jntuh.ac.in

Abstract--**Software quality assurance plays an important role to justify the software to reach the right level of quality. Its objective is to estimate the software quality and the errors in software modules before release to market place. In order to estimate the right level of quality one must apply some comprehensive techniques. To determine software quality, we present the Analytic Hierarchy Process (AHP) is the suitable approach for assessing the quality of software, with judgments by a group of experts rating. Since developing perfect or highly compatible software is not easy the AHP approach puts a threshold beyond which the quality of the new development is more than acceptable. We studied various techniques approached by different authors of software quality assurance to enable the stakeholder for choosing right kind of techniques suitable to their project.**

Index Terms—**Analytic Hierarchy Process, In Vivo Testing, Source Code Metrics, Software Quality, Divide And Conquer, Prioritization Problem.**

I. INTRODUCTION

Software runs on the machine and machine finds the errors with human interaction while development process. The development phase of SDLC (Software Development Life Cycle) includes more formal and detailed technical reviews that ensure to detect errors early. It is the time now for face-to-face communication instead of formal reviews, so the teams to decide and own the quality of each product. The product quality will be higher through the agile [1] development process that many organizations belief.

One specific form of technical debt [2] that has been studied for some time is design debt, also referred to as architecture debt. Design debt occurs whenever the software design no longer fits its intended purpose. A software project can run into design debt for various reasons. For example, adding a series of features that the initial architecture was not intended to support can cause debt and decrease the maintainability of software. Or, drifting away from a proposed architecture can bring short-term payoffs but might have consequences for the portability and interoperability of software. Reducing or eliminating design debt means in most cases that the design should be tailored and adapted towards changing requirements immediately and continuously.

We study various techniques approached by different authors of software quality assurance to enable the stakeholder for choosing right kind of techniques suitable to their project. The most important goals of the software industry is to develop high-quality and reliable software for their customers. We also consider the in vivo testing, in which tests are continuously executed in the deployment environment. However, the technical quality of source code (how well written it is) is an important determinant for software maintainability. Our survey focuses the low level source code metrics also effect to the high level quality characteristics. One must reconsider the divide and conquer principle applied consistently throughout the development (requirements documentation, design, review, coding, inspection, and testing) and maintenance of the product. However, predicting the exact number of faults is too risky, especially in the beginning of a software project when too little information is available. We conclude the analytical hierarchy process is the best suitable approach for software quality assurance.

In section II we discuss about the in vivo testing that run in the deployment environment which is hidden to the user. In section III we discuss the technical quality of source code (how well written it is) and how it affects to software maintainability. In section III we discuss the source code metrics that affect to the high level quality characteristics. In section IV we discuss the mathematical model for software quality assurance called divide and conquer where the complex job of building a software product must be reduced to a set of much simpler jobs. In section V we discuss the analytic hierarchy process consists of 6 criteria and 27 subcriteria where the prioritization problem solved to estimate the quality of software.

II. IN VIVO TESTING APPROACH

Testing at deployment environment needs attention of the developer where it runs continuously without the knowledge of user [3]. It is an improved version of unit or integration tests and focusing on aspects of the program that should hold true regardless of the state of the system. These tests keep the current state of the program while execution without affecting or altering the state that visible to users. This testing can be used to detect concurrency, security, or robustness issues.

In vivo testing [3] is a methodology by which tests are executed continuously without disturbing the state of the system that is hidden to the user. A prototype is developed in JAVA programming language called Invite (IN VIvo TEsting framework), focused on distributed execution of tests in earlier version. The current version includes a more detailed description in which it reveals the defects in real world applications.

A. In Vivo Testing Framework

The in vivo testing framework describes the steps for a software vendor regarding to use the Invite framework. The development of any new test code and the configuration of the framework must be done prior to distribute an in vivo-testable system.

1. Create test code
   The test methods must reside in the same class as the code they are testing (or in a superclass).
2. Instrument classes
   The vendor must select the methods from one or more Java classes in the application that under test for instrumentation.
3. Configure frameworks
   Each method runs with probability ρ, the vendor must configure Invite with values representing Before deployment.
4. Deploy applications
   The compiled code including the tests and the configured testing framework would ship as part of the software distribution. However, the customer would not even notice that the in vivo tests were running.

B. Testing Scenario

- The user is not aware of the presence of the testing, so his performance is not affected.
- These tests perform the following:
  - Checks the values of the individual variables
  - How the variables are related
  - Condition is held or not? – after some execution of the software

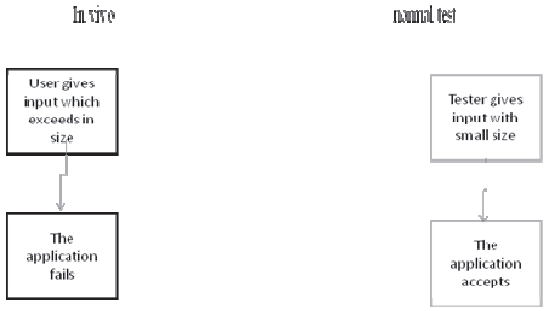

Figure 1 Testing Scenario

C. Concurrency Problem

- Function1 is used to destroy the processes that are running.
- Function 2 is used to create a new process.
- If function1 and function2 are called at the same time then function2 cannot create new process.
- This kind of defect can only be detected during run time, so In vivo testing approach is useful.

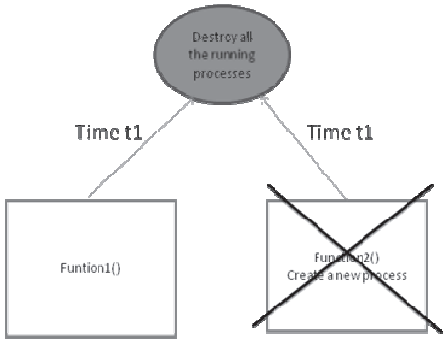

Figure 2 Concurrency problem

III. CODE QUALITY BENCHMARKING

The quality of source code also affect to software maintainability [4]. Whenever a change is required it must ensure how easy it is to perform the change, to implement the change, to avoid unexpected effects of that change and to validate the change.

Software Code Metrics

Software Improvement Group (SIG) chose 6 source code properties as key metrics for the quality assessments, namely:

1. Volume the larger the size the more to maintain since there is more information.
2. Redundancy duplicated code has to be maintained in all places where it requires.

3. Unit size the lowest-level piece of code and should be small to understand easily.
4. Complexity testing simple systems is easier than complex ones.
5. Unit interface size units with many interfaces to other units can be a symptom of bad encapsulation.
6. Coupling tightly coupled components are more resistant to change.

A. *Measurements Aggregation*

The sub characteristics are made quantifiable with the above source code metrics [5]. However, the metrics values are aggregated to a grand total of the whole system. Latter summarize to the cyclomatic complexity based on a set of thresholds. The aggregated measurements are used to determine a rating for each source code property, based on the application of another set of thresholds. These are further combined to calculate ratings for the sub characteristics and the general maintainability score for a given system [6].

B. *Standardized Evaluation Procedure*

The procedure consists of several steps, defined by SIG [7] quality model starting with the take-in of the source code by secure transmission to the evaluation laboratory and ending with the delivery of an evaluation report.

1. Intake: The source code is uploaded to a secure and standard location. For future identification of the original source a checksum is calculated.
2. Scope: it defines an unambiguous description of which software artifacts are to be covered by the evaluation. The description includes the identification (name, version, etc.) of the software system, a characterization (programming languages and the number of files analyzed) as well as a description of specific files excluded from the scope of the evaluation and why.
3. Measure: Apply an appropriate algorithm to determine the software artifacts automatically. The values of source code units are then aggregated to the level of properties of the system as a whole.
4. Rate: The values obtained in the measure step are combined and compared against target values to determine quality sub ratings and the final rating for the system.

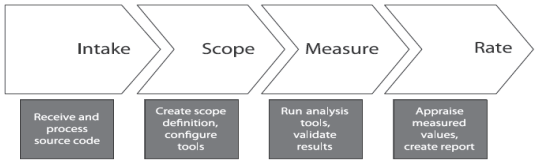

Figure 3 Evaluation framework

IV. SOURCE CODE METRICS AND MAINTAINABILITY

The ISO/IEC 9126 standard defines six high level product quality characteristics that are widely accepted both by industrial experts and academic researchers. These characteristics are: *Functionality*, *Reliability*, *Usability*, *Efficiency*, *Maintainability* and *Portability*. The characteristics are affected by low level quality properties [8], that can be *internal* (measured by looking inside the product, e.g. by analyzing the source code) or *external* (measured by executing the product, e.g. by performing testing). This work focuses on the relationship between the low level source code metrics and the high level quality characteristics defined by the standard.

Many researches propose maintainability models based on source code metrics. Bakota et al. [9] suggest a probabilistic approach for computing *maintainability* for a system. Heitlager et al. [10] also introduce a maintainability model. They transform metric value averages to the [9] discrete scale and perform an aggregation to get a measure for *maintainability*. Bansiya and Davis [11] developed a hierarchical model (QMOOD) for assessment of high level design quality attributes and validated it on two large commercial framework systems.

This work performed a manual evaluation of 570 class methods from five different aspects of quality. Now it is developed as a web-based framework to collect, store, and organize the evaluation results.

A. *Evaluated Systems*

An evaluated system JEdit is discussed, a well-known text editor designed for programmers. JEdit is a powerful tool written in Java includes syntax highlight, built-in macros, plug-in support, etc. The system selects 320 out of 700 methods to evaluate. The other evaluated system selects 250 out of 20,000 methods to evaluate. The evaluation was performed by 35 experts, who varied in age and programming experience.

B. The Evaluation Framework

The system consists of four modules:

1. AnalyzeManager - the module computes low level source code metrics and other analysis results.
2. Uploader - the module uploads the source code artifacts into a database.
3. AdminPages - the module manages the web interface and control the analysis process.
4. EvalPages - the module allow the users to evaluate the methods.

The questions are organized into the following five categories:

1. Analyzability - how easy the code to diagnose or to make a change.
2. Changeability - how easy the code to make a change in the system (includes designing, coding and documenting changes).
3. Stability - how easy the code to avoid unexpected effects after a change.
4. Testability - how easy the code to validate the software after a change.
5. Comprehension - how easy the code to comprehend (understanding its algorithm).

The author have shown the evaluator panel in fig. 4 for our better understanding.

Evaluator Panel

```
classExample{
public static void main(string args[])
{
int num=Integer.parseInt(args[0]);
int temp=num,res=0;
while(temp>0){
res=res+temp;temp--;}
```

Question: How easy it is to diagnoise the system for deficiencies or to identify where to make changes?

- o Good
- o Average
- o Poor

Figure. 4 Evaluator Screen

V. MATHEMATICAL MODELS

Present day software is more complicated where a small error can have bigger impact. With the complex task, the solution is the divide and Conquer strategy [12]. In this strategy the complex job can be reduced to a set of much simpler. This "Divide and Conquer" principle must be applied consistently throughout the development (requirements documentation, design, review, coding, inspection, and testing) and maintenance of the product

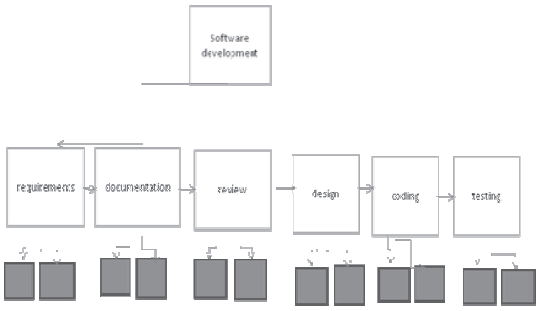

Figure 5 Divide and Conquer Model

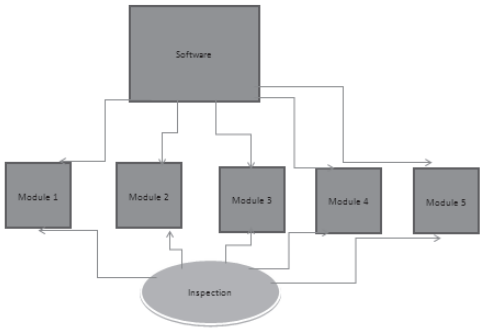

Figure 6 Inspection Using Divide and Conquer

It discusses one of three ways to measure software quality:

1. Reliability

It measures the failure rate of the software that depends on the way the software is used.

2. Correctness

It measures the correctness of a program because correctness is one property that high-quality software must have.

3. Trustworthiness

It is a question of whether users should trust a product. Some undesirable types of behavior called hazards have to be eliminated by the design and the process called hazard analysis. The more we test the more we trust in the product.

VI. ANALYTIC HIERARCHY PROCESS

The analytic hierarchy process (AHP) is the popular approach for assessing the quality of software, with judgments by a group of experts at different levels. It will explain the purpose and features of the system, what the system will do functional requirements and the constraints under which it must work. This document is

intended for the developer of software source code to understand their code quality. To determine software quality, quality metric models have been studied by many researchers. The AHP selects six criteria with 27 sub criteria in ISO/IEC 9126-1 (2001), which is the revision of 1991 version (ISO/IEC 9126, 1991) [13]. The relative rating provided by the expert contains nine scale value i.e. Equally important, Weakly important, Moderately important, Moderately plus, Strongly important, Strongly plus, Very strongly, Very very strongly and Extremely important. However the ratings provided by the experts are all fuzzy numbers. The proposed approach can help a group of various experts including developers, testers and purchasers, to measure the level of the software quality of the in-house development or the third party development.

A. Prioritization Problem

Consider a 3*3 group pair wise matrix for 3 criteria by 2 expert judgments as follows:

$$\begin{bmatrix} (1,1,1) & \begin{matrix}(3,4,5)\\(2,3,4)\end{matrix} & \begin{matrix}(5,6,7)\\(6,7,8)\end{matrix} \\ \begin{matrix}\left(\frac{1}{5},\frac{1}{4},\frac{1}{3}\right)\\\left(\frac{1}{4},\frac{1}{3},\frac{1}{2}\right)\end{matrix} & (1,1,1) & \begin{matrix}(3,4,5)\\(4,5,6)\end{matrix} \\ \begin{matrix}\left(\frac{1}{7},\frac{1}{6},\frac{1}{5}\right)\\\left(\frac{1}{8},\frac{1}{7},\frac{1}{6}\right)\end{matrix} & \begin{matrix}\left(\frac{1}{5},\frac{1}{4},\frac{1}{3}\right)\\\left(\frac{1}{6},\frac{1}{5},\frac{1}{4}\right)\end{matrix} & (1,1,1) \end{bmatrix}$$

Phase 1: expert1 matrix

Step 1: consider 3 criteria given by only 1st expert from the above matrix.

$$\begin{bmatrix} (1,1,1) & (3,4,5) & (5,6,7) \\ \left(\frac{1}{5},\frac{1}{4},\frac{1}{3}\right) & (1,1,1) & (3,4,5) \\ \left(\frac{1}{7},\frac{1}{6},\frac{1}{5}\right) & \left(\frac{1}{5},\frac{1}{4},\frac{1}{3}\right) & (1,1,1) \end{bmatrix}$$

Step 2: consider only the lower values from the above matrix (step 1).

$$\begin{bmatrix} 1 & 3 & 5 \\ \frac{1}{5} & 1 & 3 \\ \frac{1}{7} & \frac{1}{5} & 1 \end{bmatrix}$$

Step 3: consider the higher values of the above matrix(step 2) and calculate the Least Common Multiple (LCM).

$$[1 \quad 3 \quad 5]$$

LCM=15

So the factors are 1*15, 3*5, 5*3, consider the upper factors and add it i.e. 15+5+3=23.

Now calculate the reciprocal values

15/23= 0.652

5/23=0.217

3/23=0.130

Now the weighted matrix for lower values is

$$\begin{bmatrix} w_1^L \\ w_2^L \\ w_3^L \end{bmatrix} = \begin{bmatrix} 0.652 \\ 0.217 \\ 0.130 \end{bmatrix}$$

Step 4: calculate for medium values

Consider only the medium values from the above matrix (step 1).

$$\begin{bmatrix} 1 & 4 & 6 \\ \frac{1}{4} & 1 & 4 \\ \frac{1}{6} & \frac{1}{4} & 1 \end{bmatrix}$$

Step 5: consider the higher values of the above matrix(step 4) and calculate the Least Common Multiple (LCM).

$$[1 \quad 4 \quad 6]$$

LCM=12

So the factors are 1*12, 4*3, 6*2, consider the upper factors and add it i.e. 12+3+2=17.

Now calculate the reciprocal values

12/17= 0.705

3/17=0.176

2/17=0.117

Now the weighted matrix for medium values is

$$\begin{bmatrix} w_1^M \\ w_2^M \\ w_3^M \end{bmatrix} = \begin{bmatrix} 0.705 \\ 0.176 \\ 0.117 \end{bmatrix}$$

Step 6: calculate for upper values

Consider only the upper values from the above matrix (step 1).

$$\begin{bmatrix} 1 & 5 & 7 \\ \frac{1}{5} & 1 & 5 \\ \frac{1}{7} & \frac{1}{5} & 1 \end{bmatrix}$$

Step 7: consider the higher values of the above matrix (step 4) and calculate the Least Common Multiple (LCM).

$$[1 \quad 5 \quad 7]$$

LCM=35

So the factors are 1*35,5*7, 7*5, consider the upper factors and add it i.e. 35+7+5=47.

Now calculate the reciprocal values

35/47=0.744

7/47=0.148

5/47=0.106

Now the weighted matrix for upper values is

$$\begin{bmatrix} w_1^U \\ w_2^U \\ w_3^U \end{bmatrix} = \begin{bmatrix} 0.744 \\ 0.148 \\ 0.106 \end{bmatrix}$$

So the final weighted matrix for expert 1 is

$$\begin{bmatrix} w_1^L & w_1^M & w_1^U \\ w_2^L & w_2^M & w_2^U \\ w_3^L & w_3^M & w_3^U \end{bmatrix} = \begin{bmatrix} 0.652 & 0.705 & 0.744 \\ 0.217 & 0.176 & 0.148 \\ 0.130 & 0.117 & 0.106 \end{bmatrix}$$

Step 8: now divide the values with highest of upper values i.e. 0.744

$$\begin{bmatrix} w_1^L & w_1^M & w_1^U \\ w_2^L & w_2^M & w_2^U \\ w_3^L & w_3^M & w_3^U \end{bmatrix} = \begin{bmatrix} 0.876 & 0.947 & 1 \\ 0.291 & 0.236 & 0.198 \\ 0.174 & 0.157 & 0.142 \end{bmatrix}$$

Now multiply the column values of the two matrixes for the expert1

0.652*0.876 + 0.217*0.291 + 0.130*0.174= 0.657

0.705*0.947 +0.176*0.236 + 0.117*0.157= 0.726

0.744*1 + 0.148*0.198 + 0.106*0.142= 0.788

So the values for expert1 is

$$[0.657 \quad 0.726 \quad 0.788]$$

Phase 2: expert2 matrix

Step 1: consider 3 criteria given by only 2nd expert from the above matrix.

$$\begin{bmatrix} (1,1,1) & (2,3,4) & (6,7,8) \\ \left(\frac{1}{4},\frac{1}{3},\frac{1}{2}\right) & (1,1,1) & (4,5,6) \\ \left(\frac{1}{8},\frac{1}{7},\frac{1}{6}\right) & \left(\frac{1}{6},\frac{1}{5},\frac{1}{4}\right) & (1,1,1) \end{bmatrix}$$

Step 2: consider only the lower values from the above matrix (step 1).

$$\begin{bmatrix} 1 & 2 & 6 \\ \frac{1}{4} & 1 & 4 \\ \frac{1}{8} & \frac{1}{6} & 1 \end{bmatrix}$$

Step 3: consider the higher values of the above matrix(step 2) and calculate the Least Common Multiple (LCM).

$$[1 \quad 2 \quad 6]$$

LCM=12

So the factors are 1*12, 2*6, 6*2, consider the upper factors and add it i.e. 12+6+2=20.

Now calculate the reciprocal values

12/20= 0.6

6/20=0.3

2/20=0.1

Now the weighted matrix for lower values is

$$\begin{bmatrix} w_1^L \\ w_2^L \\ w_3^L \end{bmatrix} = \begin{bmatrix} 0.6 \\ 0.3 \\ 0.1 \end{bmatrix}$$

Step 4: calculate for medium values

Consider only the medium values from the above matrix (step 1).

$$\begin{bmatrix} 1 & 3 & 7 \\ \frac{1}{3} & 1 & 5 \\ \frac{1}{7} & \frac{1}{5} & 1 \end{bmatrix}$$

Step 5: consider the higher values of the above matrix (step 4) and calculate the Least Common Multiple (LCM).

$$[1 \quad 3 \quad 7]$$

LCM=21

So the factors are 1*21, 3*7, 7*3, consider the upper factors and add it i.e. 21+7+3=31.

Now calculate the reciprocal values

21/31= 0.677

7/31=0.225

3/31=0.096

Now the weighted matrix for medium values is

$$\begin{bmatrix} w_1^M \\ w_2^M \\ w_3^M \end{bmatrix} = \begin{bmatrix} 0.677 \\ 0.225 \\ 0.096 \end{bmatrix}$$

Step 6: calculate for upper values

Consider only the upper values from the above matrix (step 1).

$$\begin{bmatrix} 1 & 4 & 8 \\ \frac{1}{4} & 1 & 6 \\ \frac{1}{8} & \frac{1}{6} & 1 \end{bmatrix}$$

Step 7: consider the higher values of the above matrix (step 4) and calculate the Least Common Multiple (LCM).

$$[1 \quad 4 \quad 8]$$

LCM=8

So the factors are 1*8, 4*2, 8*1, consider the upper factors and add it i.e. 8+2+1=11.

Now calculate the reciprocal values

8/11=0.727

2/11=0.181

1/11=0.09

Now the weighted matrix for upper values is

$$\begin{bmatrix} w_1^U \\ w_2^U \\ w_3^U \end{bmatrix} = \begin{bmatrix} 0.727 \\ 0.181 \\ 0.09 \end{bmatrix}$$

So the final weighted matrix for expert 2 is

$$\begin{bmatrix} w_1^L & w_1^M & w_1^U \\ w_2^L & w_2^M & w_2^U \\ w_3^L & w_3^M & w_3^U \end{bmatrix} = \begin{bmatrix} 0.6 & 0.677 & 0.727 \\ 0.3 & 0.225 & 0.181 \\ 0.1 & 0.096 & 0.09 \end{bmatrix}$$

Step 8: now divide the values with highest of upper values i.e. 0.727

$$\begin{bmatrix} w_1^L & w_1^M & w_1^U \\ w_2^L & w_2^M & w_2^U \\ w_3^L & w_3^M & w_3^U \end{bmatrix} = \begin{bmatrix} 0.825 & 0.931 & 1 \\ 0.412 & 0.309 & 0.248 \\ 0.137 & 0.132 & 0.123 \end{bmatrix}$$

Now multiply the column values of the two matrixes for the expert2

0.6*0.825 + 0.3*0.412 + 0.1*0.137= 0.632

0.677*0.931 +0.225*0.309 + 0.096*0.132= 0.712

0.727*1 + 0.181*0.248 + 0.09*0.123= 0.782

So the values for expert2 is

$$[0.632 \quad 0.712 \quad 0.782]$$

Phase 3: Synthesis

The matrix values for expert1 is

$$[0.657 \quad 0.726 \quad 0.788]$$

And the matrix values for expert2 is

$$[0.632 \quad 0.712 \quad 0.782]$$

Now calculate the average of these two matrices

$$[0.644 \quad 0.719 \quad 0.785]$$

The final fuzzy value (0.644, 0.719, 0.785) is derived as the level of the quality. These results the quality of the new development is more than acceptable. Thus the SQA can give permission for a product of this quality to be used.

VII. CONCLUSION

We study various techniques approached by different authors of software quality assurance to enable the stakeholder for choosing right kind of techniques suitable to their project. We also consider the in vivo testing, in which tests are continuously executed in the deployment environment. However, the technical quality of source code (how well written it is) is an important determinant for software maintainability. Our survey focuses the low level source code metrics also effect to the high level quality characteristics. One must reconsider the divide and conquer principle applied consistently throughout the development (requirements documentation, design, review, coding, inspection, and testing) and maintenance of the product. We conclude the analytical hierarchy process is the best suitable approach for software quality assurance.

REFERENCES

[1] P. McBreen, “Quality Assurance and Testing in Agile Projects”, McBreen.Consulting, 2003.

[2] N. Zazworka et al., Investigating the Impact of Design Debt on Software Quality, ACM 978-1-4503-0586-0/11/05, pp. 17-23.

[3] C. Murphy et al., Quality Assurance of Software Applications Using the In Vivo Testing Approach, International Conference on Software Testing Verification and Validation, IEEE DOI 10.1109/ICST.2009.18, 2009, pp. 111-120.

[4] R. Baggen et al., Standardized code quality benchmarking for improving software maintainability, Software Qual J, Springer Pub., DOI 10.1007/s11219-011-9144-9, 2012, pp. 287–307.

[5] I. Heitlager et al., A practical model for measuring maintainability, In proceedings of 6th international conference on the quality of information and communications technology (QUATIC 2007), IEEE Computer Society, pp. 30–39.

[6] J. Correia et al., A survey-based study of the mapping of system properties to iso/iec 9126 maintainability characteristics, In 25th IEEE international conference on software maintenance (ICSM 2009), September 20–26, 2009, pp. 61–70.

[7] J. P Correia, J. Visser, Certification of technical quality of software products, In an International workshop on foundations and techniques bringing together free/libre open source software and formal methods, FLOSS-FM 2008, pp. 35–51.

[8] P´eter Heged˝us, Tibor Bakota, L´aszl´o Ill´es, Gergely Lad´anyi, Rudolf Ferenc, and Tibor Gyim´othy, Source Code Metrics and Maintainability:A Case Study, ASEA/DRBC/EL 2011, Springer-Verlag Berlin Heidelberg 2011, CCIS 257, pp. 272–284.

[9] Bakota, T., Heged˝us, P., K¨ortv´elyesi, P., Rudolf, F., Gyim´othy, T., A Probabilistic Software Quality Model, In Proceedings of the 27th IEEE International Conference on Software Maintenance, ICSM 2011, IEEE Computer Society, Williamsburg 2011, pp. 368–377.

[10] I. Heitlager, T. Kuipers, J. Visser, A Practical Model for Measuring Maintainability, In Proceedings of the 6th International Conference on Quality of Information and Communications Technology, 2007, pp. 30–39.

[11] Bansiya, J., Davis, C., A Hierarchical Model for Object-Oriented Design Quality Assessment, IEEE Transactions on Software Engineering 28, 2002, pp. 4–17.

[12] David Lorge PARNAS, The use of mathematics in software quality assurance, Front. Comput. Sci., Higher Education Press and Springer-Verlag Berlin Heidelberg, DOI10.1007/s11704-012-2904-2, 2012, pp. 3–16.

[13] K. K. F. Yuen, C.W. Lau Henry, A fuzzy group analytical hierarchy process approach for software quality assurance management, Fuzzy logarithmic least squares method, Expert Systems with Applications 38, ELSEVIER Publication, 2011, pp. 10292–10302.

Water Management Using Remote Sensing Techniques

Mr. K.V Sriharsha[1] and Dr. N.V Rao[2]
[1]CVR College of Engineering, IT Dept, Hyderabad, India
Email:harsha.mtech@gmail.com.
[2]CVR College of Engineering, CSE Dept, Hyderabad, India
Email:nvr@ieee.org

Abstract--**Water is the most conservative and natural resource for agriculture. But unfortunately in our country the well known fact is that the gap between the demand and supply of water for agriculture is becoming larger. Due to rapid increase in population growth, much of the water resources are being diverted from agricultural to non agricultural purposes. Instead of going into augmentation, water management policies emphasize each and every farmer to take an initiative in limiting water consumption by implementing need based irrigation. To do so, a systematic monitoring of water content at the surface of soil and its root zone is essential at each stage of the growth of a crop. In this process several methodologies like Gravimetric, TDR, TDT, FDR, ADR, Phase Transmission and Nuclear have evolved in determining soil moisture content and are successful to some extent. These methods are chosen based on factors like soil type, field maintenance, measurement time, operating temperature, measurement range, accuracy, power consumption, cost and ease of use. Information on soil moisture can be obtained by using above techniques but are time consuming and will have limited spatial coverage. In that case Remote Sensing Techniques provide better spatial and temporal coverage of soil moisture readings. The role of electronics and computers in Agriculture in designing sensors is very significant. This paper is limited to remote sensing techniques in this respect.**

Index terms—**Remote Sensing, Electromagnetic Spectrum, Hydrological Modeling, Soil Moisture Retrieval, Data driven Modeling, Fresnel's reflection coefficient, brightness Temperature, and Root Mean Square Error.**

I. INTRODUCTION

Remote sensing techniques are meant for observing the earth's surface or atmosphere using satellites (space borne) or using aircrafts (airborne). Any information about an object can be known without any physical contact using electromagnetic energy in remote sensing [1]. Whenever an electromagnetic energy radiation falls on a surface, some of its energy will be absorbed or transmitted and the rest is reflected. The sensing devices (cameras, scanners, radiometers, radar etc) that are mounted on aircrafts or satellites record the electromagnetic energy that is reflected or emitted by the earth's surface. The information is recorded on photographic films, videotapes or as digital data on magnetic tapes. Different objects on earth's surface return different amount of energy at different wavelengths in different bands of electromagnetic spectrum. Sensors that are mounted on satellites or on aircrafts take images of earth's surface in various wavelengths of electromagnetic spectrum. Wavelength under which object reflects or emits radiation depends on the property of material, surface roughness, angle with which ray is incident on earth's surface, intensity and wavelength of radiant energy.

A. Stages in Remote Sensing

- Emission of electromagnetic radiation from source
- Transmission of energy from source to surface of the earth
- Electromagnetic energy interaction with the earth's surface (reflection and emission of EM energy)
- Electromagnetic energy transmission from surface of the earth to the sensor
- Recording of information from the reflected or emitted electromagnetic energy in a specified format by the optical sensors.

Regions of Electromagnetic Spectrum available for Remote Sensing Systems are given in the following table1.

B. *Behavior of Electromagnetic Waves when Incident on Vegetation crops, Soil and Water*

- When an EM wave is incident on the vegetation, chlorophyll in the leaves absorb the radiation in red and blue wavelengths but reflect green wavelengths.
- When an EM wave incidents on the water, it is not reflected instead it will be either absorbed or transmitted.

- When an EM wave is incident on a soil surface, it is either reflected or absorbed but only little will be transmitted.

The reflectance property determines the characteristics of the soil.

TABLE1
Regions of EM spectrum available for Remote Sensing [1]

Photographic ultraviolet rays	0.3-0.4 micrometers	Available for remote sensing
Visible	0.4-0.4 micrometers	Available for remote sensing
Near and Mid Infrared	0.7-3 micrometers	Available for remote sensing
Thermal	3.0-14 micrometers	Available for remote sensing
microwave	0.1 to 100 cms	Available for remote sensing and can pass through cloud, fog and rain
Radio	>100 cms	Not normally used for remote sensing

II. Instruments used for remote sensing

A. *Remote Sensors*

Remote Sensor is an instrument that measure and record electromagnetic energy.
Remote sensing instruments are categorized into two types

- Passive Sensors
- Active Sensors

B. *Passive Sensors*

A passive sensor senses the electromagnetic radiation that is emitted or reflected from an object from source other than Sensor. According to Norman [2] these sensors do not produce electromagnetic energy on their own; instead depend on the external sources like Sun and sometimes the earth. These sensors cover the electromagnetic spectrum in a wavelength ranging from less than 1 picometer (gamma rays) to greater than 1meter (microwaves).

From the irrigation perspective MICROWAVE RADIOMETER is one of the most popular passive sensor instrument that is used in soil moisture estimation in the field. It is also used in mineral exploration, snow and ice detection. This instrument measures the intensity of radiation that is emitted or reflected from the object within the microwave range (0.1cm to 100cms). The depth from which energy is emitted depends on the properties of the material such as water content in the soil. The recorded electromagnetic radiation is termed as brightness temperature.

The other popular passive Sensor that comes in discussion is Aerial Camera which is termed as airborne sensor (a sensor used in aircrafts). Low orbiting satellites and NASA space shuttle Mission use the aerial Cameras for accurate navigation. Even Global Navigation Satellite systems (GPS-USA) use the Aerial camera systems to take the photographs of the objects on the earth's surface at precise points. Navigations are most essential in survey areas where especially topography maps won't work. These sensors have film which record the electromagnetic radiation in this specified wavelength range (400nm-900nm).

The other popular passive remote Sensor is Multispectral Scanner with which observations can be made point by point and line by line manner. These sensors can measure electromagnetic radiation in both visible and infrared spectrum. These sensors can give information about mineral compositions of the soil.

Imaging Spectrometer can measure intensity of radiation in very narrow spectral bands (5nm-10nm).These are used in determining chlorophyll content of surface water.

Thermal Scanner measures the electromagnetic radiation that falls within the specified range (8 micro meters to 14 micrometers). The wavelength in this range is related to temperature of the soil and hence effects of droughts on agricultural crops can be studied. The major disadvantage in passive remote sensing systems is that they are sensitive to climatic conditions especially when the sky is cloudy and the incoming radiation cannot be sensed. To overcome this problem Active remote sensing systems are used and they allow the signal to pass through clouds, fog and rain.

C. *Active Remote Sensing Systems*

The most distinguishable feature of active sensor is that they provide electromagnetic energy on their own to illuminate the object on the earth's surface. These sensors also measure the electromagnetic radiation that is emitted or reflected from the object. RADAR is one of the well noted Active Remote Sensing systems which can operate at microwave wavelength range. One of the most popular radar is Synthetic Aperture Radar [3].It transmits and receives the electromagnetic radiation that fall within the microwave range (1mm to 1m). The electromagnetic energy that is emitted from sensor can be penetrated into deeper parts in the soil mantel and can be reflected from that point. This radar system can be made to operate during daylight as well as in darkness. These sensors give the knowledge of deep and under canopy soil moisture.

RADARSAT is a popular Synthetic aperture radar operate at 5 GHZ and is used worldwide in giving response to disasters such as flooding, volcanic eruptions and severe storms.

The other active remote sensing system is ALTIMETER transmits microwave pulses and measures round trip delay with which distance from object to sensor is known. If the object is sea surface then its height can be predicted and hence wind speed is estimated. These sensors can be mounted on aircrafts and satellites and can be used for topological mapping. JASON-I is an altimeter which can provide the altitude of earth's ocean surface and is operated at frequencies of 13.6GHz to 5.3GHz.

Scatterometers are the active sensors that measure the back scattered radiation in microwave region and derive the information about the wind direction and speed over the earth's surface with the help of the maps.

TABLE 2
Characteristics of Active Remote Sensing System

D. *Measurement Principle*

The emission of microwave energy is proportional to the product of surface temperature and surface emissivity [4]. Here the brightness of an emitter of a microwave radiation is related to temperature of a source through emissivity

T_B is proportional to T_{eff}

characteristics	SAR (Synthetic Aperture radar)	Altimeter	Scatterometer
Radiated Power(W)	1500	20	100
Range(km)	695	1344	1145
Viewing Geometry	Side looking	Nadir looking	Six fan beam in azimuth
Spectrum width	20-300MHz	320MHz	5-80KHz
Service Area	Land/coastal/ ocean	Ocean/ice	Ocean/ice/land

$$T_B = (1-R)T_{eff} = eT_{eff} \quad (1)$$

R- Directional Reflectivity of surface

T_{eff} - Effective Radiation temperature

e- Effective emissivity = 1-R, which depends on dielectric constant of medium and latter can be used to determine soil moisture content.

E. *Measuring Soil Moisture content using L Band Radio Metric System*

Microwave radiometer is one such Passive remote sensing device measures the power level of the incoming radiation. The power level (P) is expressed based on the following relationship

$$P = K*T_b*B \quad (2)$$

T_b is brightness temperature (defines the measure of intensity of radiation at microwave frequencies)

K Boltzmann constant; B Bandwidth of the instrument

For a flat surface, Brightness temperature is proportional to the physical temperature of the surface as

$$T_b = e*T = (1-r)\,T \quad (3)$$

e- Emissivity; r = Fresnel's reflection coefficient

From Microwave Radiative Transfer Model [5] L-MEB (L-Band Microwave Emission of Biosphere) the brightness temperature (T_{BP}) is expressed as

$$T_{BP} = (1-w_p)(1-\gamma_p)(1+\gamma_p r_{Gp})T_c + (1-r_{GP})\gamma_p T_G \quad (4)$$

T_c,T_G - vegetative and effective soil temperatures.

r_{GP} soil reflectivity

γ_p vegetation attenuation factor

T_{BP} polarized brightness temperature, where

$\gamma_p = e^{-\tau_p/\cos\theta}$

θ Is incident angle, τ_p- vegetation optical depth

Soil reflectivity (r_{GP}) depends on dielectric properties of the soil such as permittivity, permeability, conductivity etc which in turn depend on physical properties of soil such as soil moisture, temperature, salinity and geometric roughness.

Fresnel's reflection coefficient(r) determines the reflectance of the soil

$$r \alpha \theta_I \quad (5)$$

- Small change in angle of incidence (θ_i<10°c) exhibits small change in r values with variation in dielectric properties of soil water mixture.
- Variation in soil moisture (θ) affects dielectric properties of the soil (ϵ,μ,σ,f) which in turn affects their value (reflection coefficients) and in turn the difference in received power level of the incoming radiation.

III. Analysis of Remotely Sensed Data Using Hydrological Modeling Techniques

In order to perform analysis on remotely sensed data such as soil moisture, hydrological models are mainly used. These are further classified into two categories namely physical based and empirical based. Physical based modeling technique uses mathematical equations derived from the system physical process. Hence it is necessary to know about physical parameters in detail. Especially in modeling the soil moisture component

with respect to time and/or space, the physical parameters like evapotransiration rate, infiltration rate, percolation, soil type, and vegetation cover are to be considered. The latter model which is empirical based uses mathematical equations, derived from time series data analysis. Without knowing explicitly the physical behavior of the system one can use the Data Driven Modeling (DDM). As the name implies it is based on analysis of data about a system [6]. In particular, it finds a way in relating system state variables (input and output variables) without the physical behavior of system , The model is trained on sample data of soil moisture aiming at reducing the error which is shown as difference between observed and predicted output.

A. Different Types of Data Driven Modeling Techniques

Data Driven Modeling is classified into two categories i.e. parameterized and non parameterized. Recent survey on non parameterized data driven modeling reveals the fact that statistical and Neural Network modeling (NN) approaches are simple and efficient in soil moisture retrieval.

B . Soil Moisture Retrieval using Statistical Approach

Support vector machines (SVM) and Relevance vector machines (RVM) are supervised non parametric statistical modeling techniques that are known for producing desired estimations of soil moisture content using inexpensive and readily available data. From the experiments conducted at Walnet Creek Watershed in Ames, South Central Iowa, USA, it is derived that RVM model performs much better with RMSE of soil moisture content depts. Of 5,10,20,30 and 50cm for about 227 days. On the fourth day 1cm 0.014%v/v compared to SVM whose RMSE value is 0.017%v/v [7].

Their research starts with the development of three models for soil moisture estimation. The first model uses remotely sensed input consisting of meteorological variables, field measurements and crop physiological actors for training SVM and RVM models in order to retrieve surface soil moisture at 0-6cms of top soil layer. Once the model is trained, the soil moisture content is estimated to check the model performance with a RMSE value. The second model is trained with inputs like soil temperature for 0-6 cms precipitation, number of days last rained, including soil moisture readings of model1 and surface soil moisture content at 30cm depth is estimated. The Model III is trained in two steps. In the first step RVM and SVM models are trained in a similar manner as Model I to estimate surface soil moisture content. In the second step the model is trained on remotely sensed data at a larger scale to estimate soil moisture content at 30cms depth.

In order to measure the error between observed and estimated data, the parameter, Root Mean Square Error is used. The performance of a model is directly proportional to the value of RMSE.

With reference to experimental study made on Landsat images of study area superimposed with land use in the year 2002, RMSE values obtained for soil moisture retrieval at three models during training and testing phases are tabulated as shown in table3.

TABLE 3.
RMSE values of soil Moisture Retrieval for SVM and RVM Models [7]

Phases	Training phase	Testing Phase	Training Phase	Testing Phase
Model 1	2.0%v/v	4.3%v/v	1.2%v/v	3.8%v/v
Model 2	0.36%v/v	0.66%v/v	0.02%v/v	0.48%v/v
Model 3	0.76%v/v	1.7%v/v	0.38%v/v	1.4%v/v

The results indicated in the table 3 show that RVM model comparatively provides better performance in all respects during training and test phases. This proves that it has good potential of soil moisture estimation. With reference to data taken from Soil climatic Analysis network site at Rees centre, Texas, USA, MVRM(Muitvariate Relevance Vector Machine) trained on input variables like soil temperature, depth of soil model, RMSE value for soil moisture retrieval is recorded as 1.31% which indicate that observed data and modeled values are close and model is performing well. Even at the end of the 4^{th} day at a depth of 2mts, RMSE reading is reduced to 0.15% which shows the closeness of modeled value to the observed value .Decrease in RMSE is a signature of good performance of a model.

C. Soil Moisture Retrieval using Neural Network Model

A multilayer layered feed forward Artificial Neural Network model used for research with input layer consisting of selected input variables, a hidden layer with 'n' number of hidden neurons and output layer consisting of predicted soil moisture values. The sigmoid and linear transfer functions are used in hidden and output layers. The model uses an algorithm to train the network. During forward phase the selected inputs are propagated though the network from layer to layer. An error is computed by comparing the difference between desired and predicted output. This error is propagated backwards and correspondingly weights and bias are adjusted to minimize the error. The results of the model show that with the appropriate selection of

inputs, the error is minimized and hence the accuracy in soil moisture retrieval can be improved.

With reference to the National Airborne Field Experiment 2005[8] conducted in Southern Australia for Goulburn catchment, it is explicitly stated that the near surface soil moisture measurements were taken over eight farms at the same time by using active remote sensing systems. The measurements were also taken at many locations within a farm. For the study of soil moisture estimation in a farm, a two layer perceptron model consisting of 2 nodes in the input layer, four neurons in the hidden layer and one at the output layer is chosen. The model is trained with several back propagation algorithms to adjust the weights in the hidden and input layers so as to minimize the root mean square error between actual and predicted soil moisture output measurements. The results obtained for RMSE are found to be between ranges of 3.93%v/v to 5.77%v/v, as shown in table 4.

In the table 4 it is explicitly stated that RMSE value obtained after training the network with Quasi Newton Algorithm-BFGS is comparatively less and this proves that it is the only method that is capable of retrieving soil moisture with the desired accuracy.

TABLE 4
Root Mean Square Error (RMSE) of soil moisture retrieval for various backpropogation algorithms [8]

sno	Back Propogation algorithm	RMSE (Root Mean Square Error)% v/v
1	Batch Gradient with Momentum	4.86
2	Gradient Descent with Adaptive Learning	4.88
3	Gradient descent with momentum and adaptive learning rate	4.88
4	Resilient backpropogation	4.93
5	Conjugate gradient backpropogation with Fletcher-Reeves updates	4.82
6	Conjugate gradient backpropogation Polak-Ribiere updates	4.83
7	Conjugate gradient backpropogation with Powell-Beale restarts	4.83
8	Scaled conjugate gradient backpropogation	5.77
9	Quasi-Newton Algorithm-BFGS	3.93
10	Quasi-Newton Algorithm: One step Secant algorithm	5.51
11	Levenberg-Marquardt	4.04

D. Soil Moisture Retrieval using Classification and Regression trees Algorithm (CART)

With reference to observations taken from experimental study conducted at Yongdam Basin from May 16th to August 19th, 2008[9], it is observed that use of CART algorithm and neural networks provide proper soil moisture field estimations and even represent soil moisture behavior very well.

TABLE 5
RMSE values of soil moisture retrievals at four sites

Area	RMSE(%v/v)
Jucheon	1.3925
Bugui	1.0254
Sangjeon	1.8783
Ahncheon	1.0037

For experimental study a neural network model was built with input layer consisting of five nodes, hidden layer consisting of five nodes and an output layer with one node. The input variables to the model includes in suite soil moisture measurements taken from Korean water resources corporation (KWRC), precipitation , surface temperature provided by Korean Meteorological Administration (KMA), Normalized Difference Vegetation Index (NDVI) from Moderate Resolution Imaging Spectro radiometer (MODIS).

IV. Irrisat- Water Management Service

Irrisat is an irrigation water management service uses high level technology to deliver information to the farmers. It was developed in New South Wales, Australia by CSIRO Land and Water for collecting the satellite images though remote sensing methods along with the information from local weather stations and sending the information to the farmers cell phones as an SMS so that this would help the farmers to schedule their irrigation at appropriate times [10]. The service sends one SMS per day to each farmer who subscribes the service. The whole system functions in such a way that the light reflected from the vegetation and land surface is captured by the remote sensors that are mounted on satellites and are being processed using software and hence crop vigor is extracted showing evapotranspiration rate. At the same time from local weather stations, farmers in different regions collect data on temperatures, wind speed, solar radiation and relative humidity and deliver the information to Irrisat SMS database. The weather information combined with satellite data determines the condition for actual water consumption by crops on a particular farm. The Irrisat service so far implemented successfully in Australia and can even be implemented in Asian countries too where cell phones are used extensively. Irrisat is a promising service rough with which farmers will be given a flexible irrigation management system meeting their specific needs. *In India, IFFCO SAN*CHAR Limited has been offering services on IKSL Green SIM CARD covering diverse areas including soil management/crop production.

CONCLUSIONS

This review demonstrates the role of Remote Sensing in Irrigation water Management. It is known that remotely sensed data on soil moisture at larger scales can drive the farmer to perform better water management

operations in scheduling the irrigation. A discussion has been made on different instruments that perform remote sensing, their characteristics and their applicability at various types of soil. From the observations made on L Band Radio Metric System, it is clearly noticed that the difference in received level power level of incoming radiation from the soil is an indicator of variation of soil moisture content. It is mentioned that there are several physical and data driven models that perform soil moisture estimation. The survey on these models reveals the fact that data driven modeling is one among that is dominating in recent trends. It is to mention that all over the world several countries including India, are offering water management services to the farmers by integrating remote sensing with mobile technology.

REFERENCES

[1] Baumann"Introduction To Remote Sensing", State university of Newyork, College at Oneonta, 2008.

[2] Bakker,Wimm ,"Principles Of Remote Sensing",An Introductory Textbook, 3rd Edition, Institute of Geo information Sciences and Earth Observation.

[3] Huneycutt,"requency Use and needs of space borne active sensors", ,Geo Science and remote Sensing Symposium, 2000 proceedings,Pasadena,pp.2457-2463,2000.

[4] Jackson,"Surface Hydrology & Remote Sensing", 1993.

[5] Philip," Characteristics of Rape field Microwave Emission and Implications of surface soil Moisture Retrieval", Remote Sensing,pp.247-270,2012.

[6] D. Solomantine, L.M See and R.J Abrahart," Data Driven Modeling: Concepts, Approaches and Experiences, Practical Hydro informatics", Water Science and Technology Library68, Springer,2008.

[7] Bushra Zaman",Remotely Sensed Data Assimilation Technique to develop Machine Learning Model for use in water Management", Utah State University, Logan, Utah, 2010.

[8] Soo-See Chai,Bert Veenedaal,Geoff West,Jeffrey Philip Walker,"Back Propogation Neural Network for soil moisture retrieval using NAFE '05 Data:A comparison of different training algorithms", University Of Melbourne, International Archives of the Photgrammetry, Remote Sensing and spatial Information Sciences, Vol.XXXVII. Part B4, Beijing, 2008.

[9] Gwangseob Kim,Jung ,"Soil Moisture Estimaton using Classification and Regression trees and neural networks, ,Geology and Continuum Mechanics,ISBN:978-960-474-275-2,2009.

[10] Richard Soppe ,"Remote Sensing& Cell Phone Technology deliver water management", CSIRO Land and Water, Dec1, 2010., Richard Soppe , CSIRO Land and Water,Dec1,2010.

Health Hazards of Computer users & Remedies (Computer Ergonomics)

Dr.M.N.Ramakrishna M.D. A.F.I.H
Medical officer, CVR College of Engineering
Email:drrkmn@rediffmail.com

***Abstract*---Computer users, especially those who continuously operate computers for hours together, are usually prone to certain health problems which are called 'Musculo-Skeletal Disorders' and 'Computer Vision Syndrome. These problems can be prevented to a large extent if users know a little about 'Ergonomics' of the computer. This article briefly describes computer-related-disorders and ergonomic tips for computer users.**

***Index Terms*—Computer ergonomics, computer-related disorders, Health Hazards**

I. Introduction

Computers have become an integral part of life. Newer studies show that if you don't use the computer properly when working on a computer, you chance discomfort, pain and even injury. New research shows that it takes more than just an ergonomic desk chair or a split keyboard to prevent health problems affecting millions of computer users. The repetitive motion is one factor among many that contribute to a cluster of symptoms called "computer-related disorder" (CRD).

A. Cumulative trauma disorder (CTD), and Repetitive stress injury (RSI)

Work-related musculoskeletal system disorders (WMSDs) are as follows.

1. Carpaltunnel syndrome
2. Back pain
3. Osteoarthritis
4. Tendinitis
5. Teno-synovitis
6. "Pitcher","Golfer" or"Tennis Elbow"

A. Computer Electromagnetic Radiation and Its Health Effects

B. Computer Vision Syndrome

Some visual display users have reported sore and tired eyes, blurred vision and eye fatigue after prolonged use of their terminals. It is natural for some people to experience visual discomfort if they've been using their eyes intensively over a long period of time, whether it is working at a display, studying for an exam or doing close work. While eye fatigue may be uncomfortable, it is not damaging to the eye. It also is a temporary condition and goes away with rest.

Most common work related Muscular skeletal disorder is carpal Tunnel Syndrome which is described below.

CARPAL TUNNEL SYNDROME

The carpal tunnel receives its name from the 8 bones in the wrist, called carpals that form a tunnel-like structure. The tunnel is filled with flexor tendons which control finger movement. It also provides a pathway for the MEDIAN NERVE to reach sensory cells in the hand. Repetitive flexing and extension of the wrist may cause a thickening of the protective sheaths which surround each of the tendons. The swollen tendon sheaths, or Teno-synovitis, apply increased pressure on the median nerve and produce Carpal Tunnel Syndrome

MOTOR-Thenar muscle at the base of the thumb atrophies and strength is lost.

SENSORY- Subjective or objective hypoesthesia (decreased sensation) coinciding with median nerve distributions, heat and cold sensation lost.

II. Helpful Hints for work area

Millions of people work with computers every day. There is no single "correct" posture or arrangement of components that will fit everyone. However, there are basic design goals to consider when setting up a computer workstation or performing computer-related tasks.

Creating the Ideal Computer Workstation

It is necessary to plan to create an ergonomically sound workstation for computer users. The plan should include illustrated guidelines on how to adjust furniture, computer equipment, and work aids. It must also include information on how to organize work area and tasks, and checklists to

evaluate the ergonomics of current workstation. It has to help in preparing specifications list when purchasing new equipment.

The Work Area

The following figures illustrate how a computer user should adjust his body posture and eye alignment while using a computer.

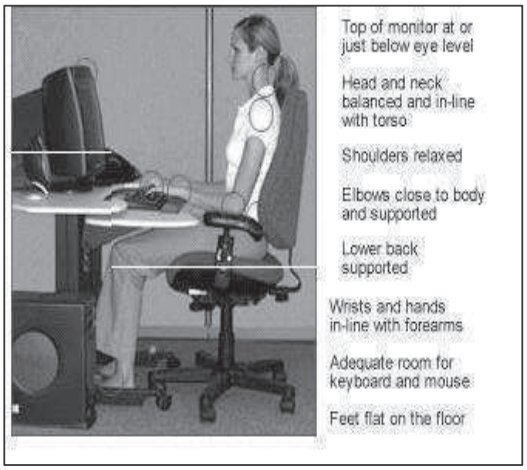

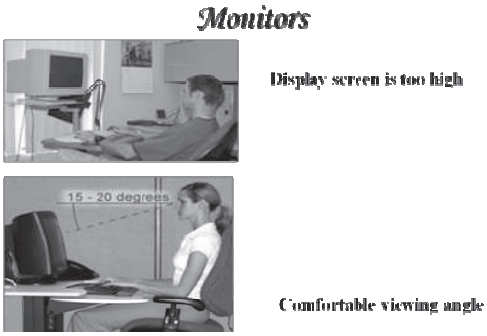

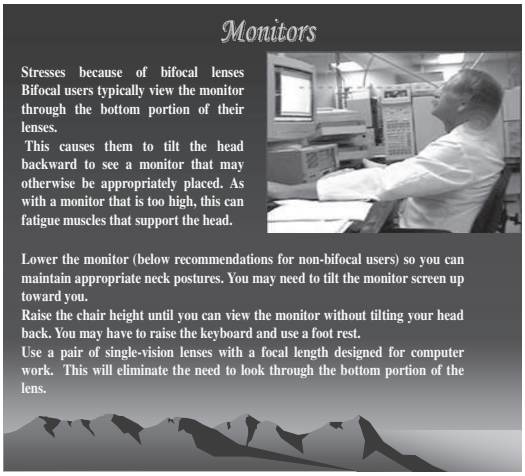

Following are some hints on how to minimize fatigue and other harmful effects while using computer.

- Eyes should rest periodically by focusing on objects that are farther away (for example, a clock on a wall 20 feet away). The user should look away, and blink at regular intervals to moisten the eyes.
- The user has to alternate duties with other non-computer tasks such as filing, phone work, or customer interaction to provide periods of rest for the eyes.
- There may be some factors that reduce image quality, make viewing more difficult and may lead to eye strain by other electrical equipment located near computer workstations. The result may be display quality distortions and dust accumulation, which are accelerated by magnetic fields associated with computer

monitors. These may reduce contrast and degrade viewing conditions.

- Computer workstations should be isolated from other equipment that may have electrostatic potentials in excess of +/- 500 volts.
- Computer monitors should be periodically cleaned and dusted.

Additional hints are given below for using related equipment with minimum discomfort.

Keyboards

- The keyboard should be directly in front of the user.
- The user's shoulders should be relaxed and your elbows close to your body.
- The wrists should be straight and in-line with your forearms
- Chair height and work surface height should be adjusted to maintain a neutral body posture.
- Elbows should be about the same height as the keyboard and should hang comfortably to the side of the body. Shoulders should be relaxed, and wrists should not bend up or down or to either side during keyboard use.
- Central pencil drawers should be removed from traditional desks if chair can not be raised high enough because of contact between the drawer and the top of the thighs. The work surface should generally be not more than 2 inches thick.

Pointer/Mouse

- The pointer/mouse should be kept close to the keyboard.
- Both hands should be used alternately while operating the pointer/mouse.
- Keyboard short cuts are to be used to reduce strain.

Wrist/Palm Supports

- Wrist rest should be used to maintain straight wrist postures and to minimize contact stress during typing and mousing tasks.

Document Holders

Documents should be at the same height and distance as the monitor.

Chairs

Desirable specifications of computer chairs are:

- Adjustable chair and backrest
- Natural S-curvature of the spine
- Seat pan with a rounded, "waterfall" edge.

Shoulders in various positions are illustrated below.

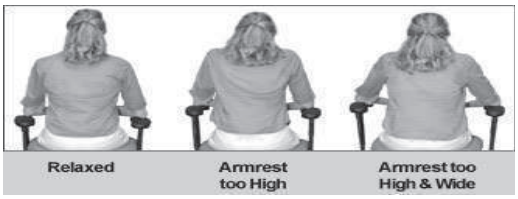

Some other precautions are as follows:

- Taking micro breaks or rest pauses
- Adjusting to have optimum lighting
- Avoiding Glare Effect on monitor

III. ERGONOMIC TIPS FOR COMPUTER USERS

Ergonomics is "Study of how people physically interact with their work, fitting the job, the equipment and the work environment to the worker".

Ideal Office

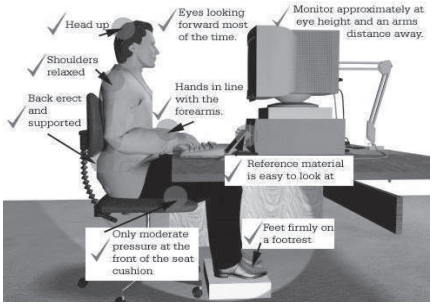

- Head Up
- Shoulders relaxed
- Back erect and supported
- Eyes looking forward most of the time.
- Hands in line with the forearms.
- Only moderate pressure at the front of the seat cushion
- Reference material is easy to look at.
- Feet firmly on a footrest.
- Monitor approximately at eye height and an arms distance away.

Exercises for the office

One of the biggest injury risk factors is static posture. This can be reduced by

- Spending at least 5 minutes every hour away from your computer.
- *Remembering* to ONLY stretch to the point of mild tension.
- Trying to incorporate the stretches into daily routine.

Hand Exercises include

- Doing hand exercises like tight clenching of hand into a fist and releasing it, fanning out the fingers, and repeating it three times.

Back and Shoulder Exercises

These include standing up straight, placing the right hand on the left shoulder and moving head back gently, and repeating it for the right shoulder.

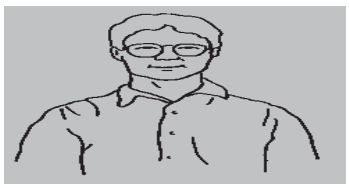

Head and Neck Exercises

These involve

- Moving head sideways from left to right and back to left.
- Moving head backward and then forward.



Computer and Desk Stretches

Sitting at a computer for long periods often causes neck and shoulder stiffness and occasionally lower back pain. This can be avoided by doing following stretches every hour or so throughout the day or whenever there is a feeling of stiffness. It helps to get up and walk around the office every now and then.

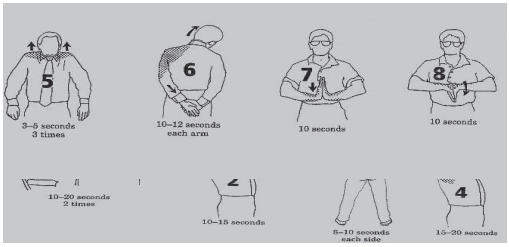

CONCLUSIONS

Many of the potential health problems associated with using computers for long duration can be avoided by following a few precautions and doing appropriate physical exercises. The present article has given an overview of these, and computer users will benefit by making them a part of their work culture.

Note: The information provided in this article is collected from following websites.
*www.cdc.gov/**NIOSH***
www.**cdc**.gov/
www.**osha**.gov/
www.**ilo**.org/
www.defense.gov/

ABOUT THE COLLEGE

CVR College of Engineering was established in 2001, and its ninth batch of students graduated from the College. CVR is ranked among the top few of more than 600 colleges in AP that started in the last decade and was also rated as the #1 co-educational college in Pass percentage among nearly 300 colleges under JNTU, Hyderabad for examinations held in May 2009, November 2009 and May 2010. It is the expectation of the academic community that CVR is on the successful path to be in the TOP-5 amongst all colleges in AP in the next few years.

The College was the first college in Osmania University area that was promoted by NRI technology professionals resident in the US. The NRI promoters are associated with cutting-edge technologies of the computer and electronics industry. They also have strong associations with other leading NRI professionals working for world-renowned companies like IBM, Intel, Cisco, Motorola, AT&T, Lucent and Nortel who have agreed to associate with the College with a vision and passion to make the College a state-of-the-art engineering institution.

The College has been given permanent Affiliation and Autonomous status by JNTUH.

CALL FOR PAPERS:

Papers in Engineering, Science and Management disciplines are invited for Publication in our Journal. Authors are requested to mail their contributions to Editor, CVR Journal of Science and Technology (Email Id:chalapatiraokv@gmail.com).

The Papers are to be written using a Standard Template, which may be obtained on request from the Editor.

CVR JOURNAL OF SCIENCE & TECHNOLOGY

CVR COLLEGE OF ENGINEERING
(An Autonomous College affiliated to JNTU Hyderabad)
Mangalpalli (V), Ibrahimpatan (M)
RR District, AP-501510
http://cvr.ac.in